AD 295 108

ANALYTICAL STUDY

OF

ILS BEAM CHARACTERISTICS

by

THE BENDIX CORPORATION
ECLIPSE-PIONEER DIVISION

FAA Contract No: ARDS-451
FAA Project No: 114-1312D
E-P Project No: AD1091

August 31, 1962

FEDERAL AVIATION AGENCY SYSTEMS RESEARCH AND DEVELOPMENT SERVICE

Analytical Study
of
ILS Beam Characteristics

by

THE BENDIX CORPORATION
ECLIPSE-PIONEER DIVISION

FAA Contract No: ARDS-451
FAA Project No: 114-1312D
E-P Project No: AD1091

August 31, 1962

FEDERAL AVIATION AGENCY
SYSTEMS RESEARCH AND DEVELOPMENT SERVICE

NOTICE

This report has been prepared by The Bendix Corporation's Eclipse-Pioneer Division for the Systems Research and Development Service (formerly Aviation Research and Development Service), Federal Aviation Agency under Contract Number ARDS-451, Project Number 114-1312D. The contents of this report reflect the views of the contractor, who is responsible for the facts and the accuracy of the data presented herein, and do not necessarily reflect the official views or policy of the FAA.

THE BENDIX CORPORATION
ECLIPSE-PIONEER DIVISION
TETERBORO, NEW JERSEY

Analytical Study of ILS Beam Characteristics for the Systems Research and Development Service Federal Aviation Agency

FAA Contract No: ARDS-451
FAA Project No: 114-1312D
E-P Project No: AD-1091

August 31, 1962

Prepared by:

J. Doniger
V. Doniger
Project Manager

Reviewed by:

K. Moses
Senior Engineer

Approved by:

W. A. Platt
W. A. Platt
Assistant Chief Engineer

P. A. Noxon
P. A. Noxon
Director of Advanced Systems
Development Department

FOREWORD

This report was prepared by the Eclipse-Pioneer Division of The Bendix Corporation as required by the Federal Aviation Agency under Contract FAA/ARDS-451, Project Number 114-1312D.

The entire study was administered by the Advanced Systems Development Laboratory with J. Doniger as Project Manager. Messrs. R. Kostanty, B. Hanisch, F. Belsky, and A. Flitt performed the analog computer studies, and J. Clair studied the applicable decision making techniques.

The cognizant FAA Project Manager was Mr. N. J. Proferes of the Aviation Research and Development Service; who together with Mr. D. J. Sheftel and Mr. A. B. Winick, provided valuable guidance throughout the project.

The Bendix Corporation, Eclipse-Pioneer Division, Teterboro, N. J.

ANALYTICAL STUDY OF ILS BEAM CHARACTERISTICS FOR THE SYSTEMS RESEARCH AND DEVELOPMENT SERVICE.
August 31, 1962. 90 pages, including 50 illustrations.

ABSTRACT

This report presents the results of analog computer studies and analyses of the noise component in the ILS glide path and localizer course structures due to terrain reflections. Actual recordings of the noise at the 25 ILS sites which will probably be used in the initial lower minimum operations below 200 feet were furnished to the contractor by the FAA. The studies included the comparison of various possible ILS course/path noise figures of merit as they related to the performance of presently accepted airborne coupler and autopilot systems with the KC-135, DC-7, and TF-102 aircraft.

An attempt was made to characterize the measured ILS course/path noise in terms of power spectral density as well as amplitude and to use such a characterization to accept or reject installations. Only weak correlations were found to exist between aircraft performance and the possible power spectral figures of merit.

A satisfactory course/path noise amplitude specification of 5 μa in the localizer and 20 μa in the glide path at low altitudes can be specified with the increased probability of rejection of some ILS facilities for approaches below the present 200 feet minimum.

The best technical solution of the acceptability criteria problem was found to be the application of the measured noise to a complete simulation of several models of airborne systems.

TABLE OF CONTENTS

LIST OF ILLUSTRATIONS

LIST OF ILLUSTRATIONS (Cont'd)

LIST OF TABLES

LIST OF TABLES (Cont'd)

LIST OF SYMBOLS

Symbol	Dimension	Definition
x	feet	distance between aircraft and transmitter
y, $\bar{y}$	feet	lateral offset of aircraft perpendicular to runway, average
Δh	feet	vertical offset of aircraft from ideal glide slope
θ, θ_c	deg	pitch attitude of aircraft, command
ϕ, ϕ_c	deg	roll attitude of aircraft, command
ψ	deg	relative heading of aircraft to runway
α	deg	angle of attack of aircraft
γ	deg	flight path angle of aircraft
δ_e	deg	elevator surface position
δ_a	deg	aileron surface position
V	ft/sec	trim airspeed of aircraft
I_{xx}	slug-ft^2	aircraft moment of inertia about roll axis
I_{yy}	slug-ft^2	aircraft moment of inertia about pitch axis
I_{zz}	slug-ft^2	aircraft moment of inertia about yaw axis
W	pounds	aircraft gross weight
c.g.	% MAC	center of gravity in % mean aerodynamic chord
ρ	slug-ft^3	atmospheric density
g	ft/sec^2	gravity constant
c	ft	aerodynamic chord length
b	ft	wing span
s	ft^2	wing area
C_ℓ	rad^{-1}	rolling moment coefficient ($C_{\ell_{\delta_a}}$ moment due to aileron deflection)
C_n	rad^{-1}	yawing moment coefficient ($C_{n_{\delta_a}}$ moment due to aileron deflection)
C_m	rad^{-1}	pitching moment coefficient (C_{m_α} moment due to angle of attack change)
C_y	rad^{-1}	side force coefficient (C_{y_r} force due to yaw rate)
C_L	rad^{-1}	lift coefficient (C_{L_α} change in lift due to change in α)
C_D	rad^{-1}	drag coefficient (C_{D_α} change in drag due to change in α)
p	deg/sec	approximately equal to roll rate ($\dot{\phi}$)
r	deg/sec	approximately equal to yaw rate ($\dot{\psi}$)
q	deg/sec	approximately equal to pitch rate ($\dot{\theta}$)

LIST OF SYMBOLS (Cont'd)

Symbol	Dimension	Definition
$\dot{\alpha}$	deg/sec	rate of change of angle of attack
β	deg	sideslip angle
$\theta_{g.s.\ trim}$	deg	trim pitch attitude of aircraft on glide slope
η	deg	glide path elevation angle
τ, T	second	time constant
$K_{D,I}$		gain parameter, displacement, integral
μa	microamperes	standard output of airborne receiver
MM		middle marker
OM		outer marker
Rwy		runway threshold
TD		touchdown point
ζ		damping factor
ω	rad/sec	natural frequency
R		desensitization ratio
m		mean value
m_N	μa	mean value of course/path noise
σ		standard deviation
σ_N	μa	standard deviation of course/path noise
σ_θ	deg	standard deviation of pitch attitude
σ_y	ft	standard deviation of lateral track error
$\sigma_{\Delta h}$	ft	standard deviation of vertical track error
σ_ϕ	deg	standard deviation of roll attitude
σ_{δ_a}	deg	standard deviation of aileron position
ξ		expected value ($\lvert m \rvert + \lvert \sigma \rvert$)
$\lvert\ \rvert$		absolute value
ξ_N	μa	expected value of course/path noise
ξ_y	ft	expected value of lateral track error
σ^2		variance
$\sigma_N{}^2$	μa^2	variance of course/path noise
$(\bar{\sigma}_N)^2$	μa^2	average variance of course/path noise
r		correlation coefficient
B	c.p.s.	bandwidth of course/path noise
n		number of degrees of statistical freedom

SUMMARY

This is the compilation of two final reports under Phase I and Phase IA of the work statement specified in Contract FAA/SRDS-451 as amended July 1962.

In Phase I of this project an attempt was made, using actual recordings of 25 major ILS facilities, to find correlation between test aircraft lateral dispersions and selected localizer course noise* power spectral parameters applied to such facilities. No significant correlation was found to exist. Only the RMS aileron and roll dispersions were found to be weakly correlated with course/path noise power. At best, these trends may provide a means of using course/path noise power spectra in a limited fashion as a secondary criterion for localizer course acceptance in addition to the present localizer course amplitude criteria. However, the correlation between aircraft performance and course noise power improved with the use of mean square values of roll and pitch attitude or lateral and vertical deviation in lieu of using instantaneous values of aircraft position.

Analysis of the glide path data revealed that the path noise is not statistically stationary in nature and that power spectral techniques consequently cannot be used.

Approach couplers which use a derived rate term to damp the track response are more susceptible to the adverse effects of course/path noise than those couplers which use attitude damping. Heading damped localizer couplers and attitude damped glide path couplers reduce the effects of course/path noise by almost three to one.

The TF-102 lateral responses to course/path noise were two to three times more severe than the KC-135 or DC-7 responses. This is due to the broader band airframe response as a result of the low moment of inertia about the roll axis and the higher approach speed of the TF-102.

*The term "noise" or "course/path noise" used in this report only relates to the irregularities in the ILS course/path structure due to terrain reflections.

The TF-102 pitch dispersions did not significantly differ from the other aircraft since the autopilot configuration masks the differences in the airframe responses.

The employment of a simple filter technique to accept ILS localizer and glide path performance did not result in sufficient correlation between the output responses of relatively simple filters and the complete ILS system simulation. This was due in part to the lower order approximation of the filter itself to the actual transfer functions, as well as to the non-Gaussian and nonstationary characteristics of the actual ILS course/path noise.

An arbitrary course/path noise variance technique to determine acceptability of ILS facilities did provide reasonable correlation between the roll, pitch, vertical and lateral deviations using a random noise generator and the actual course/path noise in the recordings. The discrepancies are due to the differences between the peculiar characteristics of the actual course/path noise, as noted above, and the characteristics of the almost purely random generator; as well as the fact that the actual noise variance does not change with range in the same manner as the generated noise was changed.

In order to minimize the possibility of accepting an unsatisfactory facility for low approach use, the results of the course/path noise variance program are as follows, based on the desire to restrict 95% of the aircraft deviations, due to this noise, in the region of the middle marker and the runway, to less than 2 degrees of roll and pitch attitude, lateral displacements to less than 15 feet and vertical displacements to less than 4 feet:

1) The localizer course noise due to terrain reflections in the region between the middle marker and the runway should not exceed 5 microamperes with 95% probability.* The course noise in the region of the outer marker can be 30 microamperes (95% probability level) without deteriorating performance at the lower altitudes. A linear relationship between the allowable

*See Section 3.2.3 for description of the test procedure to be used in verifying that an ILS facility is within the limits of the course/path noise criteria.

course noise level and the distance from the landing threshold is recommended.

2) The glide path noise, due to terrain irregularities, from the region of the middle marker to the runway should not exceed 20 microamperes with 95% probability. The noise in the region of the outer marker can be 30 microamperes (95% probability level) without deteriorating performance at the lower altitudes; with a linear relationship between the allowable path noise level and the distance from the landing threshold being recommended.

The foregoing recommendations represent an acceptable solution since they can be implemented relatively simply and immediately. This relatively easy solution also has a penalty in that in trying to prevent the possibility of falsely accepting an unsatisfactory facility some acceptable facilities may be rejected. This study has shown that the use of increasingly weighted or averaged noise characteristics can only increase the uncertainty between the predicted and actual performance.

The best technical solution, short of actually flying a series of aircraft and automatic systems that represent the types that will use the ILS facility, to determine whether the performance is acceptable, is to apply a recorded version of the ILS course/path noise corrected to account for the motion of the test aircraft to complete analog computer simulations of the various systems that will use the facility. This is the only technique that can result in one-to-one correspondence between predicted and actual performance.

1. INTRODUCTION

This document is a compilation of the final reports of Phase I and Phase IA of the ILS localizer course and glide path study program outlined in FAA/SRDS-451. The primary objective of the study was to determine a figure of merit for ILS course/path noise which provides a strong correlation with the acceptability of the approach process. In this report the term "beam noise" or course/path noise" only relates to the irregularities in the localizer course and glide path due to terrain reflections of the carrier and/or sideband energy of the transmitted signals. The vector sum of the direct and reflected course/path signal components results in a localizer or glide path reference line which is not straight but which consists of irregular granularities. As the aircraft, which is involved in the approach, moves through these regions of signal variations along the course line, the irregularities in the course/path structure cause the receiver output signal to fluctuate. The fluctuations, or course/path noise, observed in the aircraft therefore depend on the spacial distribution of the beam irregularities and the speed with which the aircraft traverses them. Automatic ILS coupler systems operate on the localizer and glide path receiver output signals to generate roll and pitch attitude commands to the respective autopilot channels to force the aircraft to fly to the indicated course/path null. Any noise in the indicated track error signals causes resulting dispersions in the actual position of the aircraft. An acceptable automatic ILS approach is one which satisfies prescribed performance criteria such as control column activity, aircraft attitude and displacement dispersions at various points along the track in response to this course/path noise.

The present figure of merit for localizer course and glide path acceptability is a maximum noise amplitude specification which does not involve approach performance criteria. This allowable amplitude, which is reasonably large, is an outgrowth of many past compromises in the selection of practical ILS subsystem component tolerances. These tolerances are adequate for the present use of the ILS to the 200 foot minimum. However, if lower minima and eventually final landings are to be accomplished with the aid of the ILS, tighter control of the beam characteristics and component tolerances should be provided. Since zero noise amplitudes cannot practically be specified, some reasonable value of a pertinent measure of noise must be used. This parameter may be a smaller value of maximum allowable amplitude based on standard deviations which provide acceptable tracking performance; or it may be, for example, a parameter which additionally specifies the course/path noise as a

function of frequency. The latter situation was assumed in Phase I of the contract work statement, which indicates that the bend power spectral density is a probable figure of merit. The Phase I analytical studies were designed to determine the extent to which the above parameters may be used as figures of merit. Section 2 of this report contains the results of the power spectral analyses of most of the localizer and glide slope data taken at 25 major airports in the U. S. that was furnished by the Federal Aviation Agency under Phase I. This FAA data was derived employing theodolite-controlled approaches wherein the aircraft tracking error was in the order of $\pm$ 2.5 feet, the data rate was approximately 1 reading per second; and the ILS course/path recorded with full scale recording deflections ($\pm$ 2 inches) of $\pm$ 30 microamperes, and a recording speed of 24 inches per minute. The recorder frequency response was approximately 25 cps. The visual tracking error was removed from the test recordings, so that the resultant tape recordings represented the actual ILS course structure with a reasonable degree of accuracy.

The effort in Phase IA included the following studies:

1. It determined the extent of the usefulness of a simple filter response technique in specifying ILS beam acceptance. This technique involved the use of relatively simple filters which simulated the response of the actual airborne systems. The trade-off between filter simplicity and correlation with the full scale analog computer responses was investigated.

2. It determined the extent of the usefulness of the noise variance program technique in specifying ILS course/path acceptance. This technique involved the use of suitably shaped random noise signals whose total power or variance was modified as a function of range to the ILS transmitters to simulate the effects of a course/path noise amplitude specification. Several variance programs were studied to determine the maximum allowable course/path noise which could be tolerated by the test systems for low approach operations.

The results of the stationarity and normality tests are presented in Section 2.1 along with the time histories of the course noise at each facility. The power spectra are presented in Section 2.2. Section 2.3 presents the closed loop simulated time responses of the KC-135, DC-7, and TF-102 aircraft under the actual course noise conditions. The time responses are shown for the two lateral control systems using heading and derived beam rate as track damping terms in the approach couplers. Section 2.4 presents the results of attempts at correlating the actual track responses with several possible course power noise figures of merit. The conclusions for the use of the power spectrum as a figure of merit for approach performance are given in Section 2.4. Section 2.5 contains the results of the glide path stationarity tests for some of the facilities. Section 2.6 contains some glide slope dispersion data for the KC-135, DC-7, and TF-102A aircraft. Section 3.1 discusses the results of the simple filter technique as applied to the three test aircraft. Section 3.2 contains the results of the course/path noise variance program technique.

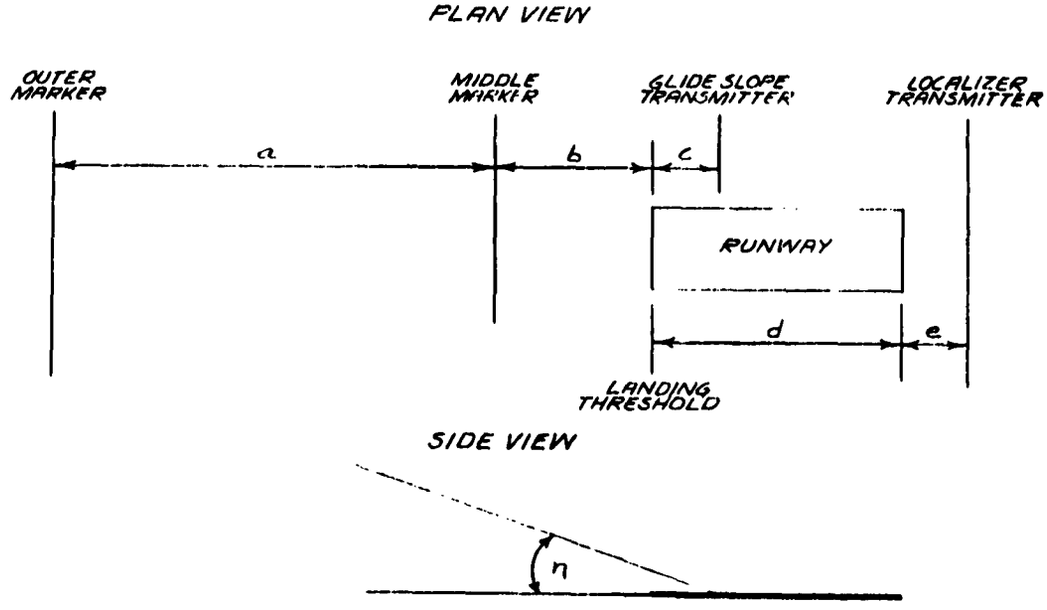

Figure 1 Airport Approach Geometry

2. PHASE I BEAM ACCEPTANCE STUDIES

2.1 LOCALIZER STATIONARITY AND PROBABILITY DISTRIBUTION TESTS

Figure 1 and Table I indicate the geometrical relationships between the localizer and glide path transmitters, the marker beacons, and the runway at each of the test facilities.

	a ft	b ft	c ft	d ft	e ft	η deg	Runway number
Atlantic City	22800	3275	1250	10000	990	2.59	13
Atlanta (Mun.)	20140	4700	1200	7500	600	2.89	9
Baltimore (Fr.)	19483	3749	(3)	10000	600	(6)	10
Birmingham	24100	3325	(3)	10000	650	(6)	5
Boston (Logan)	28764	1181	2502	10000	(5)	3.01	4R
Burbank (Lock.)	62000	10710	1251	6000	900 (2)	3.0	7
Chicago (O'Hare)	31680	3690	1102	7345	1600	3.0	14L
Cleveland (Hop.)	17430	3750	1136	6242	500	3.0	5L
Dallas (Love)	21595	3802	1000	7751	1150	2.84	13
Detroit (Metro.)	22289	3407	1200	10000	1050	(6)	3L
Duluth	22556	3794	1000	9000	2400	(6)	9
Ft. Worth (Meach.)	17632	3648	980	5200	1000	3.3	17
Houston (Int.)	21800	3430	1000	7600	800	2.65	3
Kansas City (Mun.)	29000	3900	1234	7000	(5)	3.01	18
Los Angeles (Int.)	31733	3326	1200	12000	1000	3.00	25L
Louisville (Stan.)	29100	3590	1170	7800	1000	3.0	1
Miami	19500	3650	1000	8400	700	2.50	9
Minneapolis (Wold-Cham.)	24800 (1) (1)	(4)	975	6500	1000	2.75	29L
New Orleans (Mois.)	20700	(4)	(3)	8325	(5)	2.72	10
New York (Idle.)	12355	3485	1200	8400	375	2.5	4R
Ontario (Int.)	34900	3170	740	8200	400	2.75	25
Reno	21500	13700	1216	7800	(5)	3.0	16
San Francisco (Int.)	30887	3483	1250	9500	250	2.7	28R
St. Louis (Lam.)	21300	3380	1200	7598	500	2.73	24
Washington, D.C. (Nat'l)	24700	3270	750	6700	180	2.76	36

NOTE: (1) Outer Marker to Runway
(2) Distance in front of Runway Threshold
(3) Assumed to be 1000 feet
(4) Assumed to be 3500 feet
(5) Assumed to be 700 feet
(6) Assumed to be 2.5 degrees

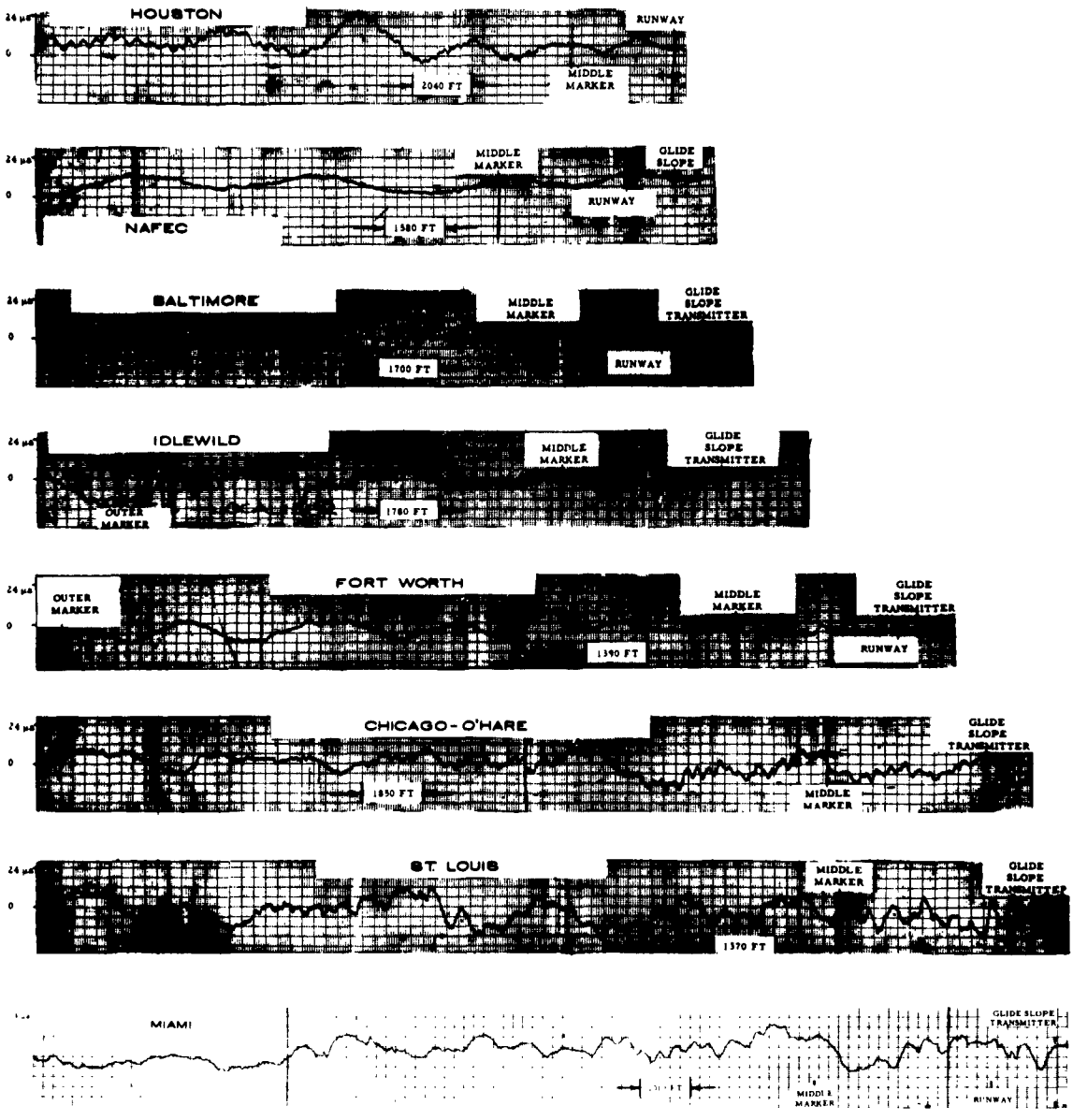

Figure 2 Theodolite Corrected Localizer Recordings

Theodolite Corrected Localizer Recordings

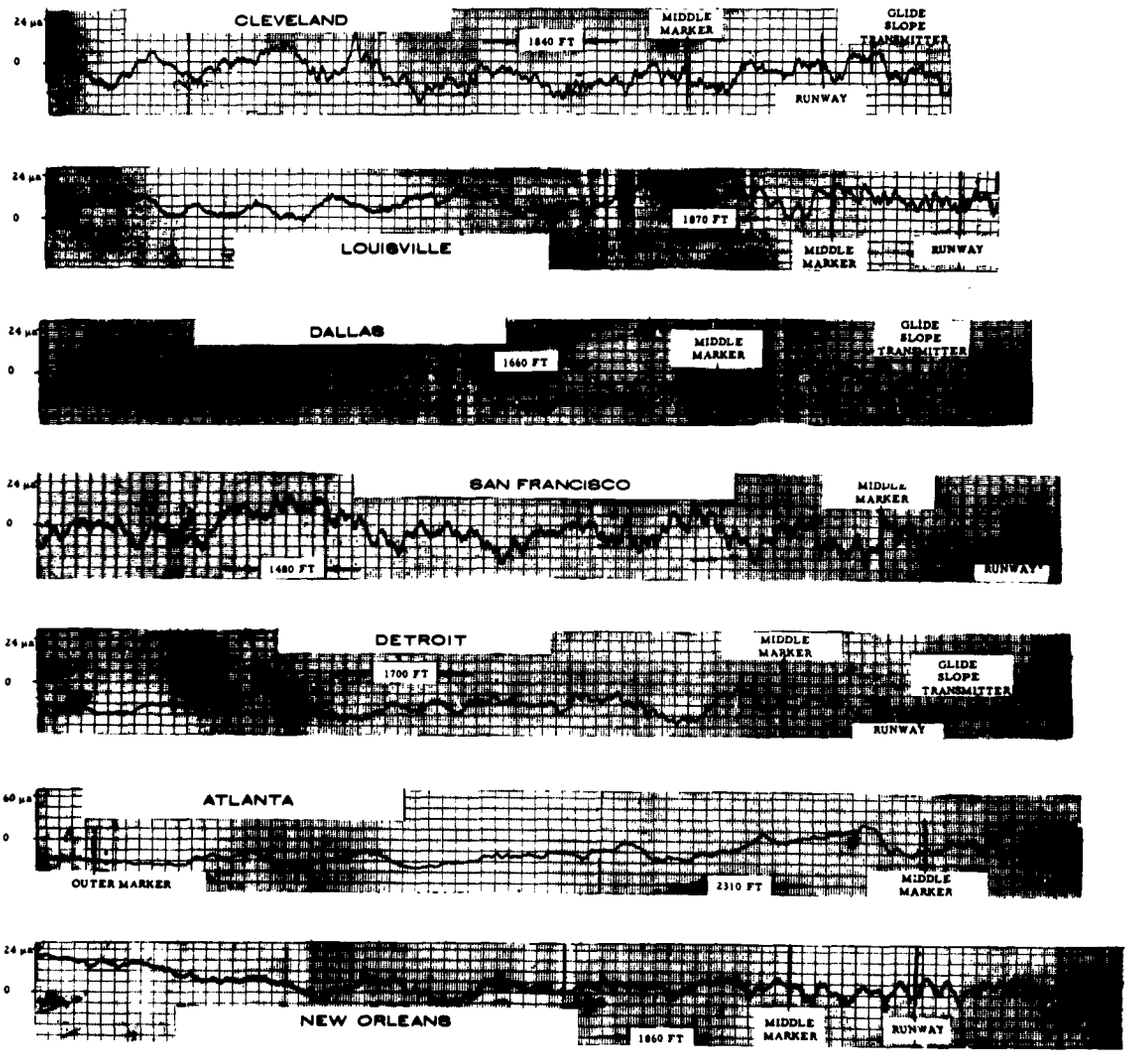

Theodolite Corrected Localizer Recordings

8 (cont'd)

Figure 2 shows the theodolite corrected course noise at each of the localizer facilities. It is this data that was tape recorded and processed to provide the statistical figures of merit. As indicated in Reference 1, knowledge of the stationarity and normality of the course/path noise is necessary prior to deriving the power spectra. As an example of the procedures outlined in that report, Table II indicates, in discrete fashion, the time history of the variance of the Miami Localizer. Although there are deviations from the average variance, they are not considered significant and the course noise at this facility is said to be at least weakly self-stationary. Table III indicates the results of the other localizer facilities.

TABLE II
STATIONARITY TEST USING BEAM NOISE VARIANCE
MIAMI LOCALIZER FACILITY

Record Time (Sec)	Subrecord Variance (σ^2) $(\mu a)^2$	Average Subrecord Variance $(\bar{\sigma})^2$ $(\mu a)^2$	Record Time (Sec)	Subrecord Variance (σ^2) $(\mu a)^2$	Average Subrecord Variance $(\bar{\sigma})^2$ $(\mu a)^2$	Record Time (Sec)	Subrecord Variance (σ^2) $(\mu a)^2$	Average Subrecord Variance $(\bar{\sigma})^2$ $(\mu a)^2$
0-5	36		70-75	0		130-135	27	
5-10	36	36	75-80	9	11.24	135-140	31.45	23.67
10-15	36		80-85	18		140-145	13.5	
15-20	12.6		85-90	18		145-150	22.5	
20-25	12.6	15.3	90-95	9		150-155	0	
25-30	10.8		95-100	0	2.25	155-160	0	7.875
30-35	25.2		100-105	0		160-165	9.0	
35-40	21.2		105-110	0		165-170	22.5	
40-45	7.2	18.45	110-115	0		170-175	13.5	
45-50	9.0		115-120	22.5	27	175-180	18.0	7.875
50-55	36		120-125	67.5		180-185	0	
55-60	28.8		125-130	18		185-190	0	
60-65	18.0	27.6						
65-70	36							

$$\bar{\sigma}^2 = \frac{L\sigma^2}{10} = \frac{19.7}{10} = 1.97$$

Subset	Time Interval T_i (sec)	Bandwidth (Assumed) B(cps)	Degrees of Freedom $\eta = 2BT_i$	$\bar{\sigma}^2$ $(\mu a)^2$	S^2 Min $(\mu a)^2$	S^2 Max $(\mu a)^2$	$\bar{\sigma}^2$ $(\mu a)^2$	
1	15	1	30	17.73	9.79	28.58	36	
2	20	1	40	17.73	10.764	26.46	15.3	
3	20	1	40	17.73	10.764	26.46	18.45	
4	15	1	30	17.73	9.79	28.58	27.6	
5	20	1	40	17.73	10.764	26.46	11.24	
6	20	1	40	17.73	10.764	26.46	2.25	
7	20	1	40	17.73	10.764	26.46	27.0	
8	20	1	40	17.73	10.764	26.46	23.62	Middle Marker Runway Region
9	20	1	40	17.73	10.764	26.46	7.91	
10	20	1	40	17.73	10.764	26.46	7.91	

A "good" facility is one for which none of the subrecord variances significantly exceeded the range of values prescribed by the Chi-square test. A "fair" facility is one for which no more than two of the ten subrecord variances significantly exceed the prescribed values. A "poor" facility is one for which more than two of the ten subrecord variances significantly exceeded the prescribed values. The results indicate that only the St. Louis facility can be considered poorly self-stationary. The only significance of this statement is that a single power spectrum for this facility would not be as useful a possible figure of merit as it would for the spectra of facilities which are at least weakly self-stationary. It does not indicate the quality of the course noise as it relates to aircraft performance.

TABLE III
RESULTS OF STATIONARITY TESTS

Facility	Qualitative Result
Duluth	Good
Detroit	"
Baltimore	"
Fort Worth	"
San Francisco	"
Ontario	"
New York	"
Dallas	"
Miami	Fair
Birmingham	"
Chicago	"
Atlantic City	"
St. Louis	Poor

Figure 3 indicates the result of the normality tests with the course noise of the Miami Localizer facility; and Table IV is a tabulation of the mean and standard deviations for this and the other facilities. The results of these tests for a majority of the localizer facilities indicate that the course noise is reasonably Gaussian in character, at least within one or two standard deviations. These results imply that those facilities which were weakly self-stationary are probably also strongly self-stationary and that a single power spectrum can be derived in most cases.

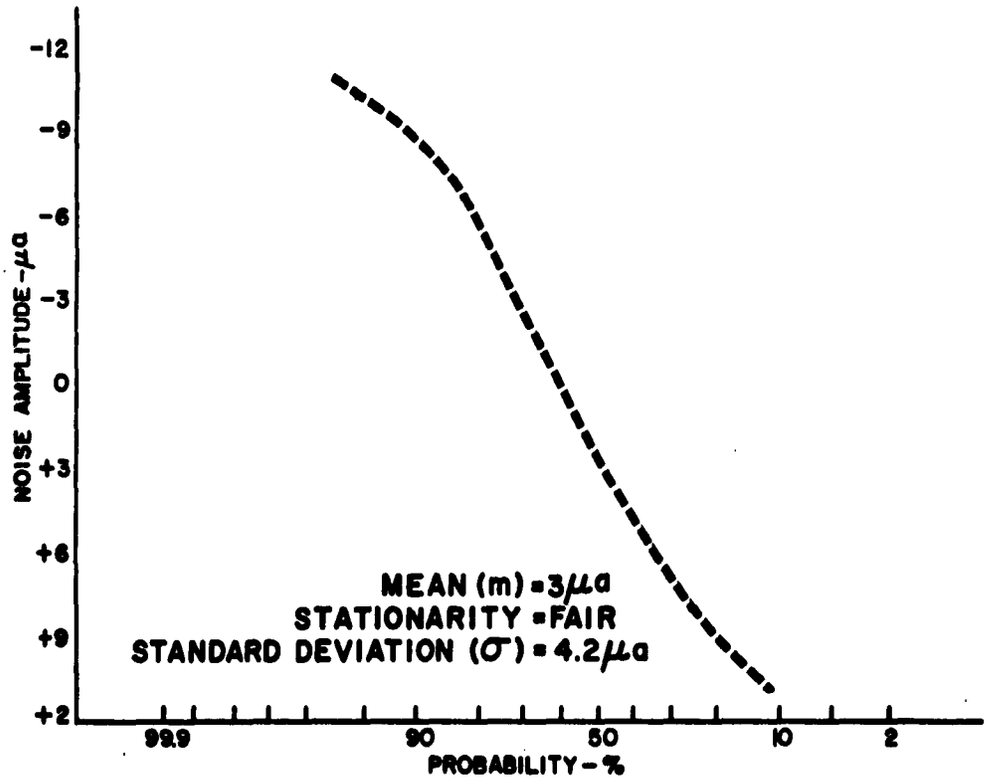

Figure 3 - Miami Localizer - Noise Amplitude Probability Distribution

2.2 LOCALIZER POWER SPECTRAL TESTS

Figure 4 indicates the results of the power spectral tests for a majority of the localizer facilities. A general trend of increasing power with decreasing frequency is quite evident. Table IV also includes a compilation of the average power in each of three spectral bands as well as the total course noise power, the mean power, the average power at the middle marker and the average power between the outer and middle markers. The starred facilities had directional localizers at the time the flight recordings were made. The NAFEC and Duluth facilities have very low noise power in the measured spectral bands. The total random noise power at the NAFEC facility is not significantly lower than the other facilities however, and this indicates that considerable power is located in the very low frequency band of the power spectrum which could not be measured directly. A glance at the time history for this facility, in Figure 2, indicates that this is true. Unfortunately, as noted in Reference 7, power measurements at these very low frequencies are unreliable due to the tape splicing effect and bias errors. As noted in Table IV the mean course noise power level at some localizer facilities is quite high. It cannot be determined whether this mean deviation is due to a theodolite offset or is actually due to a misalignment of the beam structure. The effect of the mean course deviations was subtracted from the results of the aircraft response tests since any misalignments can be accounted for in the ILS commissioning process.

TABLE IV
LOCALIZER BEAM NOISE POWER

Facility	$(\bar{v}_N)^2$ avg ran pwr MM-Rwy μa^2	$(\bar{v}_N)^2$ total pwr MM-Rwy μa^2	avg. ran pwr MM-OM μa^2	total pwr 95% Prob noise level MM-Rwy (est)	mean	mean pwr μa^2	tot ran pwr μa^2	tot avg pwr low freq μa^2	tot avg pwr mod freq μa^2	tot avg pwr hi freq μa^2
Fort Worth*	33	90	8.2	4.5	.20	26	24	.041	.015	
Detroit	11	96	4.7	13.2	170	32	105	.033	.019	
Baltimore	11	19	4.7	6	4	22		.15	.023	
San Francisco	33	90	8.2	3.6	12	62	.23	.23	.06	
Atlantic City*	9	20	4.2	3.9	15	36	.027	011	.007*	
Duluth*	3.6	1.8	2.2	8	64	3.6	.21	.02	.01	
Miami	7	13	3.8	5	9	17	46	.17	.04	
Chicago	32	41	7.9	73	5	34	.12	.05	025	
Dallas	34	27	8.3	4.7	22	29	.113	.055	.022	
Idlewild	16	27	5	3.4	2	22	.16	.041	.03	
St. Louis	16	51	5	2.1	1	48	35	12	.024	
Ontario	50	40	10	3.1	10	81				
Birmingham	55	27	10.5	3.6	12	43	.4	.13	.05	
Los Angeles	40		9	9						
Minneapolis	16		5	6						
Houston	16		5	6						
Washington, D C	41		9.1	7						
Cleveland	32		8	6						
Louisville	29		7	8						
New Orleans	20		6	2.5						
Burbank	210		20	10						
Atlanta	140		15	15						

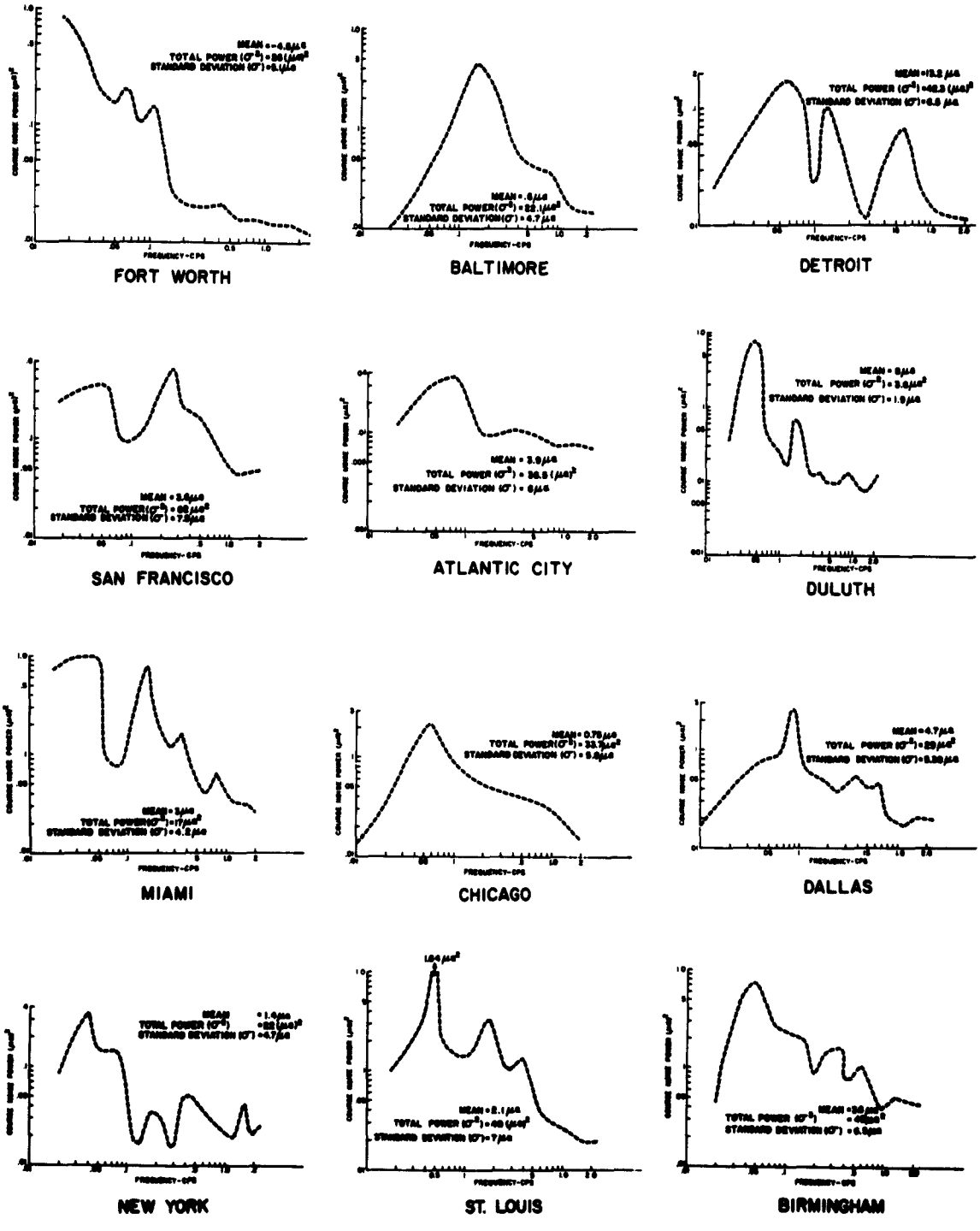

Figure 4 **Power Spectrum - Localizer Facility**

2.3 LOCALIZER TIME RESPONSE TESTS

Figures 5 and 6 are block diagrams of the lateral approach coupler systems that were simulated on the analog computer. The significant difference between the two systems is the use of a relative heading signal as a track damping term in Figure 5 in lieu of the derived beam rate signal in Figure 6.

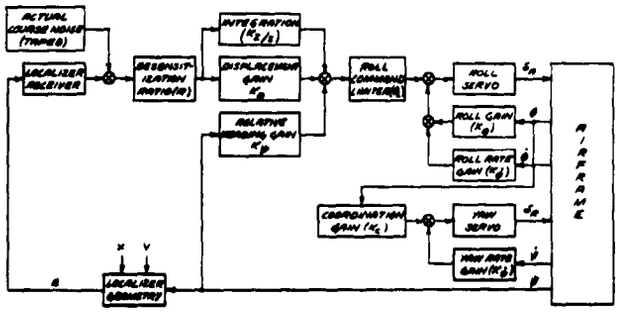

Figure 5 Heading Damped Coupler

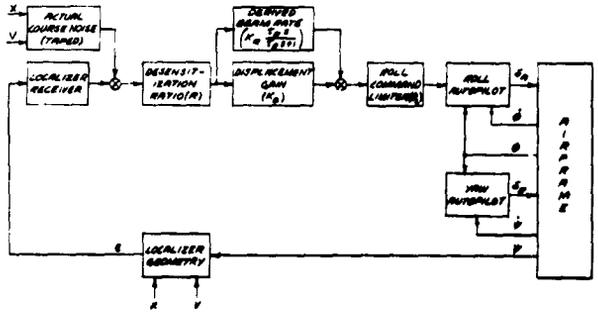

Figure 6 Beam Damped Coupler

The heading damped system requires a beam error integration signal to provide tight control under crosswind conditions. The rate filter constants K_R and τ_R were chosen on the basis of track stability and are consistent with the lowest first order lag break frequency which provides reasonable course noise rejection. Figures 7 and 8 show the simulated time responses of the KC-135 autopilot/aircraft with each coupler system with no course noise. The rate damped system track response is somewhat faster than the heading damped system due to the airplane's natural weathercocking capability. This would lead one to suspect that the track deviations under noise conditions might be smaller with the rate damped system at the expense of increased roll and stick activity due to the derived rate signal. This point is illustrated by comparing the response of each KC-135 coupler at the NAFEC facility in Figures 9 and 10. This facility has a 117 foot waveguide localizer so that the control activity with either coupler, is relatively low. However, the rate system generates two to three times more activity than the heading system. It is also worthwhile to note the difference between the actual course noise and the indicated course error in Figure 9. The aircraft track deviation (y) from the ideal center due to course noise is not much less than the deviations in Figure 10 with the heading system. The result is that although the rate system offers improved tracking responses on beams, the responses are significantly degraded when the ILS signal contains course noise.

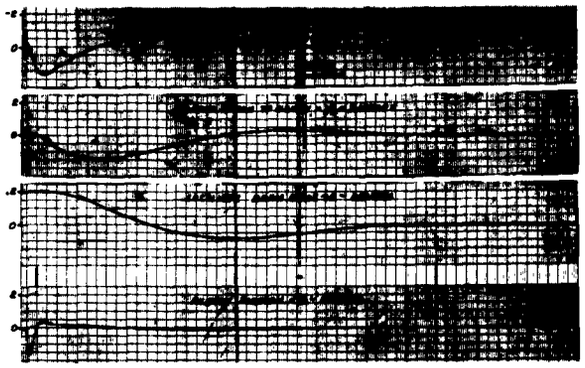

Figure 7
KC-135A Track Response
Heading Damped Coupler
No Noise

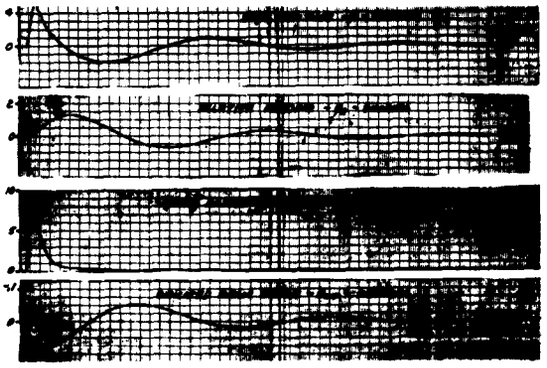

Figure 8
KC-135A Track Response
Rate Damped Coupler
No Noise

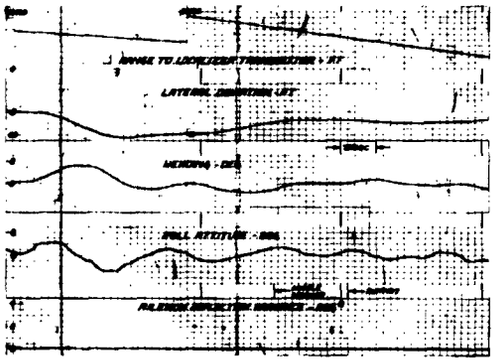

Figure 9
KC-135A Track Response
Heading Coupler
NAFEC Localizer

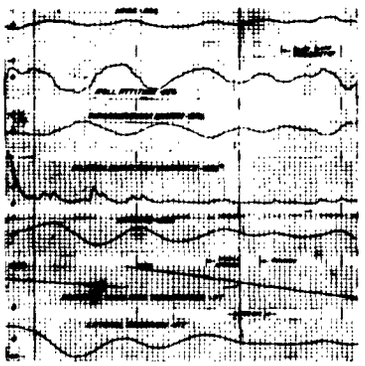

Figure 10
KC-135A Track Response
Rate Coupler
NAFEC Localizer

Tables V and VI indicate the aircraft responses to the noise at each facility at the middle marker, the runway, and the touchdown region for each type of approach coupler. Figures 11 and 12 are time histories at the Miami Localizer facility with the KC-135A aircraft with each coupler system.

TABLE V
DISPERSION DATA
HEADING SYSTEM KC-135

Facility	Middle Marker Region					Runway Threshold						Touchdown Region	
	y Ft	ε Deg	φ Deg	σ_ϕ Deg	σ_{δ_a} Deg	y Ft	ε Deg	φ Deg	σ_ϕ Deg	σ_{δ_a} Deg	$\xi_{y_{rms}}$ rwy	ξ_y rwy TD	σ_ϕ TD
Fort Worth	9	0	0.2	0	0	10	+0.1	0	0	0	5	10	.2
Detroit	15	+0.5	0	0.3	0.6	10	0	0	0	0	10	10	0
Baltimore	9	0	0	0.5	0.2	0	0	0.7	0.2	0.1	5	0	0
San Francisco	30	+0.4	0.7	0.5	1	20	+0.2	1	0.5	1.4	20	15	-
NAFEC	4	+0.5	0.75	0.5	0.1	8	0	0.5	0.1	0.1	6	8	3
Duluth	8	0	0	0	0	10	+0.1	0	0	0	8	5	.2
Miami	57	-0.5	0	0.75	0.5	34	+0.5	0.5	0.75	0.5	30	20	-
Chicago	25	+0.7	0.5	0.7	0.2	15	0	0.2	0	0.1	20	18	.45
Los Angeles	15	+0.5	1.8	0.42	0.45	7	+0.2	0.75	0.7	0.8	12	10	.9
Dallas	65	+0.5	2	0.9	0.7	20	+1	0.8	0.5	0.9	30	10	.6
Idlewild	6	+0.1	0.2	0	0	6	-0.1	0.3	0	0	4.3	4.3	0
Minneapolis	15	+0.5	0	0.7	0.5	5	+0.25	0.5	0.3	0.2	10	5	.5
Houston	30	0	0.8	0.8	0.2	15	+0.5	0	0	0.1	15	-	-
Washington, D.C.	5	+0.5	1	0.6	0.7	0	+0.4	1.2	0.7	1	6	15	.5
St. Louis	30	+0.5	0.8	0.7	0.5	15	0	0	0.7	1	15	10	0
Cleveland	40	+0.3	0.2	0.45	0.5	20	+0.8	0.2	0	0.3	30	15	.8
Ontario	20	0.1	2	1.25	0.3	30	+0.3	0.5	0.4	0.5	25	30	0
Louisville	6	+0.6	0.4	0.5	0.5	7	+0.5	0.3	0	0.5	7	-	-
New Orleans	60	+0.7	0.5	0.3	0.3	32	+0.3	0.2	0	0.4	45	28	0
Birmingham	45	-0.3	0.5	0.4	0.4	45	+0.7	0	0.5	0.7	49	30	.5
Burbank	90	-2.5	4	1.4	0.85	12	-2.0	4	3	1.4	36	-	-
Atlanta	32	-0.5	3.5	2.8	1.2	6	+1.5	1	0.5	1	20	-	-

Note: +ε - closing to runway centerline
-ε - departing runway centerline

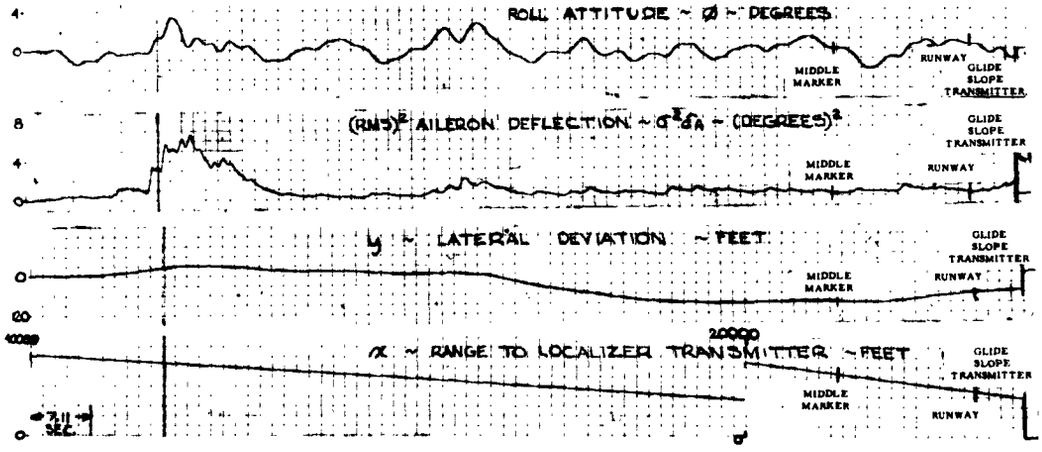

Figure 11 KC-135A - Heading Coupler - Miami Localizer

This facility was chosen as being representative of nondirectional localizers. The advantage of the NAFEC installation is apparent when comparing Figures 9 and 10 with 11 and 12 since the attitude and track deviations are significantly improved with the lower noise content of the directional localizer.

TABLE VI
DISPERSION DATA
RATE SYSTEM KC-135

Facility	Middle Marker Region					Runway Threshold Region						Touchdown Region	
	Y ft	$\dot{\psi}$ deg	ϕ deg	σ_ϕ deg	σ_{δ_a} deg	Y ft	$\dot{\psi}$ deg	ϕ deg	σ_ϕ deg	σ_{δ_a} deg	ξ_y mm rwy ft	ξ_y rwy TD ft	σ_ϕ TD deg
Fort Worth	15	-0.8	2.5	1.4	1	19	0	0.5	0.5	1.3	12	10	0
Detroit	15	+1.5	1	2.4	2.7	30	-0.8	1	1.4	1.6	15	15	1.5
Baltimore	0	-1.2	0	1.4	2	20	+1	2	2.4	1.6	15	6	.9
San Francisco	6	-1.3	1.2	2.2	4.9	21	+1.8	2.8	2.7	7.1	15	10	-
NAFEC	20	0.8	1.5	1.7	0.5	0	0	0.4	0.6	0.3	13	13	.5
Duluth	15	0.2	0	0	0.7	8	0	0.3	0	0.7	7	9	1.3
Miami	23	-2.3	2	2.2	3	7	-1	1	2.1	3	10	10	0.5
Chicago	27	-1.5	4	2.4	1.9	21	0	1	1.4	1.3	22	22	3.5
Los Angeles	4	0	3.2	2.5	2.6	6	0	1.2	2.5	2.8	6	6	2.6
Dallas	35	+0.3	6.5	4.4	3.1	10	+0.1	0	4	5	25	5	1.2
Idlewild	3	+0.3	2	2	1.3	3	-0.2	0	0.5	1.2	3	4	.4
Minneapolis	6	+0.4	0.6	0.9	1.3	14	+0.6	1.6	1.7	0.8	10	15	1.4
Houston	0	0	0	1.4	0.5	5	0	.5	.5	0	5	-	-
Washington, D.C.	45	+1.3	1.8	0.8	2.6	18	+0.2	2	3.2	4.5	20	15	3.7
St. Louis	7.5	+0.25	2	5	3	15	-1.2	1	2	7	15	20	-
Cleveland	15	+1.4	0.5	1.4	2.9	7	+1	0.5	1	1.9	7	12	2.5
Ontario	23	+1.3	3.8	4	1.3	10	-0.3	0.8	1.3	2.4	16	11	1.8
Louisville	30	-1.75	6	3.5	4.5	24	+1.5	0	1.8	3.1	40	-	-
New Orleans	20	+1.2	2	1.2	2.1	30	.5	3	1.4	2.6	15	-	1.3
Birmingham	33	-0.4	2	1.7	2.2	3	+1.8	2	1.4	3.3	33	8	1.1
Burbank	120	+1.3	5	11m	1	24	-0.7	5	4.5	2	35	-	-
Atlanta	110	+1	5	4.4	1.5	3	+2.4	2	1.4	4	70	-	-

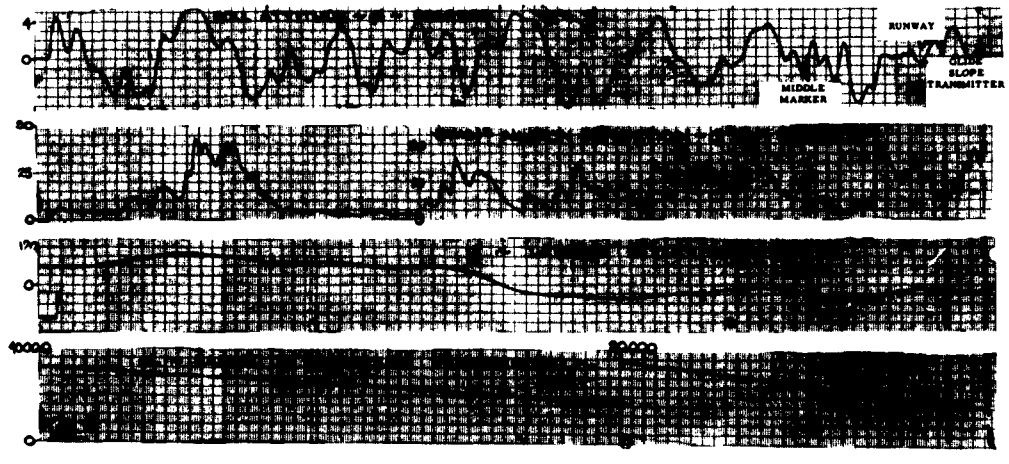

Figure 12 KC-135A Track Response - Rate Coupler Miami Localizer

The localizer course noise at some of the facilities was also applied with each coupler system to the TF-102A and DC-7C aircraft. Table VII contains the dispersion data for the TF-102 and Table VIII contains the data for the DC-7C. Comparing these results with those shown in Tables V and VI for the KC-135A indicates that they are in reasonable agreement.

TABLE VII
TF-102A AIRCRAFT LOCALIZER
DISPERSIONS AT MIDDLE MARKER AND RUNWAY

HEADING DAMPED SYSTEM

Facility	Middle Marker Y	ψ_{deg}	ϕ_{deg}	$\sigma_{\phi deg}$	Runway Threshold Y	ψ_{deg}	ϕ_{deg}	$\sigma_{\phi deg}$	ξ_y mm - rwy ft	Touch-down ξ_y rwy - TD ft	σ_ϕ TD deg	Remarks
Nafec	5	±.25	1	.6	5	-.1	.6	.3	8	5	.3	
St. Louis	22	+.4	.8		11	0	1	.9	15	10	.5	
Burbank*	50	-.4	5		8	+.1	-	-	30	-	-	
San Francisco	2	+.2	1.2		8	-	0	1.6	5	-	-	
Dallas	40	+.3	.9		5	-	1.2	1.2	25	10	1.1	
BEAM RATE DAMPED SYSTEM												
Nafec	15	+1.2	3.8	3.5	0	-.2	2.6	2.5	10	5	2.4	
St. Louis	0	+1	3	5.8	12	+1	0	3	10	18	5.5	
Burbank*	150	+.75	10	10	24	-	-	-	45	-	-	roll limiting inside rnm
Dallas	15	-1	7	7	16	-1	3	5	15	10	3.7	

*See Table VIIInote

TABLE VIII
DC-7 AIRCRAFT LOCALIZER
DISPERSIONS AT MIDDLE MARKER AND RUNWAY

HEADING DAMPED COUPLER

Facility	Middle Marker Y	ψ_{deg}	$\sigma_{\phi deg}$	$\sigma_{\delta deg}$	Runway Threshold Y	ψ_{deg}	$\sigma_{\phi deg}$	$\sigma_{\delta deg}$	ξ_y mm rwy ft	Touch-down ξ_y rwy TD ft	σ_ϕ rwy TD deg
Nafec	28	-.25	.5	.2	10	+.25	.2	.3	15	8	.45
St. Louis	21	+.8	.55	.82	15	-.1	.42	1	5	18	.45
Burbank*	60	-1.6	2.2	2	12	+.6	.52	.42	40	-	-
San Francisco	6	+.2	.62	.86	15	0	.7	1.5	10	-	-
Dallas	40	+.5	.91	1	2	+.8	.55	1.1	30	4	.6
BEAM RATE DAMPED COUPLER											
Nafec	30	+1	2.2	1	15	-.4	1.6	1.4	15	10	.7
St. Louis	30	-.4	2.5	3.5	22	-.6	1.0	5	27	20	-
Burbank*	120	-3.5	4	4	12	-1	3.1	4	50	-	-
San Francisco	25	+.7	1.4	4.4	10	+1	2.2	7	10	-	-
Dallas	15	0	3.0	2	25	0	1.5	1.5	10	15	1

*Burbank localiser transmitter is 900 feet in front of the approach end of the ILS runway. The runway parameters for this facility were actually taken 700 feet in front of the transmitter.

The conclusions in Section 2.4 therefore also pertain to these aircraft.

The 95% probability levels of course noise in the middle marker runway region are listed in Table IV for each facility. They indicate that the test facilities have 95% noise amplitudes between 3 and 20 μa. However only nine of the selected facilities would pass a 5 μa 95% noise amplitude specification while 19 facilities would pass a 10 μa specification. It should be noted that all the facilities pass the present 15 μa specification in this region of the approach, except Burbank.

The airborne system configurations for these aircraft are identical to those used with the KC-135A aircraft. Different gain parameters are used however to provide adequate body axis and track stability.

TABLE IX
LATERAL CONTROL SYSTEM PARAMETERS

	KC-135A	DC-7C	TF-102A
Autopilot			
ail and rud servo natural freq - ω_n (rad/sec)	10	10	10
ail and rud servo damping - ξ	.7	.7	first order lag
roll att rate gain - K_ϕ (deg aileron/deg roll rate)	1.1	1.1	5
roll att gain - K_ϕ (deg aileron/deg roll)	2.1	2.1	1.75
yaw rate gain - K'_ϕ (deg rudder/deg yaw rate)	9.5	9.5	2.5
coordination gain - K_{c_ϕ} (deg rudder/deg roll)	1.59	1.9	.25
roll att limit - ϕ_c (deg roll)	10	10	6
Heading Coupler			
displacement gain K_D (deg roll/deg beam error)	14.3	14.3	23
integral gain - K_I (deg roll/sec / deg beam error)	.143	.143	.48
heading gain - K_ϕ (deg roll/deg hdg error)	.95	.95	2
desensitization ratio - R	3:1	3:1	3:1
Rate Coupler			
displacement gain - K_D (deg roll/deg beam error)	7.5	15	15.5
rate gain - K_R (deg roll/deg/sec beam error)	190	190	310
rate time constant - τ_R (seconds)	2.5	2.5	2.2
desensitization ratio	3:1	3:1	3:1
receiver lag - τ (seconds)	.5	.5	.5

Table IX provides a listing of the pertinent automatic control system parameters that were used with each aircraft-coupler combination.

Table X presents a compilation of the lateral aerodynamic parameters used in the study.

TABLE X
LATERAL AERODYNAMIC PARAMETERS

		KC-135A	DC-7C	TF-102A
Airspeed (ft/sec)		210	202	290
I_{xx}	slug-ft^2	2.611×10^6	1.32×10^6	$.0192 \times 10^6$
I_{zz}	slug-ft^2	4.59×10^6	1.57×10^6	$.144 \times 10^6$
I_{xz}	slug-ft^2	0	0	$-.0254 \times 10^6$
W	pounds	160,000	100,000	23,400
$C_{l_{\delta_a}}$	rad^{-1}	-.004	-.086	-.854
$C_{l_{\delta_R}}$	rad^{-1}	+.00025	+.0163	+.0224
C_{l_p}	rad^{-1}	-.385	-.531	-.216
C_{l_r}	rad^{-1}	+.33	+.358	+.252
C_{l_β}	rad^{-1}	-.215	-.0774	-.120
$C_{n_{\delta R}}$	rad^{-1}	-.0017	-.1604	-.0401
$C_{n_{\delta_a}}$	rad^{-1}	-.00016	-.0152	+.0344
C_{n_r}	rad^{-1}	-.17	-.1604	-.291
C_{n_p}	rad^{-1}	-.18	-.118	-.0912
C_{n_β}	rad^{-1}	+.1346	+.1346	+.12
C_{y_β}	rad^{-1}	-.687	-.676	-.561
C_{y_r}	rad^{-1}	+.41	0	+.831

2.4 CORRELATION OF LOCALIZER TIME RESPONSES AND NOISE POWER DATA

Figures 13 through 21 are attempts at correlating the output time responses in Tables V and VI at the various facilities with the respective course/path noise power parameters in Table IV. Figures 13, 14, and 15 are graphs of lateral deviation, RMS roll attitude and RMS aileron deflection at the middle marker and the runway of a majority of the localizer facilities with respect to the average power in the course noise spectral bands.

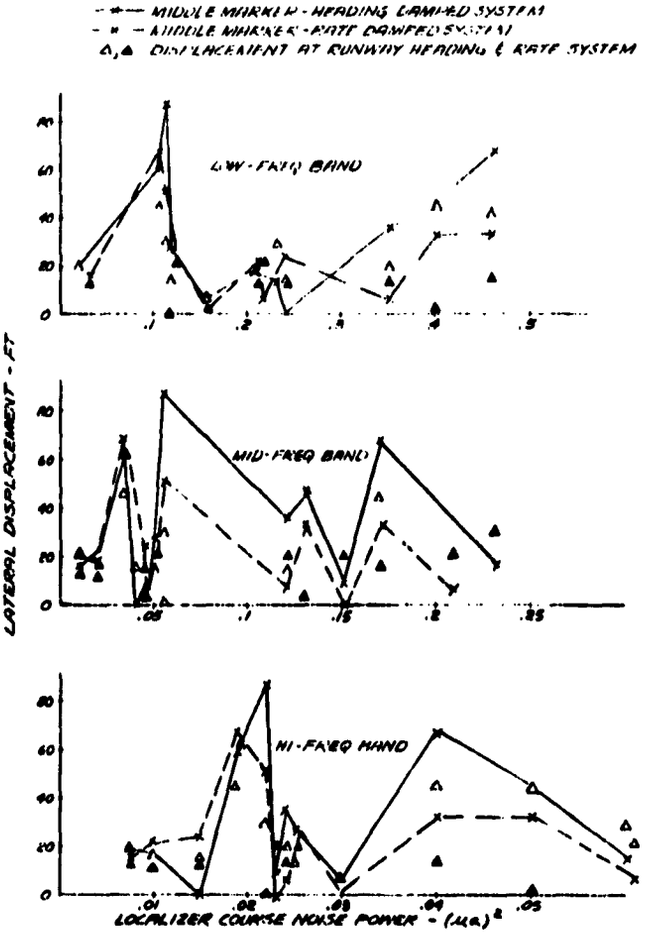

Figure 13 Lateral Dispersions vs Average Noise Power in Spectral Bands

The low frequency band is defined from .02 to .1 cps, the mid-frequency band from .1 to .6 cps, and the high frequency band from .6 to 2 cps. The rate damped system does provide somewhat smaller lateral dispersions than the heading system but the roll and aileron activity is nearly four times the same dispersions for the heading system.

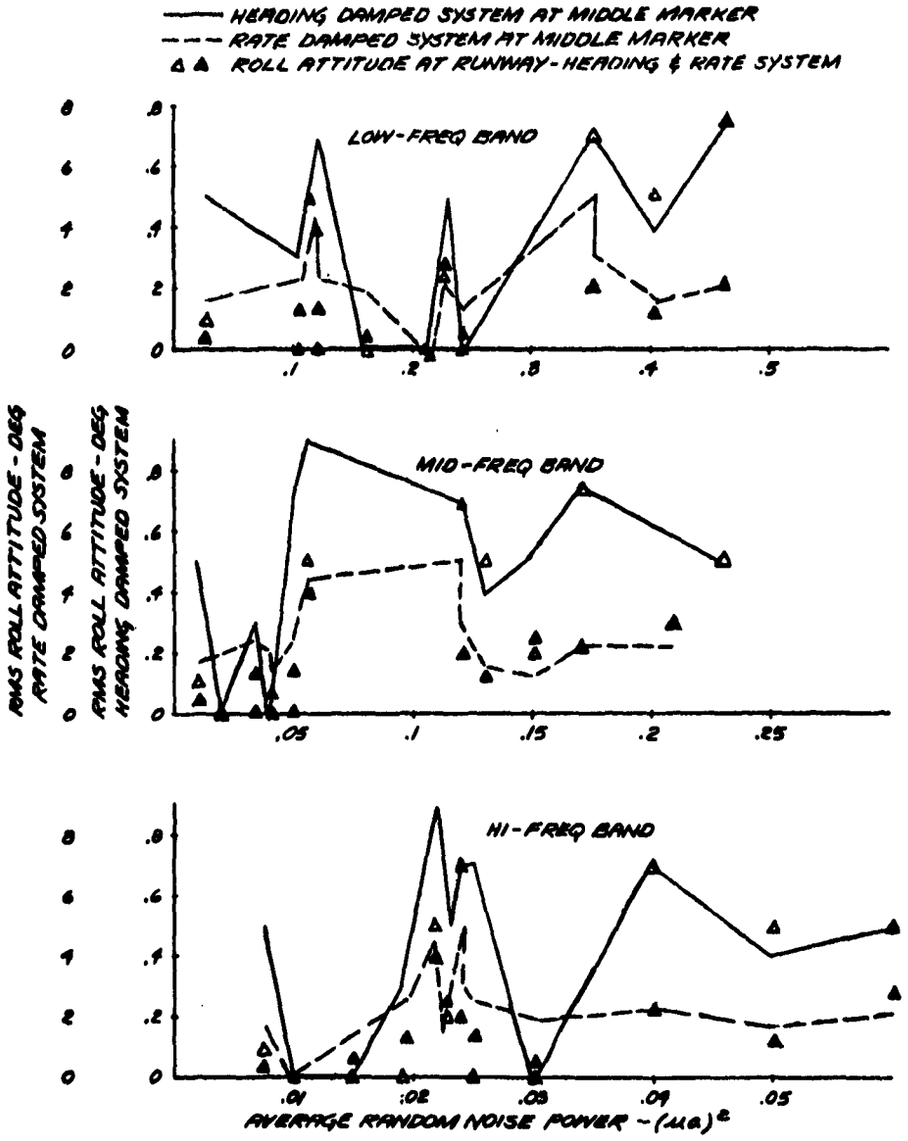

Figure 14 RMS Roll Attitude Dispersions vs Average Noise Power in the Spectral Bands

There are weak trends toward increasing aileron and roll activity with average spectral course noise power in the mid and high frequencies. However, there does not appear to be any significant trend of this kind for lateral dispersion at any frequency. This is due in part to the inherent problem of attempting to correlate an instantaneous output parameter with an average lumped course noise parameter such as power.

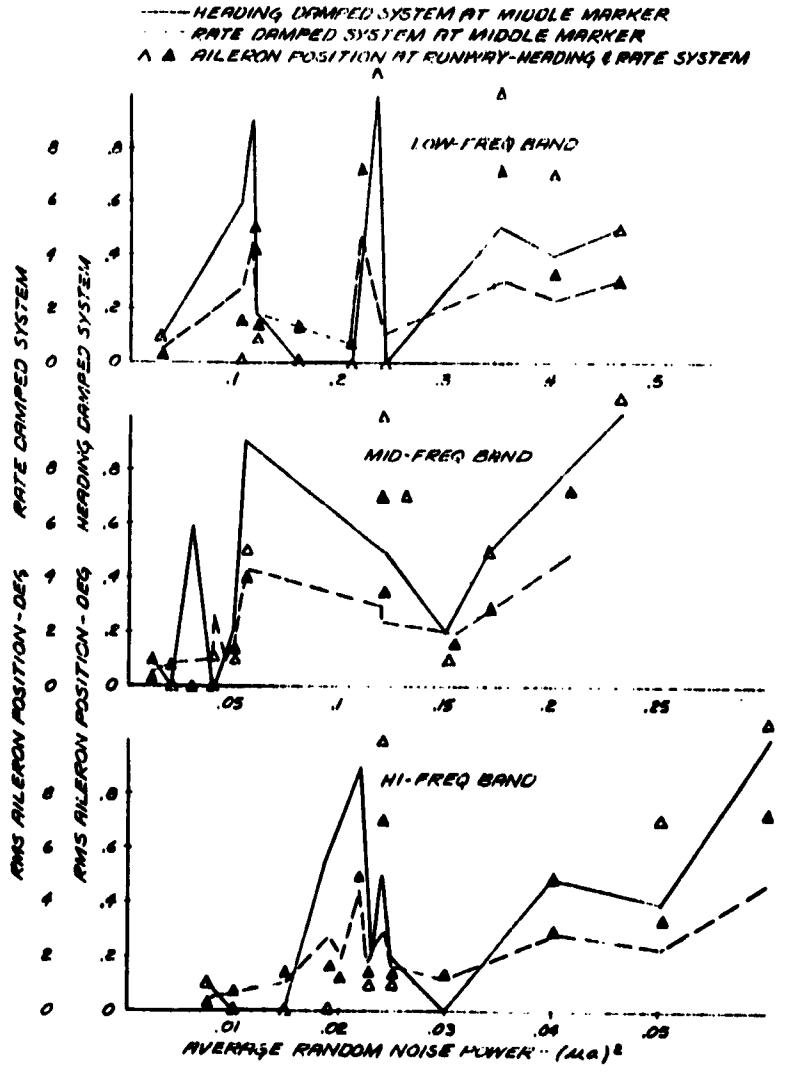

Figure 15 RMS Aileron Position Dispersion vs Average Noise Power in Spectral Bands

Figure 16 shows the relationship of the three output functions with the total random course noise power as denoted by the average variance of the course noise measured during the normality tests for each facility. Here again there are only weak trends toward increasing roll and surface activity with increasing total course noise power.

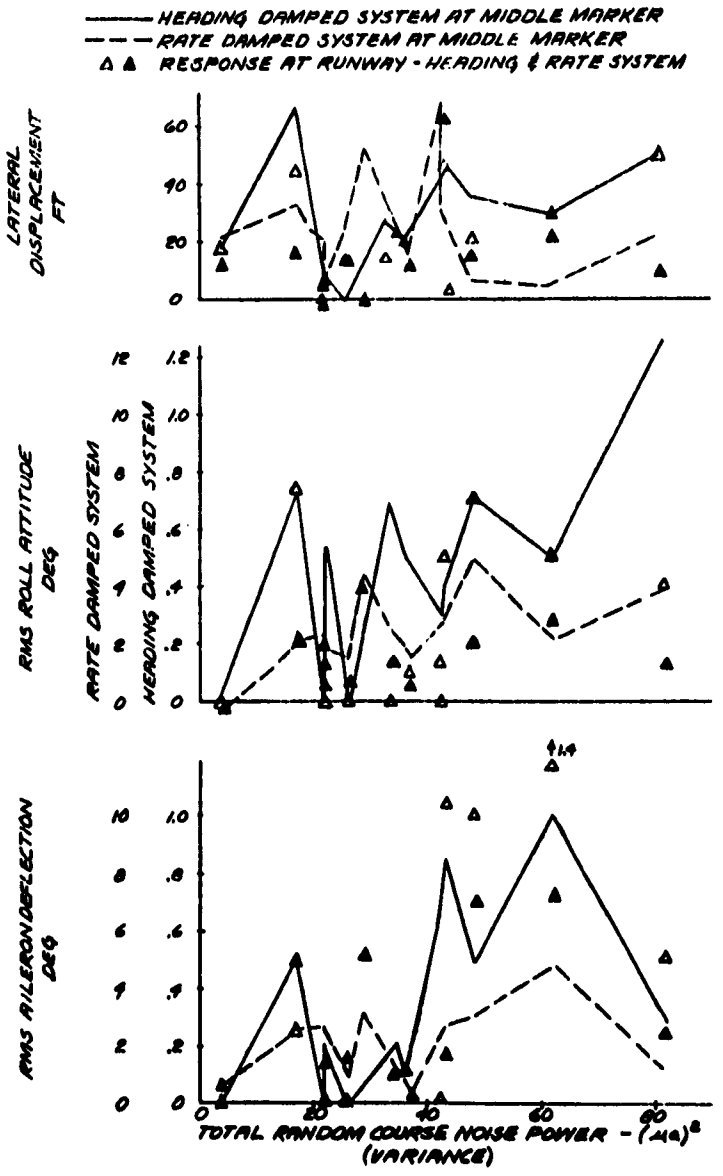

Figure 16 Aircraft Dispersion vs Random Noise Power

Figure 17 shows the relationships of the output parameters to the mean value of the localizer course noise. As expected, only the lateral deviation is reasonably correlated with this noise parameter.

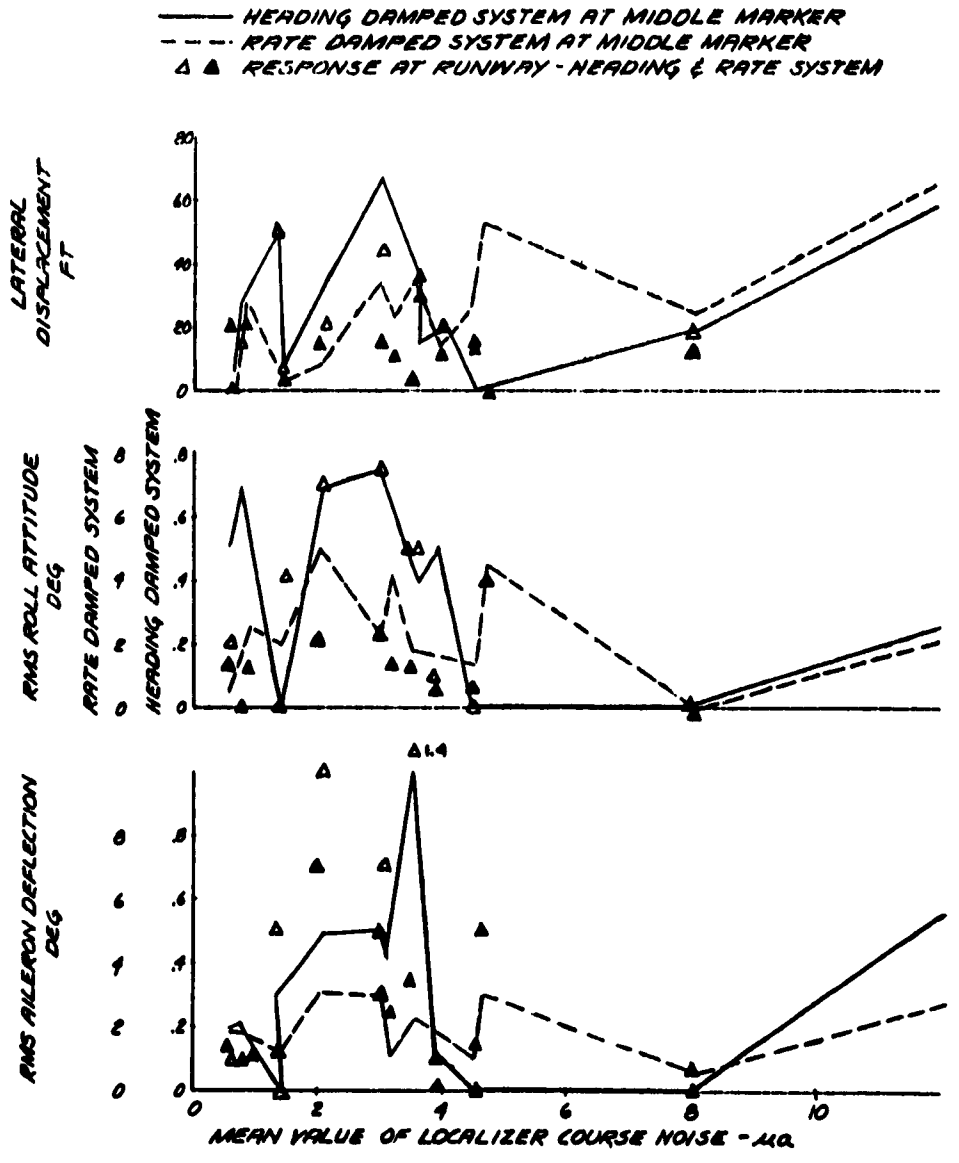

Figure 17 Aircraft Dispersions vs Mean Localizer Beam Error

Figure 18 shows the output parameters as functions of mean noise power plus the total random noise power. The addition of the mean does not materially improve the lateral deviation correlation shown in Figure 14 for the total random noise power.

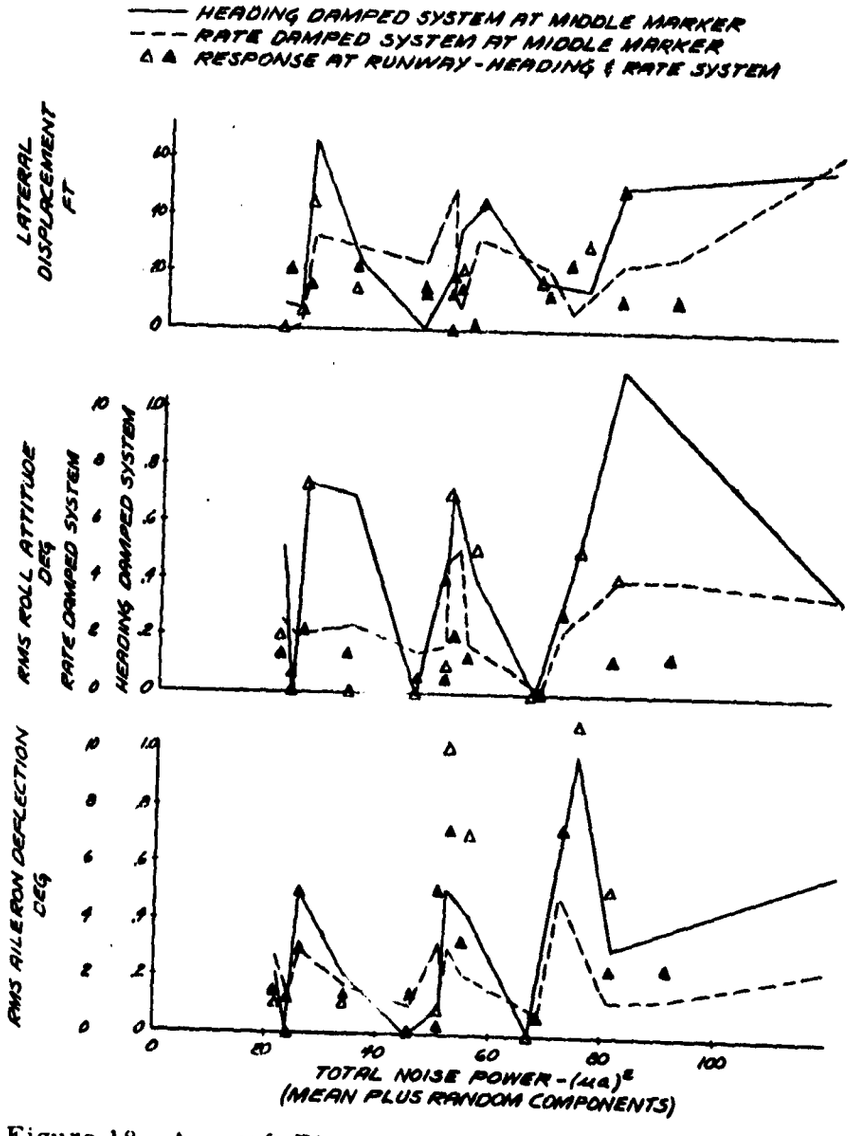

Figure 18 Aircraft Dispersions vs Total Noise Power

Figures 19 and 20, respectively, show the variation of the output parameters with the average random course noise power in the region of the middle marker and the region between the middle and outer markers. The weak correlations of the output parameters in Figure 15 are not materially enhanced.

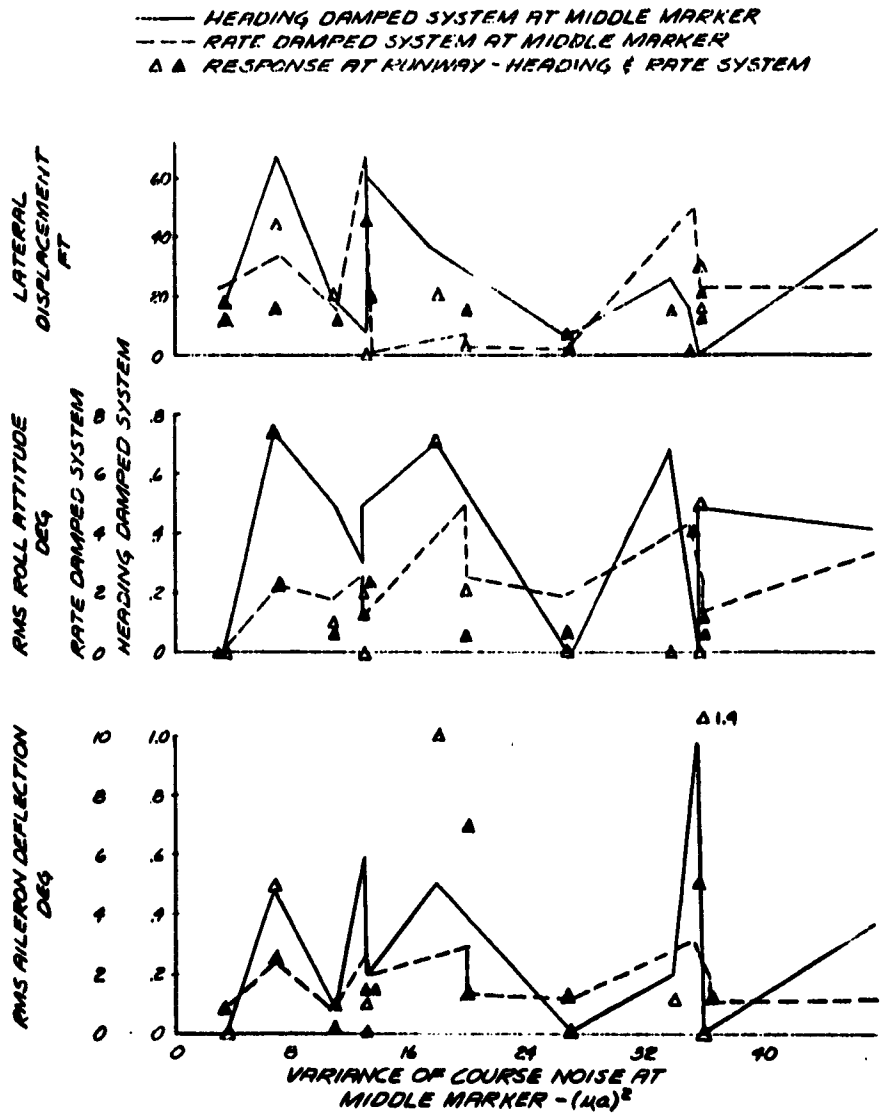

Figure 19 Aircraft Dispersion vs Average Random Power Near Middle Marker

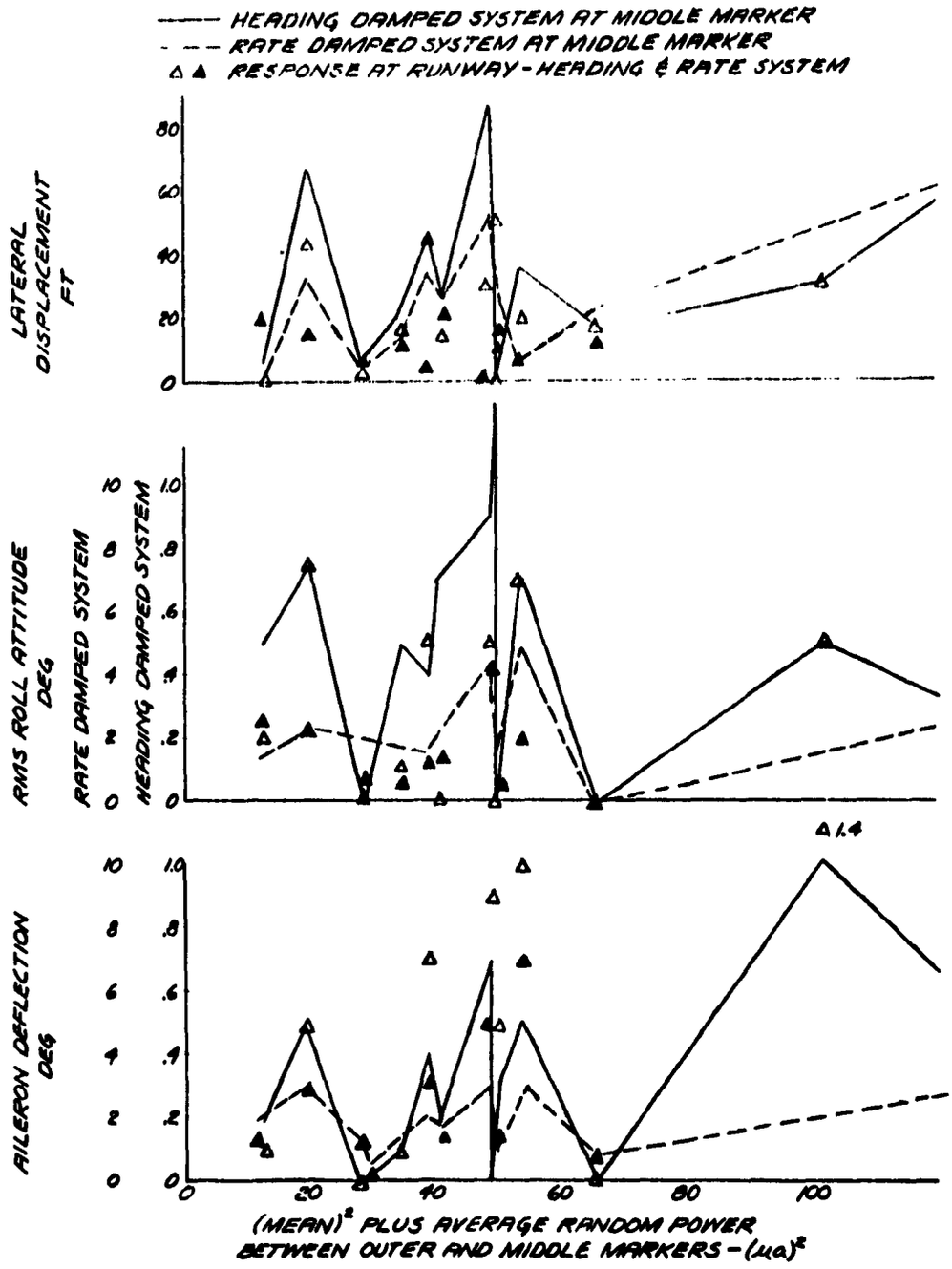

Figure 20 Aircraft Dispersion vs Average Random Power Between Marker Beacons

Figure 21 shows the relationship between the total random power and the mean power and the average spectral power in the three bands. The lack of correlation is quite apparent.

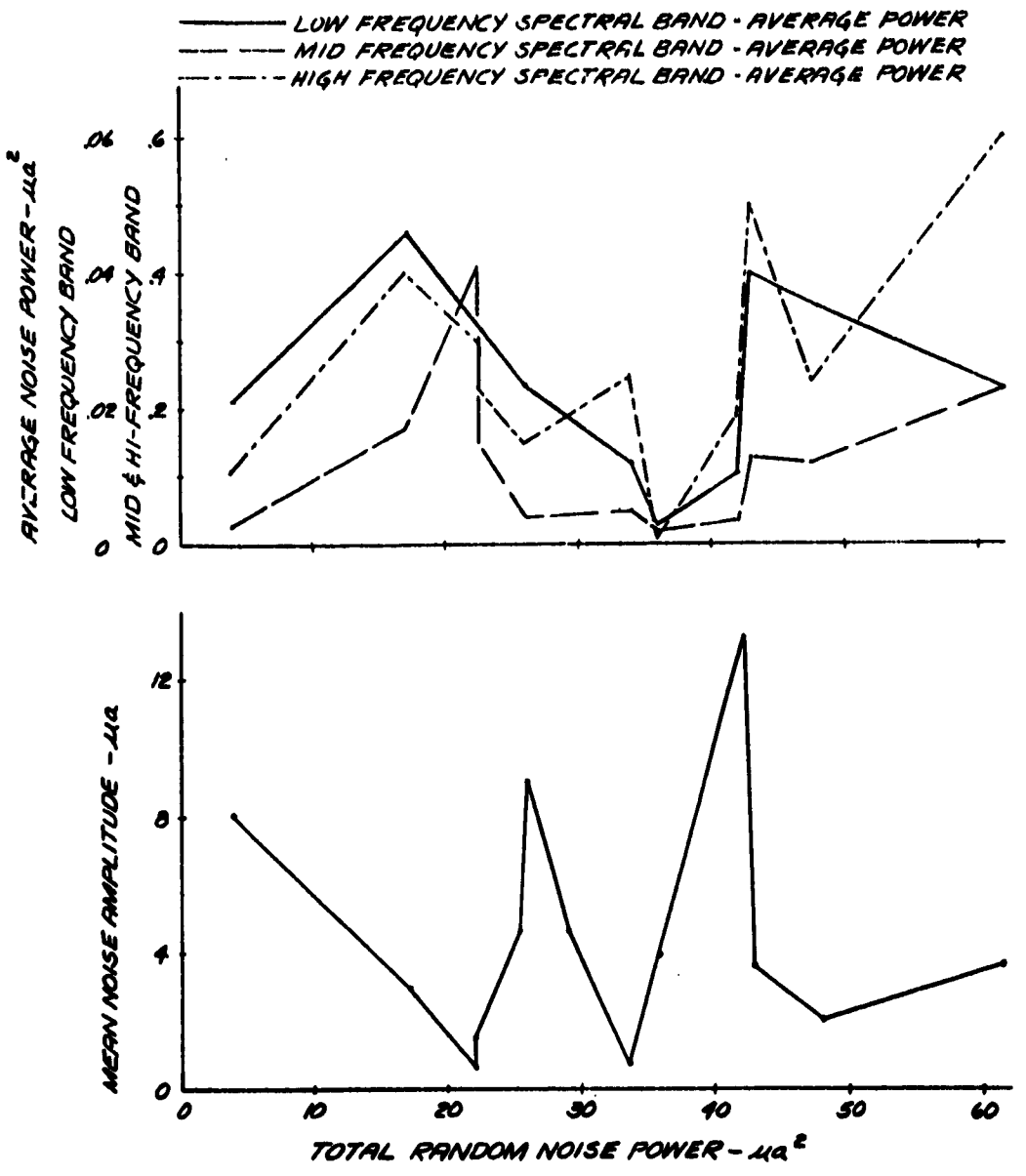

Figure 21 Average Spectral Noise Power vs Total Noise Power

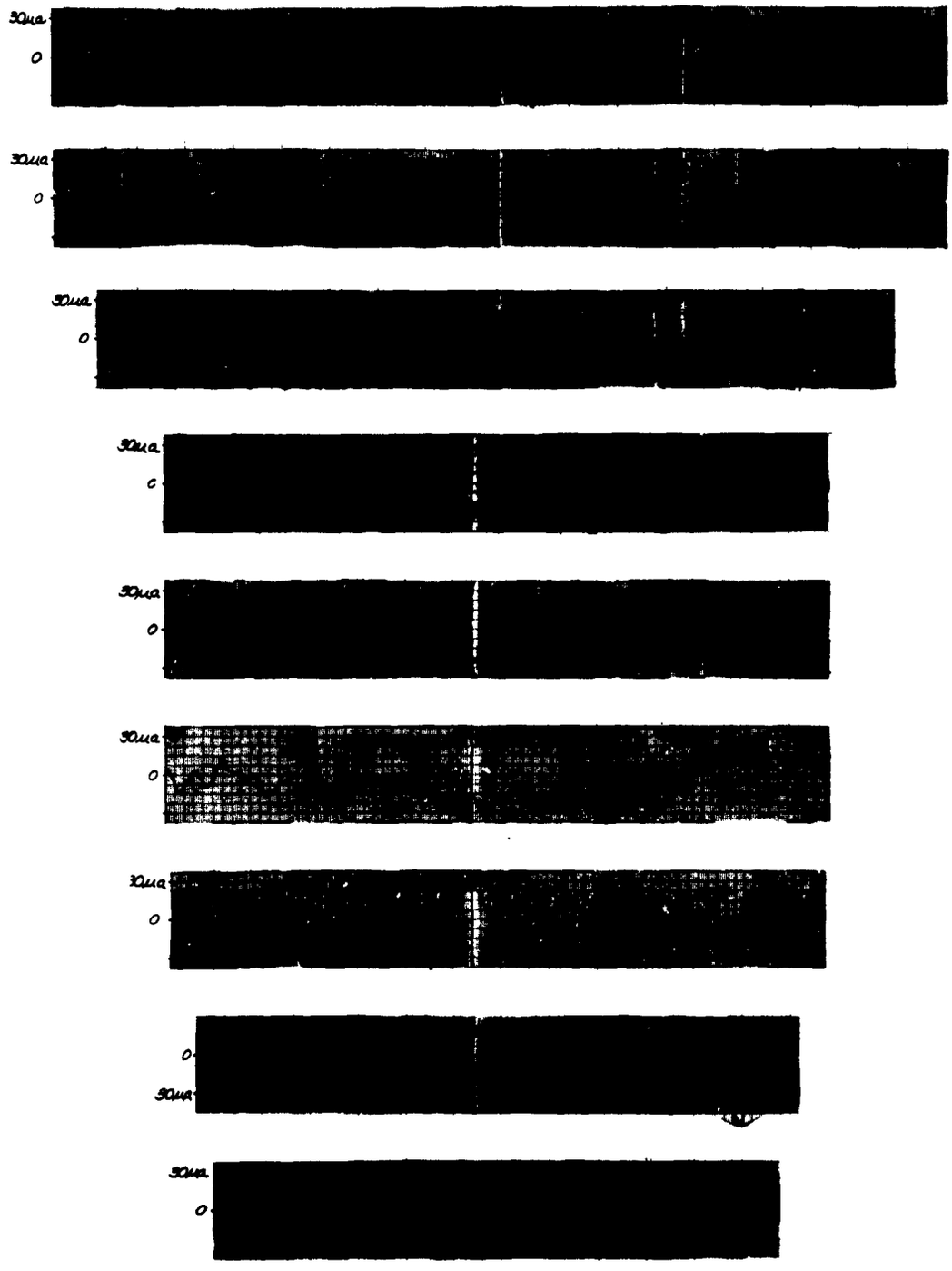

Figure 22 Theodolite Corrected Glide Path Recordings

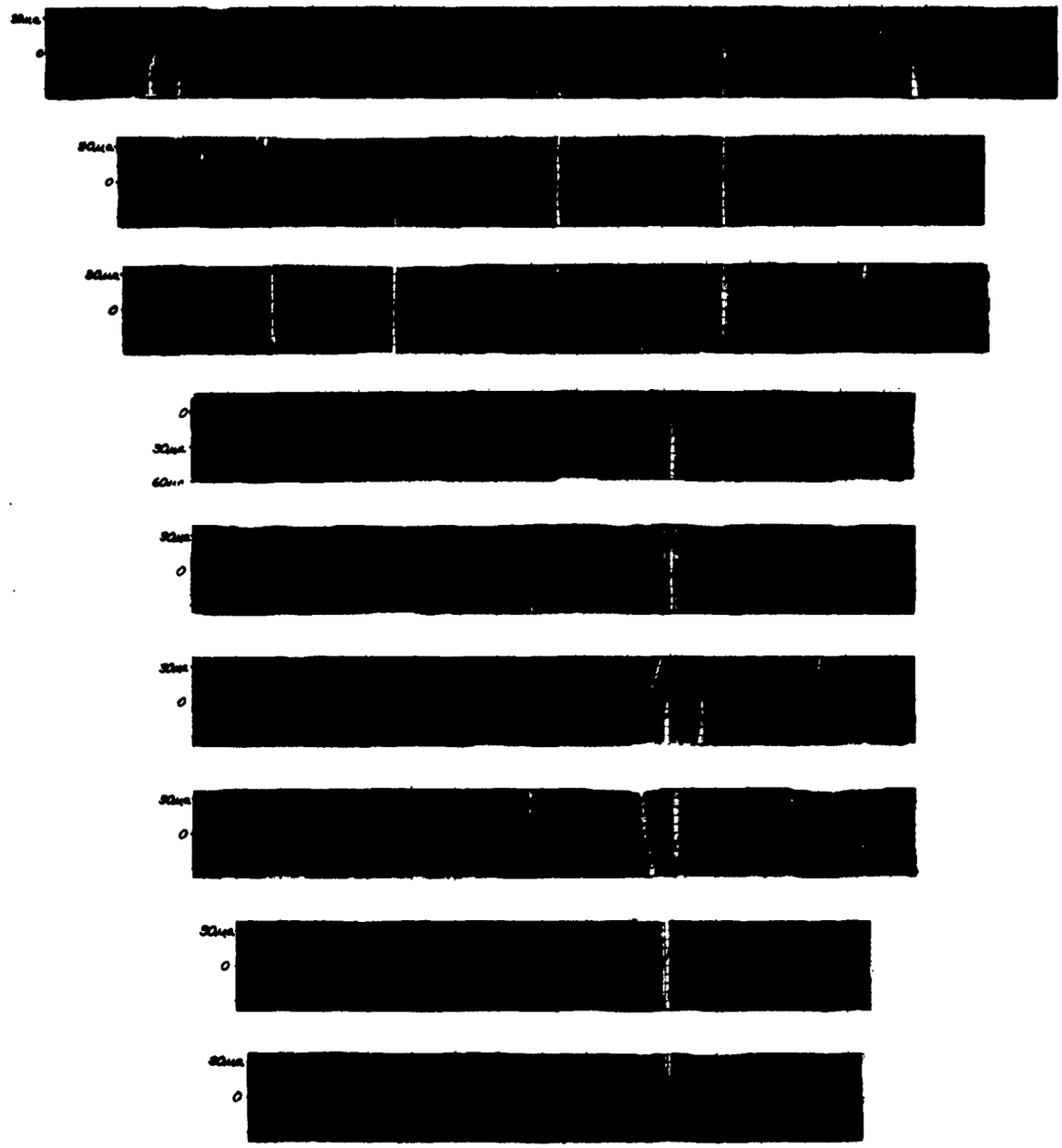

Theodolite Corrected Glide Path Recordings

2.5 GLIDE PATH STATIONARITY TESTS

Figure 22 shows the actual theodolite corrected glide path noise at each of the test facilities. Refer to Figure 1 and Table I for the geometrical relationships between the glide slope transmitter, the markers, and the runway.

The glide path noise at some of the facilities was tested for stationarity. All of the selected sites failed this test due primarily to significant shifts in the mean and standard deviations of the noise subrecords near the runway. Table XI shows the variance fluctuations for five facilities. It is impossible to determine from the records whether this path noise characteristic in the latter portion of the approach actuall exists or is apparent path noise due to aircraft motion, low theodolite data rate, or inaccuracies in the manual theodolite technique at close range. In any event the records cannot be used to derive power spectral data. However, the alternate techniques discussed in Section 3 are applicable to the glide path problem.

TABLE XI
GLIDE PATH
AVERAGE SUBRECORD VARIANCES $(Volts)^2$

Subrecord	Facilities					Remarks
	Wash.	Ontario	New Orleans	St. Louis	Chicago	
1			4.0			
2		9.6	8.3	11.5	5.52	
3	8.8	5.4	4	4.6	5.2	
4	3.2	7.2	24	4.3	16.4	
5	4.8	3.6	19	2.8	21	Runway threshold region
6	42	40	57	32	13.8	
total avg. variance (σ^2)	14.7	15	19	11	11	

NOTE: 1 $volt^2$ = 9 μa^2

TABLE XII
LONGITUDINAL AERODYNAMIC PARAMETERS

AIRCRAFT		KC-135A	DC-7C	TF-102A
W	(pounds)	160,000	100,000	23,400
c.g.	(% MAC)		14	
V	(ft/sec)	210	182	290
I_{yy}	(slug-ft^2)	2.09×10^6	1.84×10^6	$.144 \times 10^6$
ρ	(slugs/ft^3)	.00238	.00238	.00238
g	(ft/sec^2)	32.2	32.2	32.2
c	(feet)	20.2	14.07	23.8
S	(ft^2)	2433	1637	662
C_{m_q}	(rad)$^{-1}$	-16.4	-33.2	-.675
C_{m_α}	(rad)$^{-1}$	-.968	-1.4	-.157
$C_{m_{\dot\alpha}}$	(rad/sec)$^{-1}$	-5.98	10.1	-.675
$C_{m_{\delta_e}}$	(rad)$^{-1}$	.618	-1.97	+.354
$C_{L_{\delta_e}}$	(rad)$^{-1}$	0	.478	-.831
C_{L_α}	(rad)$^{-1}$	4.49	5.38	2.45
C_D	(rad)$^{-1}$	.18	.1677	.0547

TABLE XIII
LONGITUDINAL CONTROL SYSTEM PARAMETERS

AIRCRAFT	KC-135A	DC-7C	TF-102A
Autopilot			
Pitch servo natural freq - ω_n (rad/sec)	10	10	10
Pitch servo damping - ζ	.7	.7	first order lag
Attitude gain - K_θ (deg elevator/deg pitch)	2.5	3	2.5
Attitude rate gain - $K_{\dot\theta}$ (deg elevator/deg/sec pitch)	.4	.02	1
Coupler			
Displacement Gain - K_D (deg pitch/deg beam error)	20	20	20
Integral Gain - K_I (deg pitch/sec/deg beam error)	1	1	1
Desensitization ratio - R	3: 1	3: 1	3: 1
Receiver lag - τ (seconds)	.5	.5	.5

Note: The simulations used the published value of the glide slope angle at each facility as noted in Table I.

2.6 GLIDE PATH TIME RESPONSE TESTS

Figure 23 indicates the control system that was used to evaluate the effects of the glide path noise. The approach coupler is of a standard form using path error displacement and integral terms to generate a pitch command. The autopilot pitch attitude control system is used to damp the glide slope track response. Tables XII and XIII are compilations of the aerodynamic and control system parameters, respectively, that were used with each test aircraft.

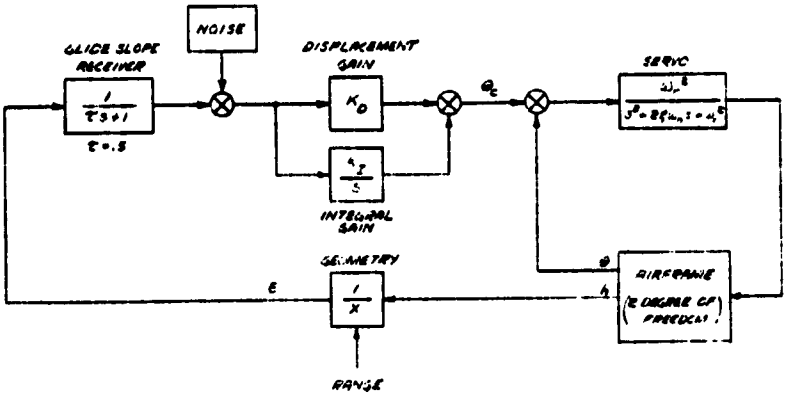

Figure 23 Glide Path Control System

The simulated aircraft were trimmed to fly the published glide slope angles in the tests which involved the path noise at each facility. The noise was injected into the system at the receiver output since the original flight test recordings were derived from that source. Parameters such as pitch attitude, range, altitude error with respect to the ideal track and elevator position were recorded for evaluation.

The autopilot gain parameters were adjusted to provide adequate response and damping to step signal inputs. Similar tests were conducted with the approach coupler parameters to provide reasonable pulse elevator disturbances at several close range positions to check the effect of desensitization on system stability.

TABLE XIV
GLIDE PATH RESPONSES - KC-135 AIRCRAFT
ATTITUDE DAMPED TRACK SYSTEM

	Noise in Middle Marker-Runway Region		Responses in Middle Marker Region			Responses in Runway Region			Responses in Middle Marker-Runway Region	
Glide Slope Facility	95% Prob Level	Mean Level	Δh	θ	σθ	Δh	θ	σθ	ℓΔh	σθ
	μa	μa	ft	deg	deg	ft	deg	deg	ft	deg
Burbank	22	15	6	.5	.85	6	.1	.45	8	.8
Ontario	30	28	0	.7	.45	10	.5	1	12	.8
San Fran.	15	7.5	4	.17	.31	0	.05	.31	2	.45xx
St. Louis	25	21	8.5	.15	.39	2	7.5	.92	5	.77
NAFEC	42	36	18	.5	.55	-	-	-	-	.8xx
Chicago	18	10	0	0	.45	2	0	.77	4	.85xx
Wash. D.C.	12	7.5	16	.2	.7	2	.8	1.4	10	1
Louisville	12	6	4	.1	.3	5	0	.7	5	.85
New Orleans	18	15	4	.5	.62	3	1	.85	3	.95xx
Houston	25	15	7	.3	.44	3	1	1	3	.75xx
Minn.	15	12	6	.1	.38	2	.3	.44	3	.31xx
Kansas City	25	4	7	.1	.3	5	1.5	1.2	5	.7xx
Atlanta	10	6	3	.4	.7	0	.4	.7	5.5	.63
Idlewild	30	25	12	0	.31	2	.25	.7	10	.63
Detroit	25	15	7	0	.45	-	-	-	-	-
Miami	15	5	0	.25	.45	2.5	.25	.6	3	.55
Cleveland	45	34	4	.25	.39	9	.4	.46	7	.38

x runway not recorded
xx last point near runway used

TABLE XV
GLIDE PATH RESPONSES - DC-7 AIRCRAFT
ATTITUDE DAMPED TRACK SYSTEM

	Middle Marker Region			Runway Threshold Region				
Facility	Δh ft	θ deg	σθ deg	Δh ft	θ deg	σθ deg	ℓΔh mm-rwy ft	$\bar{\sigma\theta}$ mm-rwy deg
Burbank	8	.5	.85	8	.25	.5	10	.3
Ontario	4.5	.5	.5	6	.4	.4	5	.45
San Francisco	4.5	.2	.3	0	.4	.32	2.5	.39
St. Louis	8	.1	.39	1	.4	.84	5	.63
NAFEC	17	.5	.63	-	-	-	-	-

TABLE XVI
GLIDE PATH RESPONSES - TF-102A AIRCRAFT
ATTITUDE DAMPED TRACK SYSTEM

	Middle Marker Region			Runway Threshold Region					
Facility	Δh ft	θ deg	σθ deg	Δh ft	θ deg	σθ deg	ℓΔh mm-rwy ft	$\bar{\sigma\theta}$ mm-rwy deg	Remarks
St. Louis	-10	.1	.34	0	0	.31	5	.4	
Nafec	16	.4	.55	4	.4	.7	14	.67	*
Burbank	5	.5	.7	5	.7	.5	8	.6	**
San Francisco	4	.15	.31	0	.7	.6	2	.5	
Ontario	2	.5	.44	7	.5	.54	6	.5	

*rwy data taken at R = 3000 ft to glide slope transmitter
**rwy data taken at R = 4500 ft to glide slope transmitter

Tables XIV, XV, and XVI are compilations, at each facility, of the performance of each aircraft. Figure 24, as a typical example, is the response of the KC-135A aircraft to the Miami Glide Slope signal.

Figure 24 KC-135A Track Response - Miami Glide Slope

These results indicate that the pitch dispersions of the three aircraft with the path noise do not differ significantly. The autopilot configuration tends to mask the differences in the airframe responses of the test aircraft. However, the altitude deviations at the runway range from two to ten feet. This variation is significant since the aircraft is only fifty feet above the ground at the runway threshold. If touchdown dispersions are to be minimized, the glide slope should provide more precise guidance in the form of a higher signal to noise ratio. The alternate path acceptance techniques described in the next section were used to determine this more acceptable level of path noise.

The path noise figures listed in column one of Table XIV indicate that the test facilities have two-sigma path noise values which range from 10 to 45 microamperes. The present glide slope noise specification does not define an acceptable level of path noise in the region of the middle marker and runway although 30 μa is taken as an acceptable value prior to reaching the middle marker. Any path noise amplitude specification should at least reduce this amplitude in the middle marker-runway region. The 95% probability level of noise, in column one of Table XIV indicates that only two of the selected facilities would fail a maximum amplitude noise specification of 30 μa; and nine would fail a 20 μa specification.

3. PHASE IA LOCALIZER COURSE/GLIDE PATH ACCEPTANCE STUDIES

As discussed in the previous section, the course/path noise power spectral technique, or any of the long term average noise power estimates, have not allowed the approach performance to be specified. This lack of statistical correlation is due in part to the finite and short process time of the approach. These results indicate however that there is some improvement in correlating the average output dispersions with short term average course noise estimates. Since the performance of the landing aircraft is of prime importance to the approach process, some methods of including the behavior of the airborne system in the beam acceptance process were studied.

The two techniques that were studied in this phase of the program were:

1) Course/Path Noise Variance Program

This technique provides a course/path noise amplitude specification as an acceptance criterion for ILS facilities. It operated in the following way.

A random noise signal, properly filtered, is applied to the simulated airframe/autopilot coupler combination. The noise variance (σ_N^2), which is a measure of the allowable course noise excursion ($2\sigma_N$) is arranged to vary in a smoothly decreasing manner between the outer marker and the runway. For example, the SC-79 maximum amplitude recommendations can be used. In this case, the localizer variance will change from 225 μa^2 ($2\sigma_N$ = 30 μa) at the outer marker, to 6 μa^2 ($2\sigma_N$ = 5 μa) at the middle marker, 3500 feet from the runway.

A set of simulated approaches was then made and the aircraft track and body axis dispersions were measured at the runway and the middle marker. If the 2σ lateral deviation was less than 20 feet and the 2σ roll attitude and aileron position were less than 2 degrees, the variance program was considered acceptable The actual time histories of the responses at the test facilities using the theodolite corrected data could then be evaluated to determine the individual noise variance at each facility. If the actual variance changes are within the acceptable range, then the facility can be used for low approaches. The converse is true if the program is outside the acceptable range.

Several ideal programs were tested to determine whether the SC-79 amplitude restrictions are realistic or are too severe. This technique has the advantage of simplicity in its application to the present FAA flight inspection procedures. However, it has the disadvantage of not explicitly minimizing the false acceptance or rejection probability of any facility for low approaches since the ideal variance program is artificially produced.

2) Filter Response Techniques

Technically the best method, short of actually flying a series of typical aircraft at each facility, is to record the actual course/path noise and present it to a complete simulation of the airborne system. The resulting responses, such as roll and pitch attitude, surface deflection, and track deviations can then be measured directly to determine if preselected allowable dispersions have been exceeded. If the simulation is accurate enough, there would be very little uncertainty between the analog results and any actual flight test.

However, a complete analog computer facility is not readily transportable so that the results would have to be obtained at some central FAA computing station. A set of simple filters, which could be carried in the inspection aircraft, could be used to generate approximate model transfer functions of the desired dispersion parameters. The noise could be applied to these circuits and the dispersions determined directly.

3.1 FILTER TECHNIQUE

The results of power spectral studies in Section 2 indicate that it is the individual bends of the course noise and not the effects of any long term average of the noise that influence the performance of the approach. Any method that attempts to correlate performance with noise should account for these short term course noise effects.

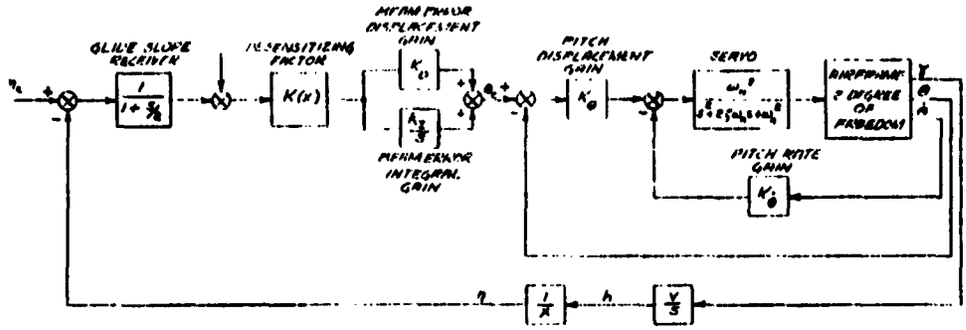

Figure 25 Pitch Attitude Longitudinal Damped Coupler System

However it is desirable that the decision to commission or revalidate an ILS facility for low approach use should be made, by the flight inspection team, on-site. It was the purpose of this section to determine the extent to which the rather complicated analog computer simulation could be simplified so as to be capable of being airborne and still provide useful correlation between the noise and aircraft performance. Simplifying the equivalent filter, that represents the ground and airborne portions of the ILS, causes some uncertainty in the results and therefore increases the probability of accepting an unsatisfactory beam and rejecting a useable one. It was felt, however, that any simple filter should not exceed third or at most fourth order complexity in an effort to maintain simplicity in the airborne or field environment. The analyses were conducted using the KC-135 aircraft but the results are applicable to other aircraft in the approach environment. In the lateral channel, the filters were designed to provide the roll attitude and lateral track deviation functions with respect to the localizer course noise input. In the pitch channel the filters were designed to represent the pitch attitude and vertical track deviations with respect to the glide path noise input.

3.1.1 Glide Path Filter Response

The pitch attitude damped coupler system shown in Figure 25 was used as a model for the glide path filters, and represents the complete analog computer simulation for the KC-135 aircraft. It is based on a linear two-degree-of-freedom, constant airspeed, airframe, and a standard pitch attitude referenced autopilot. The system gain parameters are listed in Tables XII and XIII. The actual transfer functions of pitch attitude to beam error noise, $\theta/f(t)$, and altitude to beam error noise, $h/f(t)$, are:

$$\frac{\theta}{K(x)f(t)} = \frac{-5104\, s\,(s+.025)(s+.568)(s+2)}{(s+.03)(s+2.02)(s^2+1.44s+3.31)(s^2+.221\,s+.03)(s^2+17.08s+148.6)} \quad (1)$$

$$\frac{h}{K(x)f(t)} = \frac{-8790\,(s+.025)(s+2)}{(s+.03(s+2.02)(s^2+1.44\,s+3.31)(s^2+.221\,s+.03)(s^2+17.08\,s+148.6)} \quad (2)$$

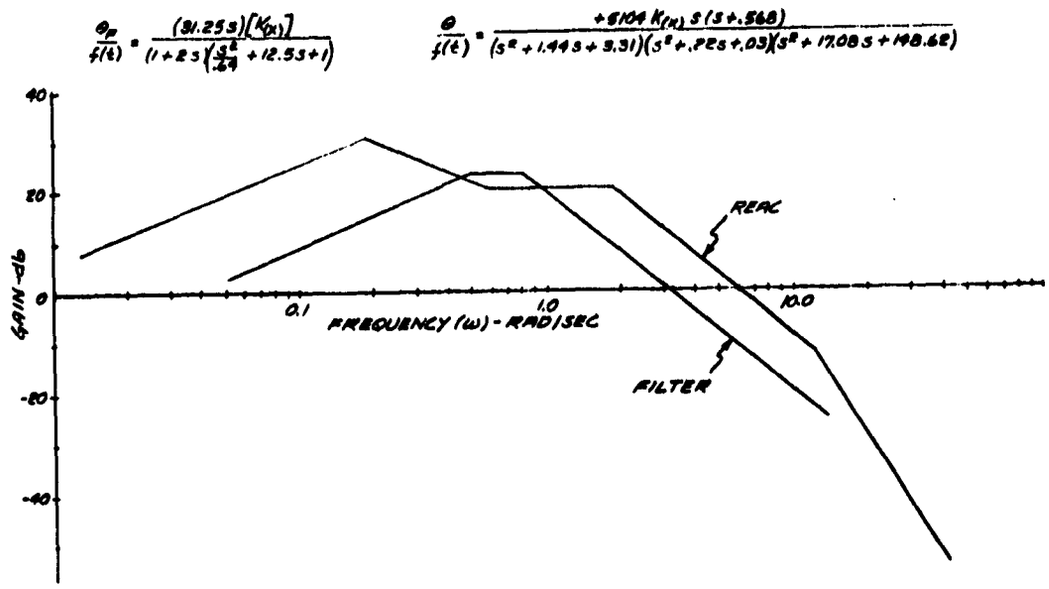

Figure 26 Bode Plot of Pitch Attitude/Beam Responses

TABLE XVII
SIMPLE FILTER PARAMETER VALUES

	Longitudinal Simple Filter									Lateral Simple Filter				
Parameter	Third Order Filter				Fourth Order Filter					Parameter	Third Order Filter			
	K	τ	ζ	ω_n	K	τ	τ_1	ζ	ω_n		K	τ	ζ	ω_n
Pitch (θ)	31.2	2	5	.8	.2	2	2.5	5	.8	Roll (ϕ)	112	5	1.44	2.24
Altitude (h)	.06	2	5	.8						Lateral Displacement (y)	14K	500	1.89	.316

The factor, K(x), on the left side of both equations represents the desensitizing factor that is normally used in the approach couplers to account for beam convergence. A frequency response of the function in Equation 1 is shown in Figure 26.

The simple filter design was a third order approximation whose parameters were adjusted to obtain the best approximation, for a step input, between the exact analog computer response and the filter response. The filter transfer functions used were, for pitch deviation,

$$\frac{\theta_F}{K(x)\ f(t)} = \frac{-KS}{(1+TS)\left(\frac{S^2}{\omega_F{}^2} + \frac{2\xi_F}{\omega_F}S + 1\right)} \tag{3}$$

and for altitude deviation,

$$\frac{h_F}{K(x)\ f(t)} = \frac{-K}{(1+TS)\left(\frac{S^2}{\omega_F{}^2} + \frac{2\xi_F}{\omega_F}S + 1\right)} \tag{4}$$

The parameters K, T, ξ_F, and ω_F of the filters were optimized by minimizing the difference

$$\Sigma\ (\theta - \theta_F(K, T, \xi_F, \omega_F)) = \text{minimum} \tag{5}$$

between the filter (θ_F) and respective computer output (θ).

Repeated trials, with many variations of the filter parameters, were used to determine the best approximation. However Equation 5 can never be equal to zero since the computer response is generated by an eighth order system while the simple filter response is generated by the third order filter. It was therefore necessary to minimize the error in Equation 5 in a particular time interval of the step response tests. The first fifteen seconds was taken as a desirable time interval since it tends to match most of the short term attitude and track motions. The results of the parameter variations are shown in Table XVII. It should be stressed that the optimization was based on responses to step inputs. Somewhat different filter parameters would perhaps have been chosen if other types of

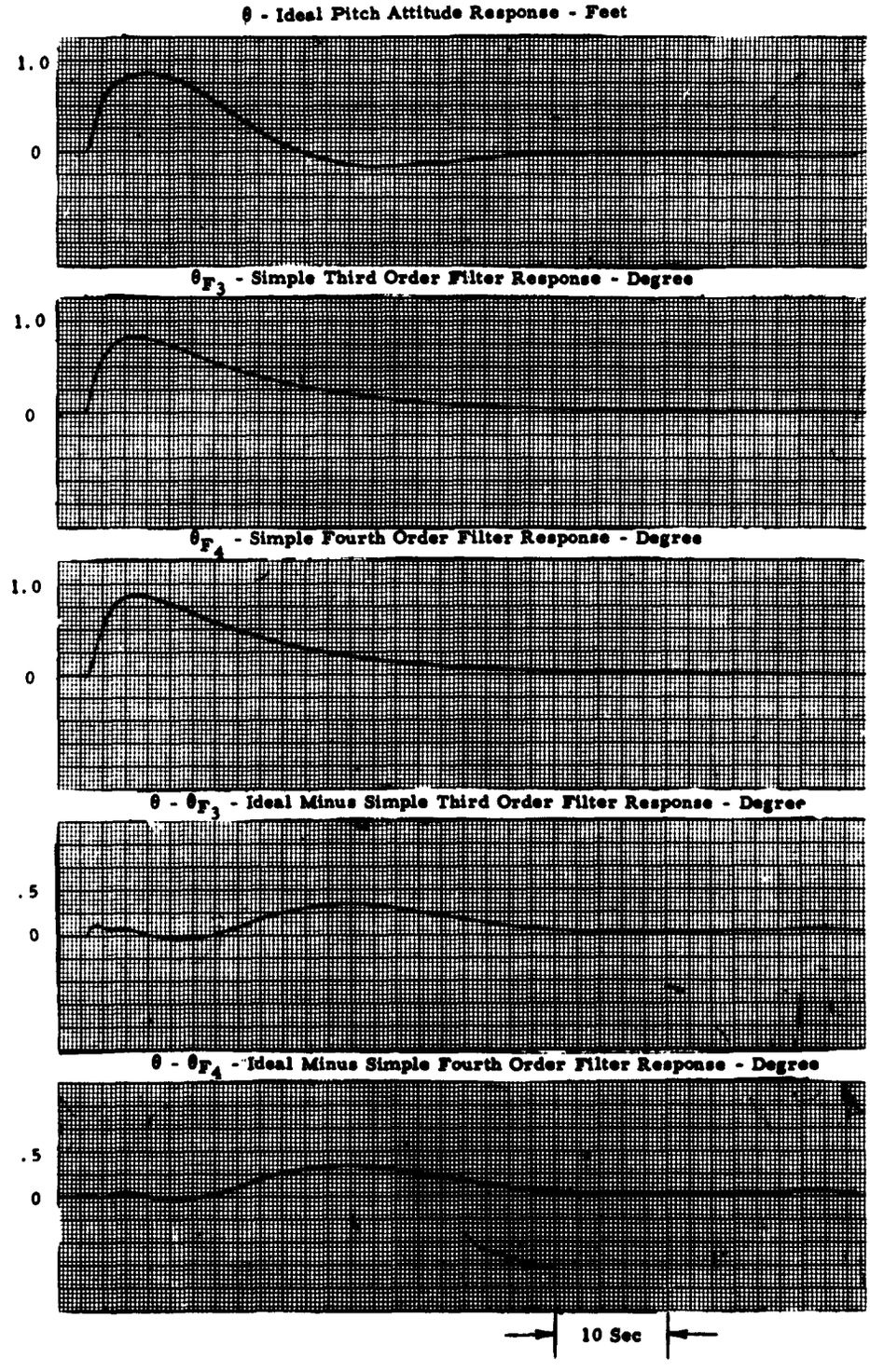

Figure 27 **Ideal Pitch Attitude and Simple Filter Responses to Step Noise**

input signals were used or if other matching time intervals were desired. Figure 27 shows the analog computer, filter, and the difference signal representing Equation 5 for the pitch attitude response. The initial conditions of the simulated aircraft in this test series were such that it was flying along a 2.5 degree glide slope and the results in Figure 27 show the deviations in the parameters from the steady state flight condition. The primary difference, in the first fifteen seconds, between the computer and filter output signals is in the initial responses to a step beam displacement. Beyond fifteen seconds the error signal again becomes large. These differences are due to the compromise in high and low frequency matching of the simpler filter to the more complex computer simulation. In order to reduce the discrepancies at either end of the frequency spectrum, a fourth order filter of the form

$$\frac{\theta_F}{K(x)f(t)} = \frac{-KS}{(1+TS)(1+T_1S)\left(\frac{S^2}{\omega_F{}^2} + \frac{2\xi_F}{\omega_F} S+1\right)} \qquad (8)$$

was also implemented. Figure 27 also shows the response of this filter after an identical optimization procedure was performed. Table XVII also lists the resulting values of parameters for this filter. Comparing the output responses of each filter shows that no significant improvement has been obtained. It was therefore concluded that for practical considerations any simple filter for the pitch channel should not exceed third order since much closer correspondence to the computer output can only be accomplished when the filter has nearly the same order, and therefore complexity, as the computer simulation.

Figure 28 shows the response of the third order altitude filter and the computer to a step beam displacement. The two signals are matched to almost the same extent as the pitch responses. The altitude filter parameters are also given in Table XVII.

The final filter designs were used in conjunction with the complete simulation to compare the results when the theodolite corrected course noise was applied to each.

The attitude and altitude responses at the runway threshold were tabulated for the computer simulation and the filters. If the filter and the computer time responses coincided throughout the tests then there would

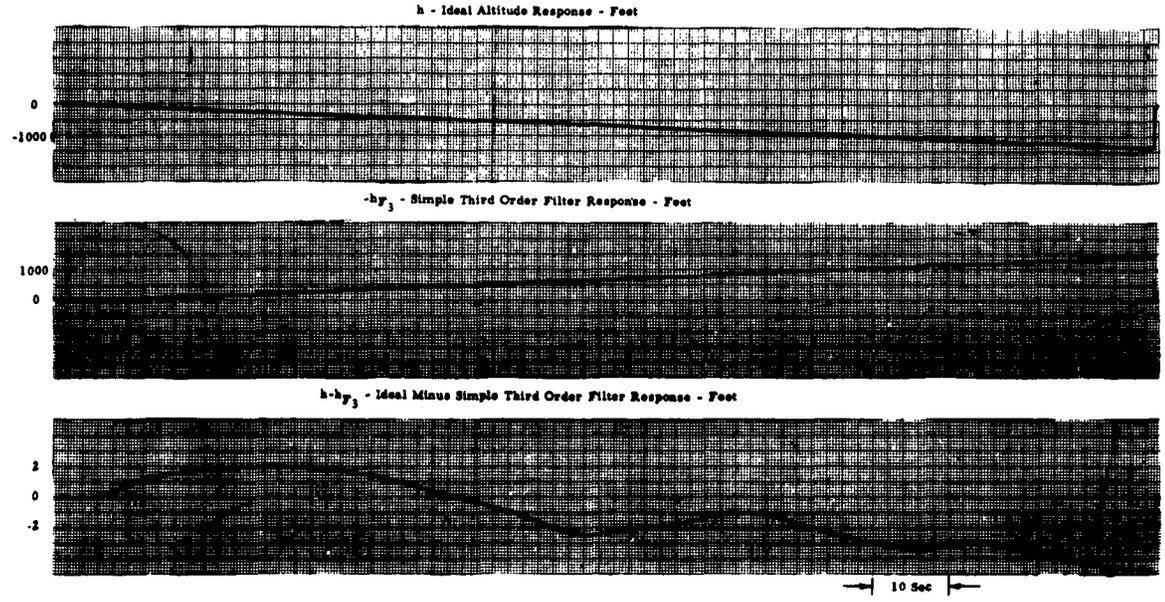

Figure 28 Ideal Altitude and Simple Filter Response to Step Noise

TABLE XVIII
TYPICAL COMPUTATION OF THE CORRELATION COEFFICIENT (r) FOR THE NAFEC GLIDE SLOPE FACILITY

$$r = \frac{n\Sigma\theta_R\theta_F - \Sigma\theta_R\Sigma\theta_F}{n\Sigma\theta_R^2 - (\Sigma\theta_R)^2\, n\Sigma\theta_F^2 - (\Sigma\theta_F)^2} = \frac{(18)(.6887) - 1.40 \times 5.15}{18 \times .3296 - 1.96 \;\; 18 \times 1.8635 - 26.5225}$$

$$= .9823$$

n	θ_R	θ_F	$\theta_R \cdot \theta_F$
1	-.06	+.04	-.0024
2	-.05	+.07	-.0035
3	-.05	+.10	-.0050
4	-.04	+.13	-.0052
5	-.03	+.16	-.0048
6	-.02	+.18	-.0036
7	0	+.21	0
8	+.02	+.24	+.0048
9	+.05	+.28	+.0140
10	+.07	+.31	+.0217
11	+.10	+.34	+.0340
12	+.12	+.36	+.0432
13	+.15	+.39	+.0585
14	+.18	+.42	+.0756
15	+.22	+.46	+.1012
16	+.24	+.48	+.1152
17	+.25	+.49	+.1225
18	+.25	.49	+.1225
	$\Sigma\theta_R = 1.40$	$\Sigma\theta_F = 5.15$	$\Sigma\theta_R \cdot \theta_F = +.6887$

$\Sigma\theta_R^2 = .3296$ $\Sigma\theta_F^2 = 1.8635$ $(\Sigma\theta_R)^2 = 1.96$ $(\Sigma\theta_F)^2 = 26.5225$

NOTE: θ_R = Ideal Pitch Attitude Response
θ_F = Simple Filter Pitch Attitude Response
n = Test points between Middle Marker and Runway

be a one-to-one correspondence, or perfect correlation. A plot of the two output signals would then be a straight line with a 45 degree slope. Obviously such coincidence in the time domain requires that there be corresponding coincidence in the frequency domain. However, comparing the actual computer transfer functions in Equations 1 with the filter transfer function in Equations 3 shows that only some degree of correlation can exist between the two signals. Figure 26 includes the frequency response of the simple pitch filter for comparison with the computer frequency response.

A qualitative measure of the degree of correspondence between the filter and the computer output signals is the correlation coefficient, r. The correlation coefficient is ± 1 when the ideal response can be exactly predicted from the simple filter response. The value of r is zero when there is no relationship between the two signals. In between 0 and $\pm$ 1, the value of r indicates that only a degree of predictability exists and that some error must always be expected. The sign of r indicates whether the simple filter response increases when the computer output is decreasing. A quantitative measure of the degree of correspondence between the computer and filter output signals is provided by the correlation coefficient squared, r^2. This parameter represents the decimal percentage of the variance of the simple filter response that can be accounted for by the relationship with the computer response. Therefore if the correlation coefficient between the two responses is 0.8 then 64% ($r^2 = 0.64$) of the expected variation can be attributed to the relationship between the responses. The remaining 36 per cent of the variation between the responses is due to other factors such as the statistical nature of the actual beam noise, and the simple filter approximations to the complete system response.

A 95% variance was taken as an acceptable value of correlation in an effort to minimize the resulting false acceptance probability for both the glide slope and localizer filter design. Table XVIII shows a typical calculation for the correlation coefficient using the NAFEC Glide Path facility.

Ten glide slope facilities were used to test the degree of correspondence between the filter and the computer responses. Typical computer and filter responses are shown in Figure 29 using the NAFEC facility as an example. Table XIX is a tabulation of the correlation coefficient r and r^2 for the responses in the middle marker/runway

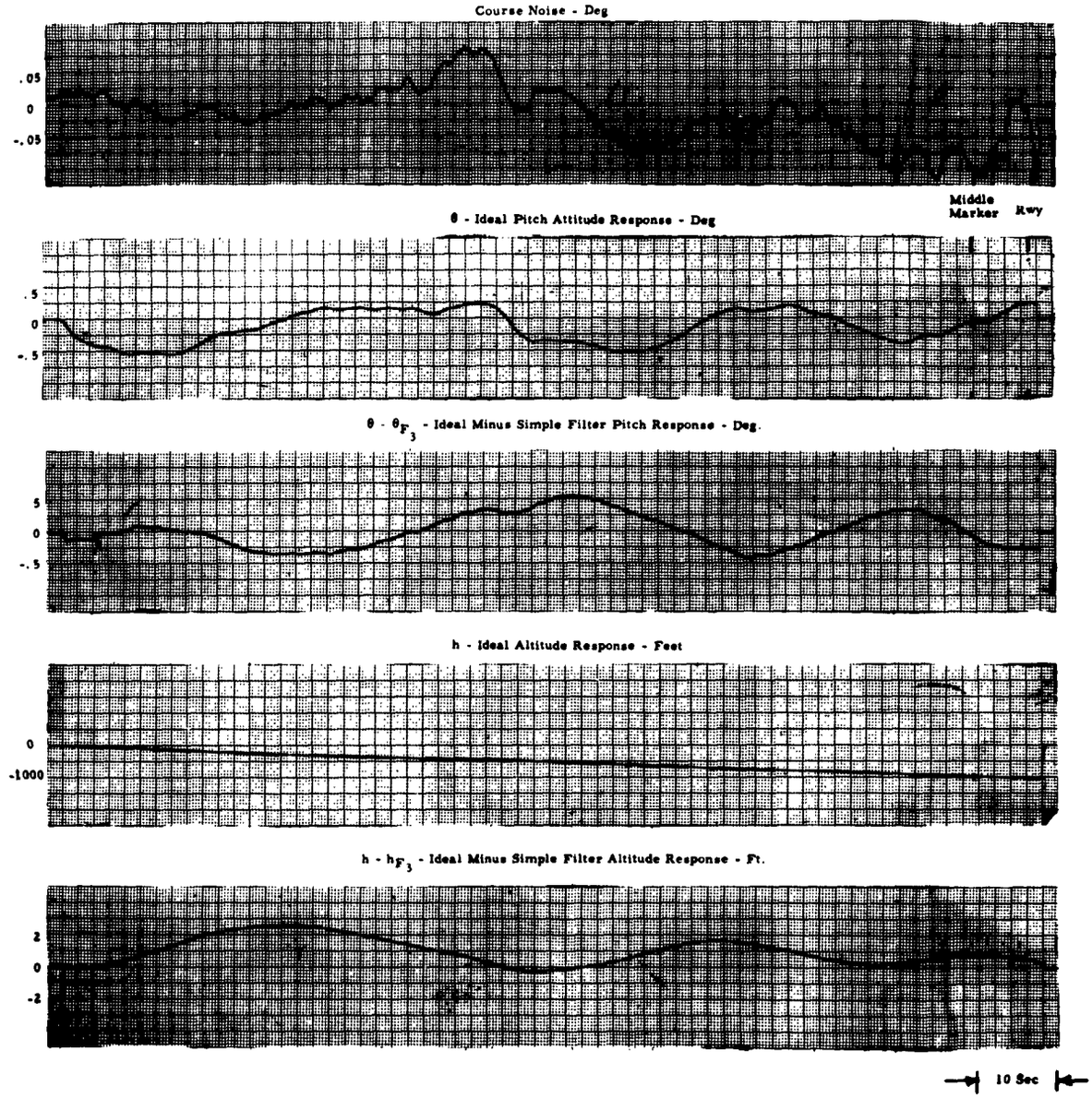

Figure 29 **Ideal and Simple Third Order Filter Responses to Beam Noise NAFEC Glide Slope Facility**

TABLE XIX
A SUMMARY OF PITCH ATTITUDE CORRELATION COEFFICIENTS
FOR TEN GLIDE SLOPE FACILITIES

Glide Slope Facility	Correlation Coefficient r	Square of Correlation Coefficient (Per Cent) r^2
LOUISVILLE	-.078	0.6
BURBANK	+.962	92.5
HOUSTON	+.953	90.8
WASHINTON, D.C.	+.673	45.3
CHICAGO	+.845	71.4
ONTARIO	-.228	5.2
ST. LOUIS	+.910	82.8
SAN FRANCISCO	+.957	91.6
NEW ORLEANS	+.833	69.4
NAFEC	+.982	96.4

region of each facility. The wide range of values of r^2 indicates that there is significant variation in the correlation between the filter and the computer responses. For example, the NAFEC facility has a high degree of correlation, (r^2 = .964) while the Louisville facility has a very poor relationship (r^2 = .006). The wide range of r^2 values is related to the uniformity of the ILS beam error signals. As shown in Section 2 the statistical characteristics of the glide slope signal in the vicinity of the middle marker and runway are not uniform. Therefore the simple filter responses fail to approximate the ideal computer responses with equivalent errors.

The frequency responses in Figure 26 indicate that if the beam noise has significant power at frequencies below .05 cps and above 1 cps the responses will be poorly correlated, since a best fit occurs only in the mid-frequency band.

Table XX summarizes the responses of the filter and the computer with the noise at each facility in terms of their means and standard deviations. It complements the lack of correlation shown in Table XIX.

TABLE XX
A SUMMARY OF LONGITUDINAL STATISTICAL CHARACTERISTICS FOR TEN GLIDE SLOPE FACILITIES

Facility	Ideal Pitch θ Deg.	Pitch Filter θ_{F_3} Deg.	Ideal Altitude h Ft.	Altitude Filter h_{F_3} Ft.	Ideal Pitch θ Deg.	Pitch Filter θ_{F_3} Deg.	Ideal Altitude h_{F_3} Ft.	Altitude Filter h_{F_3} Ft.	Ideal Pitch θ Deg.	Pitch Filter θ_{F_3} Deg.	Ideal Altitude h Ft.	Altitude Filter h_{F_3} Ft.	Ideal Pitch θ Deg.	Pitch Filter θ_{F_3} Deg.	Ideal Altitude h Ft.	Altitude Filter h_{F_3} Ft.	Ideal Pitch θ	Pitch Filter θ_{F_3} Deg.	Ideal Altitude h Ft.	Altitude Filter h_{F_3} Ft.
Louisville	-.10	-.08	-1140	-1141.7	0	-.36	-1300	-1302.1	-.15	-.01	-1216.7	-1218.4	.26	.20	61.2	61.5	+.11	+.19	-1155.5	-1156.9
Burbank	-.95	-1.32	- 720	- 722.5	-.41	-.94	-1040	-1044.5	-.20	-.39	- 880	- 883.8	.45	.63	112.1	112.6	+.25	+.23	- 767.9	- 771.1
Houston	0	-.04	- 980	- 981.7	+.12	+.03	-1100	-1101.9	-.10	-.16	-1047.5	-1049.3	.17	.19	45.3	45.4	+.07	+.03	-1002.2	-1003.9
Wash. D.C.	+.25	+.47	-1060	-1060.5	+.13	-.32	-1200	-1222.2	-.64	-.30	-1137.8	-1138.9	.56	.34	56.1	56.7	+.08	+.03	-1081.7	-1082.7
Chicago	-.15	+.03	- 920	- 921.3	+.13	-.02	-1080	-1081.9	-.22	-.16	-1000	-1001.6	.23	.19	56.0	56.2	+.01	+.03	- 944.0	- 945.4
Ontario	-.15	-.50	-1150	-1154.6	-.45	-1.30	-1220	-1224.6	-.16	-.66	-1184.3	-1188.9	.20	.39	25.1	25.1	+.04	-.27	-1159.2	-1163.8
St. Louis	+.20	-.12	-1040	-1039.7	+.13	0	-1200	-1200.6	-.31	-.67	-1111.4	-1111.4	.35	.52	57.4	57.9	+.04	-.15	-1054.0	-1053.4
San Franc.	-.10	-.28	-1100	-1100.6	-.20	-.58	-1180	-1180.4	-.10	-.38	-1134.9	-1135.3	.16	.19	29.8	29.8	+.06	-.19	-1105.0	-1105.6
New Orleans	-.61	-.13	- 740	- 741.0	-1.03	-1.17	- 940	- 941.8	-.34	-.26	- 837.1	- 838.7	36	.41	74.3	74.6	+.02	+.16	- 762.8	- 764.1
NAFEC	-.05	+.05	- 980	- 980.7	+.25	+.50	-1020	-1020.6	+.09	+.32	-1002.0	-1002.7	.13	.19	15.0	14.8	+.23	+.51	- 987.0	- 987.9

3.1.2 Localizer Filter Responses

The roll attitude and localizer track deviation filters were designed in an identical manner to that described above for the glide slope responses. The system that was used is shown in Figure 30. The simulator parameters are listed in Tables IX and X.

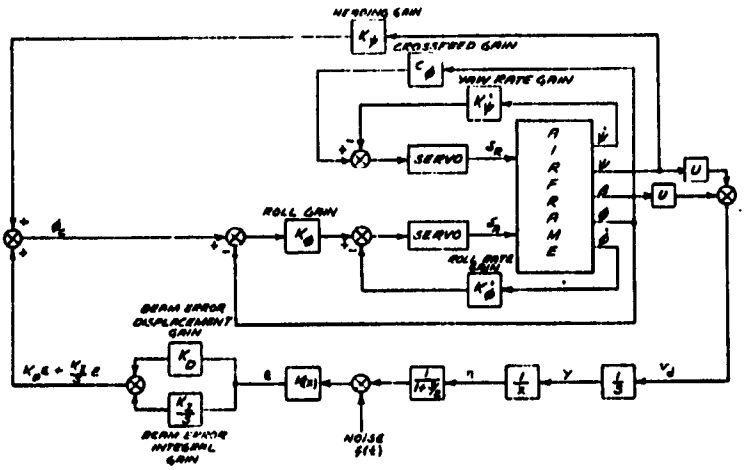

Figure 30 Heading Damped Localizer Coupler System

Frequency responses of each lateral parameter are shown in Figures 31 and 32.

The simple filter designs were third order systems given by

$$\frac{\phi F}{K(x)f(t)} = \frac{K_1 s}{(1+Ts)\left(\frac{s^2}{\omega_{F_1}^2} + \frac{2\xi_F}{\omega_{F_1}} s + 1\right)} \tag{9}$$

$$\frac{yF}{K(x)f(t)} = \frac{K_2 s}{(1+T_2 s)\left(\frac{s^2}{\omega_{F_2}^2} + \frac{2\xi_F}{\omega_{F_2}} s + 1\right)} \tag{10}$$

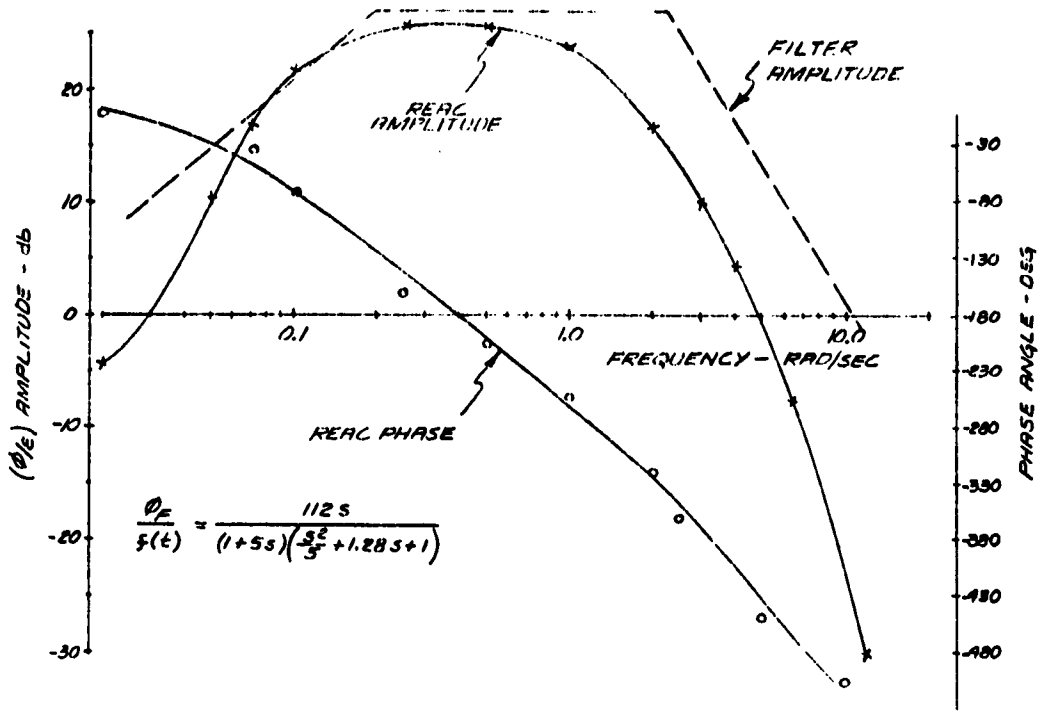

Figure 31 Bode Plot Roll Attitude/Beam Response

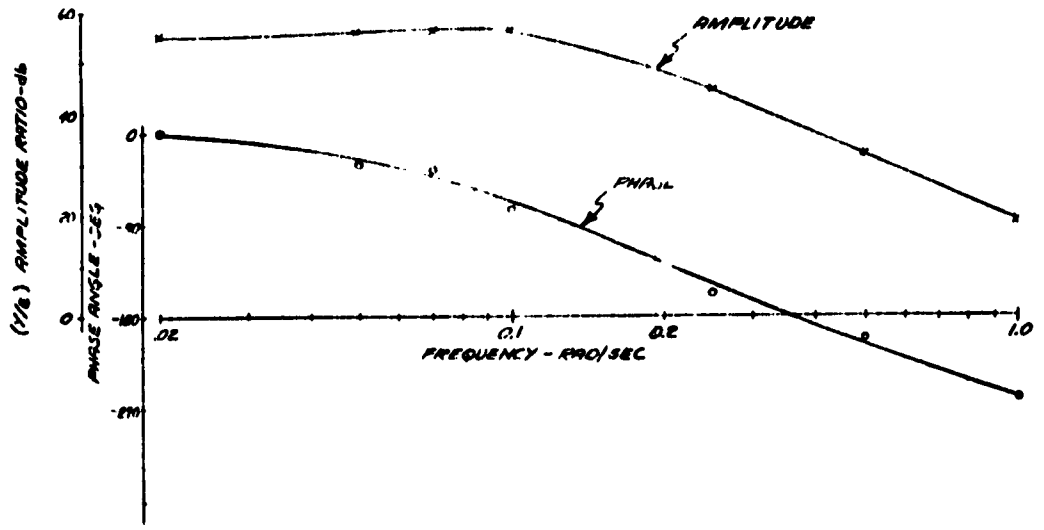

Figure 32 Bode Plot Lateral Displacement/Beam Response

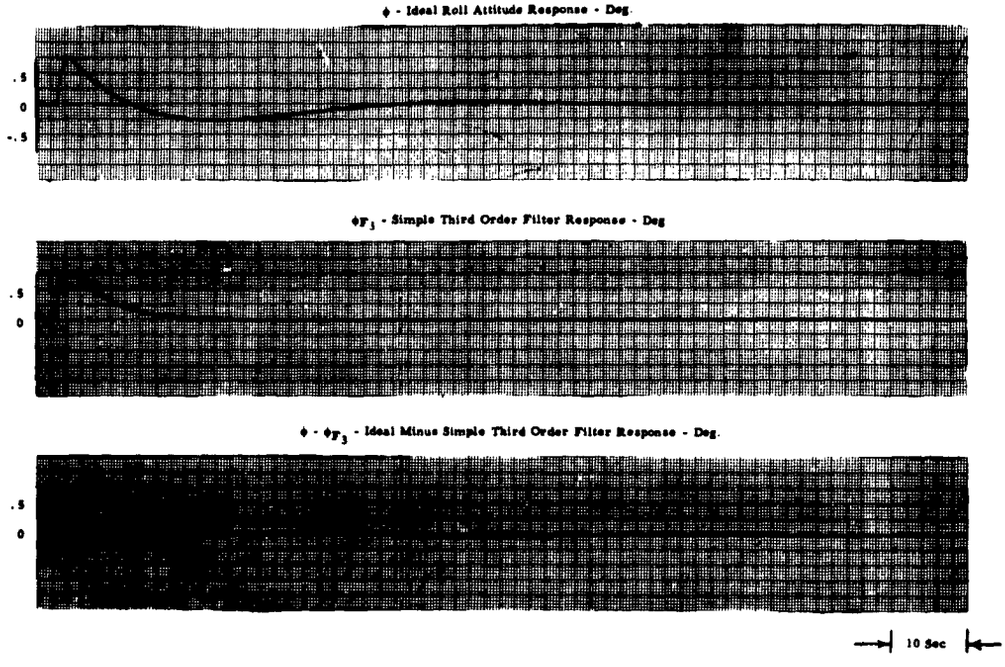

Figure 33 **Ideal Roll Attitude and Simple Filter Response to Step Noise**

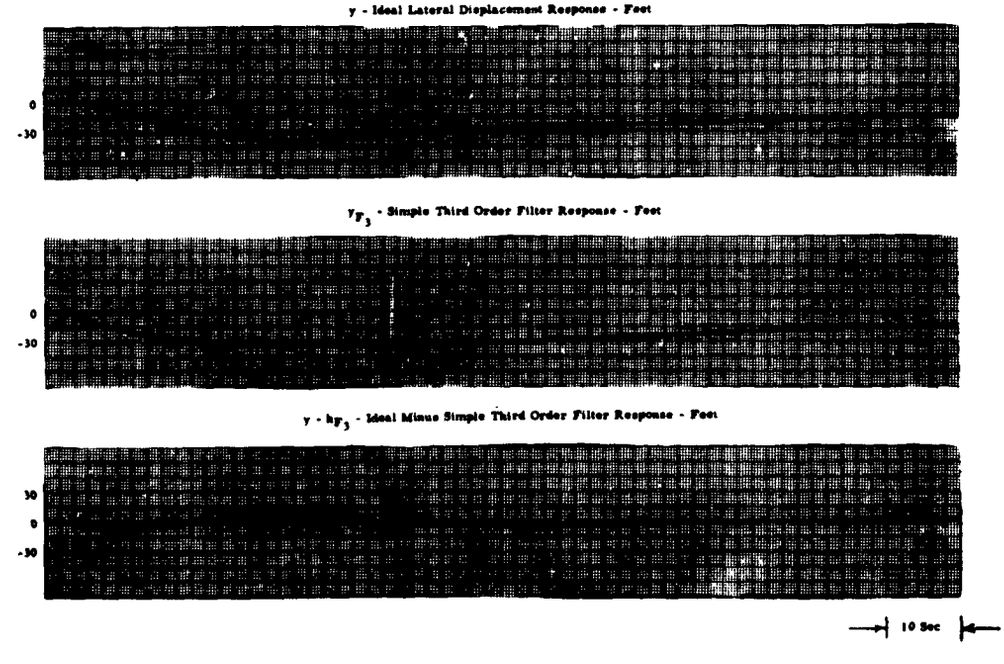

Figure 34 **Ideal Lateral Displacement and Simple Filter Response to Step Noise**

The optimization of the filter parameters, K, T, ξ, ω_n provided minimum error between the computer and filter signals in the first 15 seconds of the response to step localizer beam displacements. Table XVII presents the resulting parameters and Figures 33 and 34 show the responses that resulted from the step beam error inputs. As in the case of the glide slope responses, there is a discrepancy in the initial transient responses and during the long periods after 15 seconds. The simulated aircraft was initially positioned along the runway centerline with wings level and the displacements due to the ILS course noise are deviations about these initial conditions.

Ten localizer facilities were used to test the simple filter technique. Figures 35 and 36 show the typical responses at the New Orleans and Chicago localizer facilities. The roll attitude correlations, r and r^2 are given in Table XXI. The resulting variations in r^2 indicate that the degree of correlation between the filter and computer responses is not adequate (i. e., less than 95%) for all the facilities. Only the responses using the noise of the Burbank, Chicago and Ontario facilities indicate a high degree of correlation. It is interesting to note that there is improved correlation for the lateral results over the longitudinal results. This is due in part to the fact that the localizer course noise as shown in Section 2 is more statistically uniform or stationary, than the glide path noise in the vicinity of the middle marker and the runway.

TABLE XXI
A SUMMARY OF ROLL ATTITUDE CORRELATION COEFFICIENTS
FOR TEN LOCALIZER FACILITIES

Localizer Facility	Correlation Coefficient (r)	Square of Correlation Coefficient (Per Cent) (r^2)
LOUISVILLE	.944	89.1
BURBANK	.998	99.7
BALTIMORE	.944	89.1
WASHINGTON, D.C.	.907	82.3
CHICAGO	.995	98.9
ONTARIO	.993	98.7
ST. LOUIS	.642	42.1
SAN FRANCISCO	.813	66.1
NEW ORLEANS	.928	86.1
NAFEC	.936	87.6

A summary of the responses of the exact computer simulation and the approximation filters is listed in Table XXII. This data augments the correlation data presented in Table XXI.

The results of the simple filter technique as presented above indicate that there is not sufficient correlation between the responses of a relatively simple filter and a complete simulation to adequately protect against falsely accepting an undesirable facility or rejecting a desirable facility. To improve the degree of prediction it is necessary to increase the complexity of filter design to almost coincide with the complete simulation and to ensure that the ILS course/path noise characteristics are more uniform than they are at present. The simple filter technique is therefore not recommended for use by the FAA in commissioning ILS facilities.

TABLE XXII
A SUMMARY OF LATERAL STATISTICAL CHARACTERISTICS FOR TEN LOCALIZER FACILITIES

Facility	Ideal Roll ϕ Deg	Roll Filter ϕ_{F_3} Deg	Ideal Cen Distance y Ft	Cen Distance Filter y_{F_3} Ft	Ideal Roll ϕ Deg	Roll Filter ϕ_{F_3} Deg	Ideal Cen Distance y Ft	Cen Distance Filter y_{F_3} Ft
Louisville	+ 07	+ 51	+12 0	+ 22 2	- 20	- 08	15 0	16 2
Burbank	-1 15	-2 95	117 3	- 79 2	-3 05	-3 10	-49 8	-52 2
Baltimore	- 30	- 50	-7 8	+ 10 8	- 90	- 55	-16 8	-7 8
Wash D C	+1 13	+ 30	32 3	+ 8 1	-1 69	-1 12	-1 8	-9 0
Chicago	+ 36	+ 40	+30 9	+ 4 8	- 13	- 05	+12 0	+17 4
Ontario	+1 20	+1 55	+18 3	+ 7 2	- 40	- 20	0	+7 2
St Louis	- 40	- 20	+15 9	+ 10 5	- 30	- 05	+8 4	+21 9
San Franc	- 50	- 30	+16 5	+ 27 0	- 50	+ 80	+33 6	0
New Orleans	- 48	- 51	+60 0	+ 65 4	- 33	+ 05	+60 0	+59 4
NAFEC	+1 46	+ 90	+12 3	+ 9 0	+ 65	+ 85	-5 4	-12 9

TABLE XXII (cont'd)

Facility	Ideal Roll ϕ Deg	Roll Filter ϕ_{F_3} Deg	Ideal Cen Distance y Ft	Cen Dist Filter y_{F_3} Ft	Ideal Roll ϕ Deg	Roll Filter ϕ_{F_3} Deg	Ideal Cen Distance y Ft	Cen Dist Filter y_{F_3} Ft	Ideal Roll ϕ Deg	Roll Filter ϕ_{F_3} Deg	Ideal Cen Distance y Ft	Cen Dist Filter y_{F_3} Ft
Louisville	+ 15	+ 07	13 9	15 2	34	28	1 04	3 81	+ 48	+ 35	+14 9	+19 0
Burbank	- 47	- 55	-70 1	-50 8	1 89	1 81	27 0	16 0	+1 42	+1 26	-43 1	-34 8
Baltimore	0	+ 09	- 8 0	- 4 8	81	66	6 4	10.7	+ 81	+ 75	- 1 6	+ 5 8
Wash D C	+ 37	+ 25	+18 5	- 0 2	1 1	74	12 9	8 8	+1 43	+1 00	+31 4	+ 8 6
Chicago	- 19	- 08	+17 9	+12 1	36	34	7 1	5 0	+ 18	+ 26	+25 0	+17 1
Ontario	- 27	- 03	+ 5 3	+ 5 8	1 02	1 01	6 8	3 1	+ 75	+ 97	+12 2	+ 8 9
St Louis	- 32	- 20	+ 9 4	+14 8	14	18	3 4	3.8	- 18	- 02	+12 8	+18 6
San Franc	+ 15	+ 12	+25 3	+24 3	62	59	6.7	11 7	+ 77	+ 72	+31 9	+35 9
New Orleans	- 13	- 20	+59 4	+63 09	31	22	71	2 4	+ 18	+ 02	+60 1	+65 5
NAFEC	+ 53	+ 38	+ 5 8	- 5 6	76	58	8 10	7 9	+1 3	+ 96	+13 9	

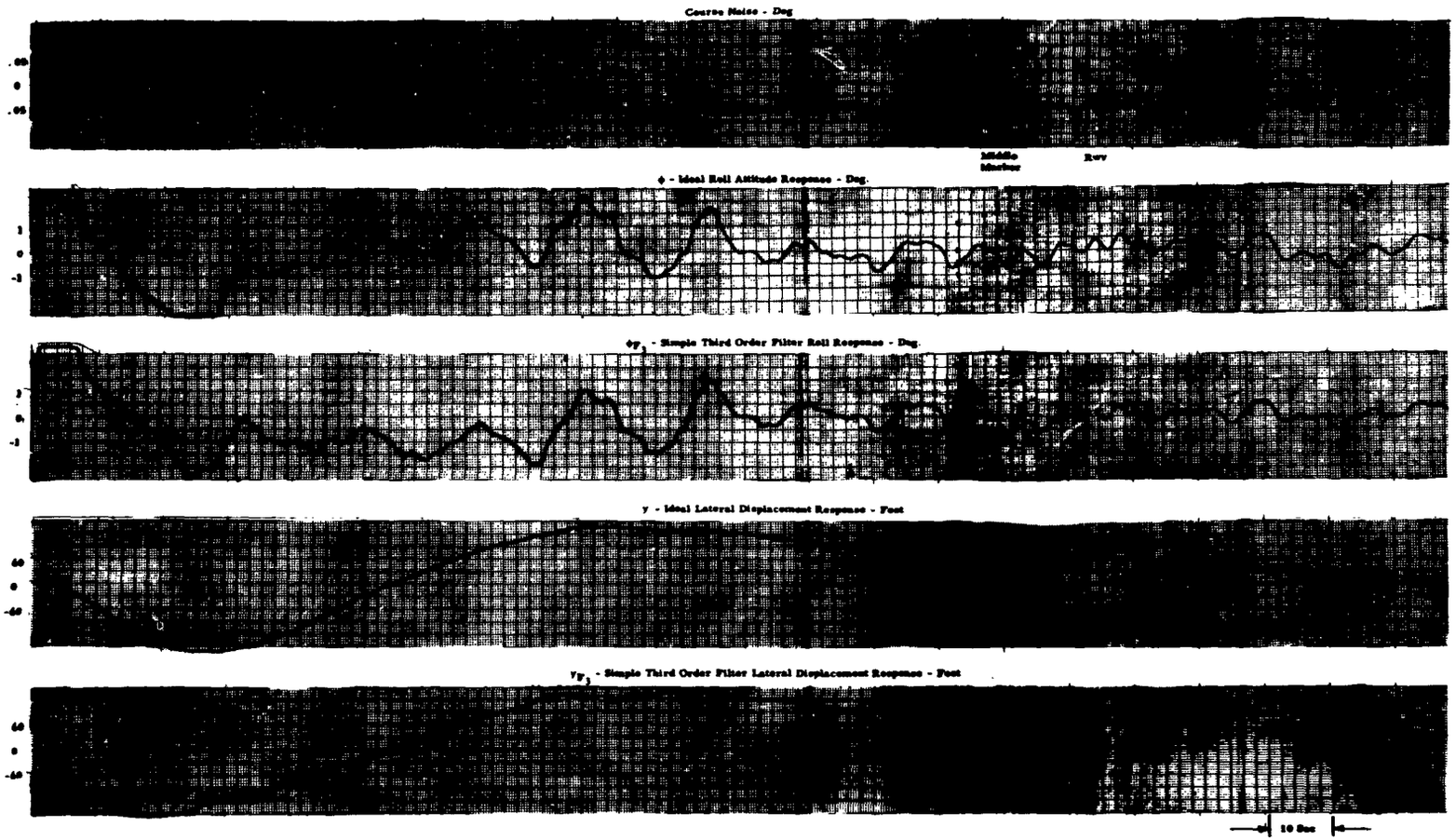

Figure 35 **New Orleans Localizer Facility - Filter Responses**

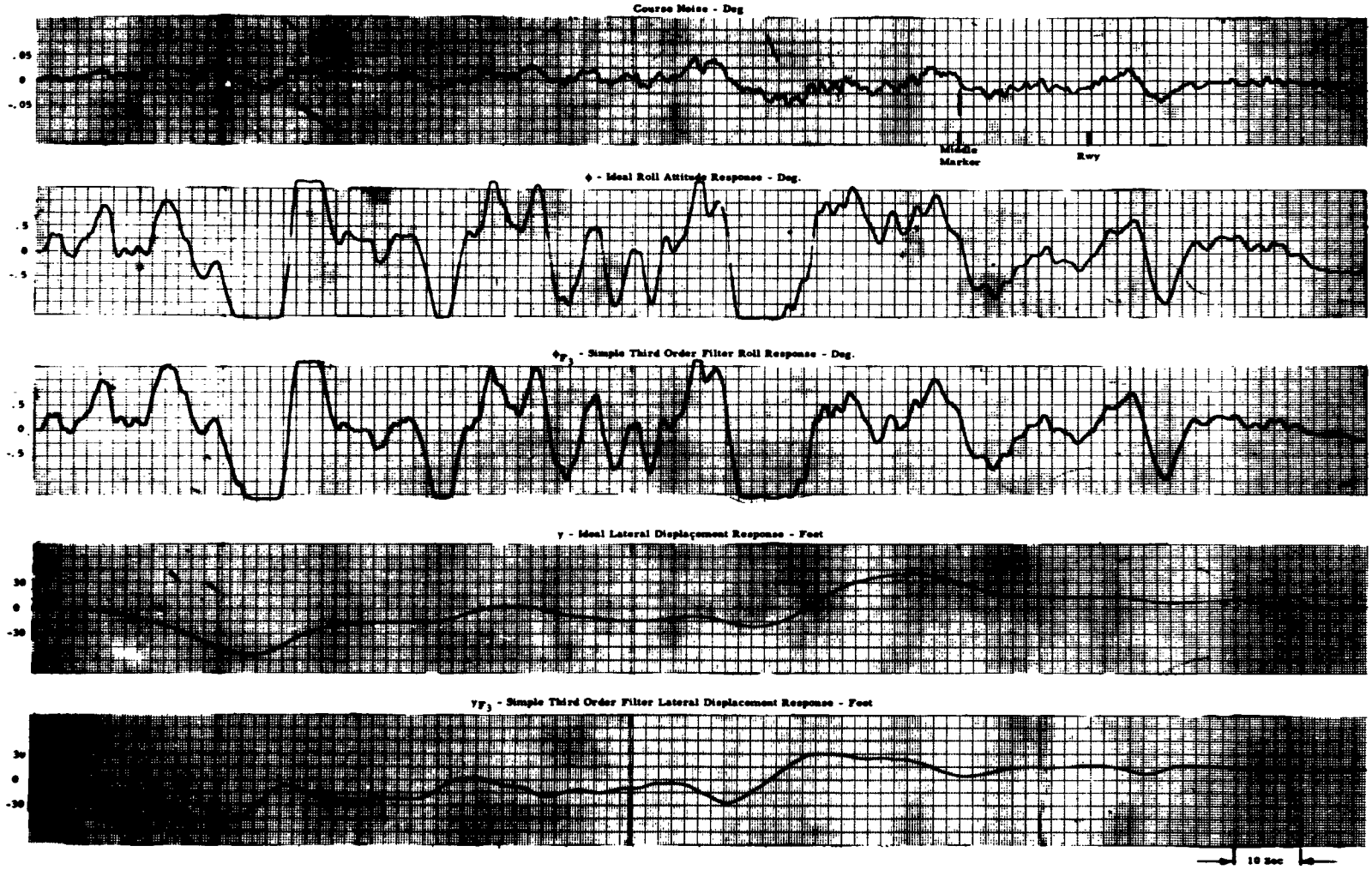

Figure 36 Chicago Localizer Facility - Filter Responses

3.2 NOISE VARIANCE STUDY

3.2.1 Localizer Noise Variance Study

The object of this portion of the study was to determine whether an amplitude specification can be used as an acceptable criterion for low approaches. The test procedure was to generate, using a random noise source, a signal whose standard deviation was a prescribed function of the range to the transmitter. Figure 37 shows the assumed noise variation and the present ILS course/path noise amplitude specification assuming that the maxumum noise amplitude actually represents two standard deviations. The maximum course noise amplitude at the outer marker was kept at a 2σ value of $\pm$ 30 μa and the final value at a point 7000 feet from the runway was adjusted during the tests from a 2σ value of 5 μa to 30 μa. The course/path noise variation between the outer and middle markers was chosen to be a uniformly decreasing function instead of the present step specification since that characteristic is more likely to be encountered in practice. The course/path noise standard deviation was kept constant from the 7000 foot point throughout the rest of the approach.

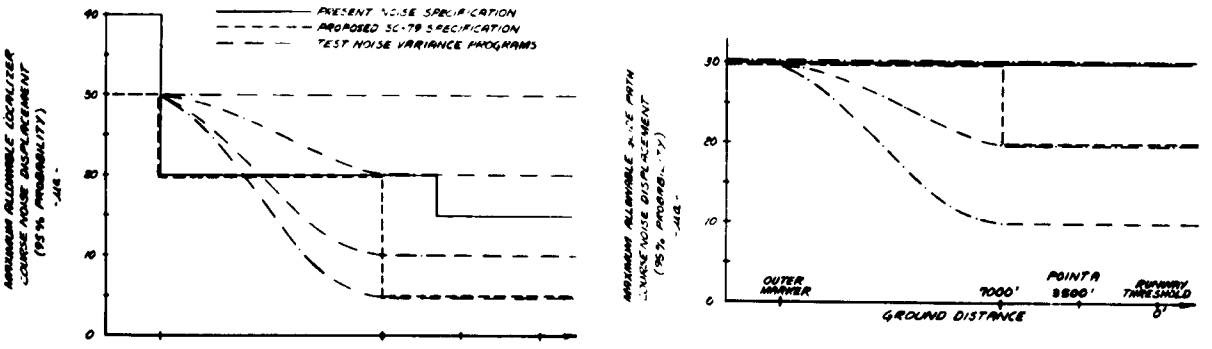

Figure 37 Localizer and Glide Path Noise Variance Programs

Since the simulated course/path noise was random in amplitude and frequency content up to a corner frequency of 3 radians/second, approximately twenty tests were conducted for each condition to ascertain the average or most likely responses.

In the lateral study the pertinent responses were considered to be the lateral deviation from the runway centerline and the rolling activity. In the longitudinal glide slope study, the pertinent responses were taken to be the altitude deviation from the ideal glide path and the pitch attitude activity.

Table XXIII shows the results of the lateral study and Table XXIV shows the longitudinal results for the KC-135, TF-102, and DC-7 aircraft.

TABLE XXIII
SUMMARY OF LOCALIZER RESULTS
CONTINUOUS VARIATION OF STANDARD DEVIATION
OF SIMULATED COURSE NOISE

KC-135A

$2\sigma_{n_{rwy}}$	μa	5	10	20	30
Heading Damped					
$\bar{y}_{MM}$	ft	-7.62		-16.2	-11.5
$\sigma_{y_{MM}}$	ft	10.3		9.5	16.1
$\bar{\sigma}_{\phi_{MM}}$	deg				.99
$\bar{y}_{rwy}$	ft	-.31		-16.7	-8.1
$\sigma_{y_{rwy}}$	ft	11.77		7.07	13.3
$\bar{\sigma}_{\phi_{rwy}}$	deg	.069			.94
Rate Damped					
$\bar{y}_{MM}$	ft	3.3	7.6	8.2	33
$\sigma_{y_{MM}}$	ft	10.7	14.1	22	23.4
$\bar{\sigma}_{\phi_{MM}}$	deg	.778	1.44	2.08	2.09
$\bar{y}_{rwy}$	ft	.86	3.5	6.7	22.2
$\sigma_{y_{rwy}}$	ft	3.36	10	12	20.3
$\bar{\sigma}_{\phi_{rwy}}$	deg	.466	1.34	2.00	2.19

DC-7

$2\sigma_{n_{rwy}}$	μa	10	30
Heading Damped			
$\bar{y}_{MM}$	ft	-4.75	-7.35
$\sigma_{y_{MM}}$	ft	4.9	18.5
$\bar{\sigma}_{\phi_{MM}}$	deg	.157	.799
$\bar{y}_{rwy}$	ft	-1.8	-8.6
$\sigma_{y_{rwy}}$	ft	10.3	11.8
$\bar{\sigma}_{\phi_{rwy}}$	deg	.825	.659
Rate Damped			
$\bar{y}_{MM}$	ft	-3.8	-11.8
$\sigma_{y_{MM}}$	ft	10.3	30.6
$\sigma_{\phi_{MM}}$	deg	.825	1.62
$\bar{y}_{rwy}$	ft	.66	-13.9
$\sigma_{y_{rwy}}$	ft	9.78	12.9
$\bar{\sigma}_{\phi_{rwy}}$	deg	1.07	1.33

TF-102

$2\sigma_{n_{rwy}}$	μa	10	20	30
Heading Damped				
$\bar{y}_{rwy}$	ft	-1.15	.435	-4.73
$\sigma_{y_{rwy}}$	ft	5.53	7.19	10.4
$\bar{\sigma}_{\phi_{rwy}}$	deg	.692	1.25	1.75
$\bar{y}_{MM}$	ft	-1.81	.17	-3.09
$\sigma_{y_{MM}}$	ft	7.27	15.8	17.7
$\bar{\sigma}_{\phi_{MM}}$	deg	.069	1.37	1.81

TABLE XXIV
SUMMARY OF RESULTS
CONTINUOUS VARIATION OF STANDARD DEVIATION OF SIMULATED GLIDE PATH NOISE

DC-7

$2\sigma_{n_{rwy}}$	μa	10	30
Δh_{MM}	ft	+ .135	+ .184
$\sigma\Delta h_{MM}$	ft	+ .575	2.27
$\bar{\sigma}\theta_{MM}$	deg	.271	.515
Δh_{rwy}	ft	+ .019	- .180
$\sigma\Delta h_{rwy}$	ft	+ .239	1.88
$\bar{\sigma}\theta_{rwy}$	deg	.294	.550

KC-135A

$2\sigma_{n_{rwy}}$	μa	10	20	30
Δh_{MM}	ft	.668	1.52	.141
$\sigma\Delta h_{MM}$	ft	.987	1.67	2.50
$\bar{\sigma}\theta_{MM}$	deg	.058	.116	.459
Δh_{rwy}	ft	.048	.677	.041
$\sigma\Delta h_{rwy}$	ft	.539	.86	1.91
$\bar{\sigma}\theta_{rwy}$	deg	.075	.149	.4135

TF-102

Noise Bandwidth (Rad/Sec)		1.96		3.14	
$2\sigma_{n_{rwy}}$	μa	10	30	10	30
Δh_{MM}	ft	.148	.062	-.096	.265
$\sigma\Delta h_{MM}$	ft	.717	3.09	.995	3.33
$\bar{\sigma}\theta_{MM}$	deg	.305	.510	.300	.531
Δh_{rwy}	ft	.042	.234	+.108	.404
$\sigma\Delta h_{rwy}$	ft	.933	1.79	.882	2.60
$\bar{\sigma}\theta_{rwy}$	deg	.357	.546	.337	.653

In an effort to aid in validating any course/path noise amplitude specification using the simulated noise source, the data using that noise was combined with the results of similar responses using the actual theodolite corrected ILS recordings as described in Section 2.

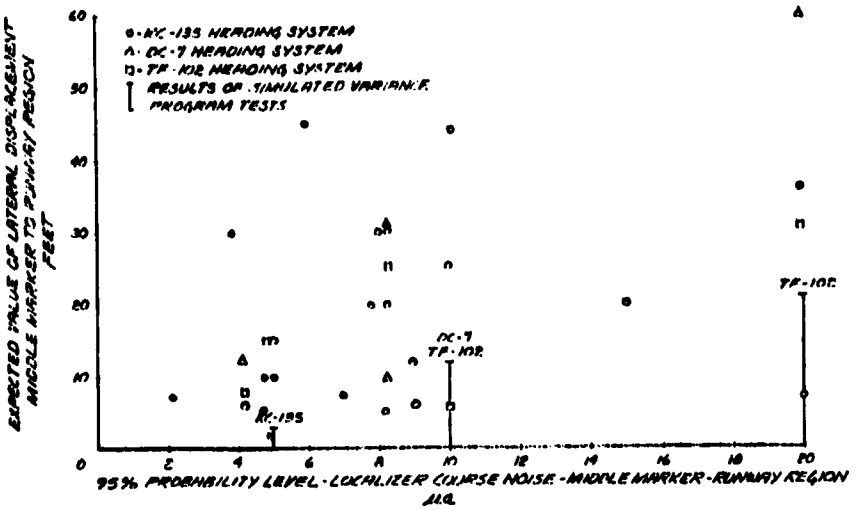

Figure 38 Localizer - Lateral Deviation Results - Heading System

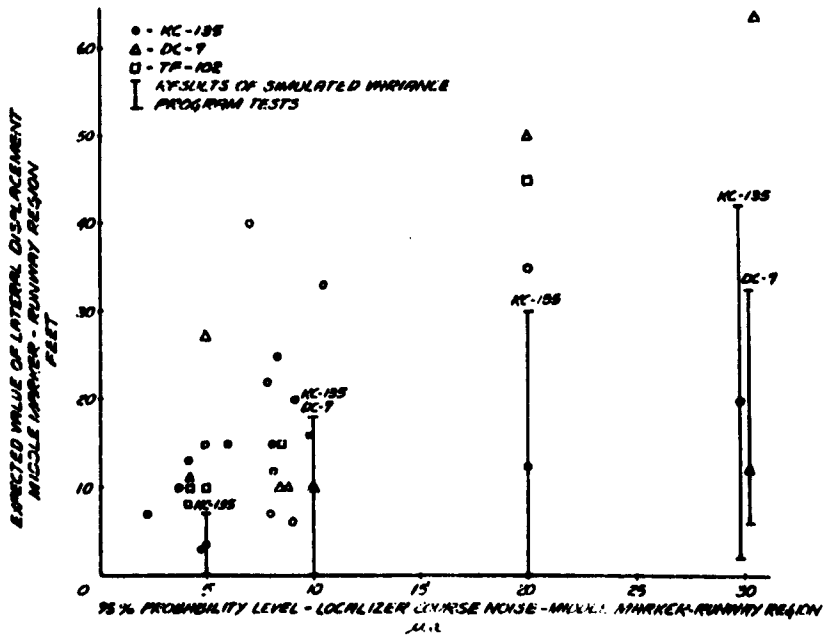

Figure 39 Localizer - Lateral Deviation Results - Beam Rate System

Figures 38 through 41 show the results of combining the actual and simulated course noise for the localizer mode of operation. The vertical bars are capped at the minimum and maximum attitude or displacement that was found during each of the simulated noise test sequences. The single marked point in each bar represents the standard deviation of the particular parameter. The individual points shown in these figures represent the results of the response tests at each of the ILS facilities using the theodolite corrected data.

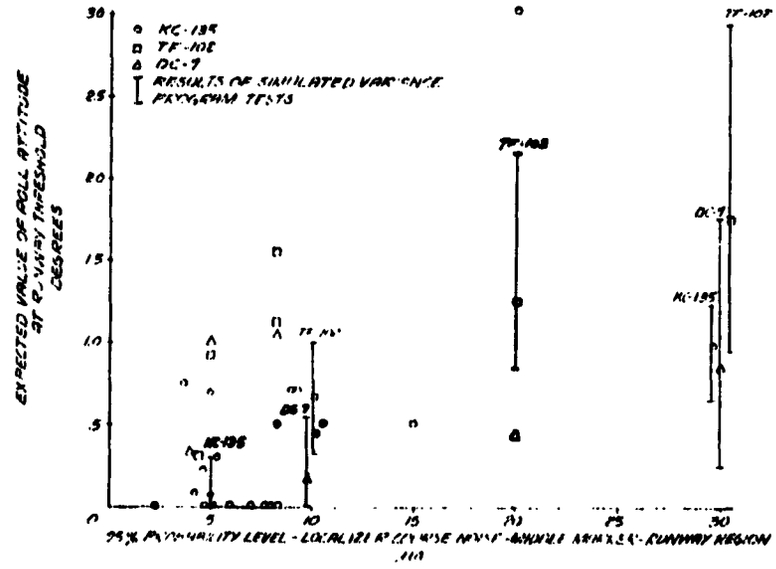

Figure 40 Localizer - Roll Attitude Results - Heading System

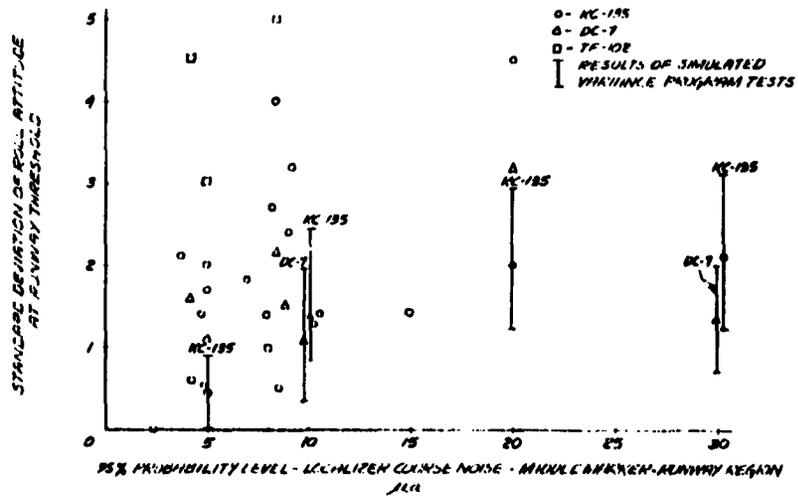

Figure 41 Localizer - Roll Attitude Results - Beam Rate System

The results of the simulated versus actual course noise tests only agree with one another on the average since the simulated noise is derived from an almost perfect random noise generator, and the actual course bends are not nearly as statistically stationary. Another reason for the disagreement is the fact that the actual course noise standard deviations do not change in the same manner as the simulated noise was allowed to change. However, for both types of localizer coupler systems, a two-sigma noise value of 5 μa in the middle marker-runway region would restrict the expected value (mean plus standard deviation) of the lateral deviations to below 15 feet and the expected value of roll attitude to below two degrees. It is believed that this low value of course noise may be used as the criterion for the future use of the ILS localizer since the additional aircraft responses to gusts and other disturbances would increase the deviations. Referring to Figures 38 through 41 indicates however that choosing this low value of maximum course noise forces the rejection of some of the present localizer systems even though, in the case of some of the systems with higher noise content, acceptable performance can in fact be obtained.

Even more importantly there is one facility which fails the performance specifications but passes the 95% probability level course noise amplitude specification. Table XXV which is a compilation of these facilities which pass or fail the performance or noise specifications shows this very clearly. A conflict is indicated when the results of the performance or noise amplitude specifications do not agree. For the heading damped system there are five conflicts if the maximum lateral offset specification is fifteen feet. The results at Miami, however, indicate that this facility would pass the noise specification and not pass the maximum lateral deviation specification. This is true even if that specification were increased to 20 feet instead of 15. With the 20 foot specification, the San Francisco and Chicago facilities are added to the conflict list wherein the noise specification is failed but the performance is acceptable.

The right hand position of Table XXV shows the same type of results for the rate damped control system. In this case the conflicts between the performance and noise specifications also include the undesirable case in which the Miami facility passes the amplitude criteria; but, the rolling activity is beyond the acceptable 2 degree level. All the other conflicts would unnecessarily penalize the localizer facilities. Table XXVI shows that there is considerable agreement between the results of applying the performance and noise amplitude specifications to the three test aircraft. Only one unsatisfactory conflict occurs and this with the St. Louis facility, with the DC-7 beam rate coupler system.

TABLE XXV

APPLICATION OF PERFORMANCE AND COURSE NOISE AMPLITUDE SPECIFICATIONS TO TEST LOCALIZER FACILITIES

KC-135

Facility	95% Prob Noise Ampl ≤ 5 μa MM-Rwy	Heading Damped System			Rate Damped System		
		$\epsilon_y \leq 15$ (or 20) MM-Rwy Feet	$\sigma\phi \leq 2$ Rwy Deg	Conflict	$\epsilon_y \leq 15$ (or 20) MM-Rwy Feet	$\sigma\phi \leq 2$ Rwy Deg	Conflict
Fort Worth	No	Yes	Yes	Yes	Yes	Yes	Yes
Detroit	Yes	Yes	Yes		Yes	Yes	
Baltimore	Yes	Yes	Yes		Yes	Yes	
San Francisco	No	No (yes)	Yes	No (yes)	Yes	No	Yes
Atlantic City	Yes	Yes	Yes		Yes	Yes	
Duluth	Yes	Yes	Yes		Yes	Yes	
Miami	Yes	No (no)	Yes	Yes (yes)	Yes	No	Yes
Chicago	No	No (yes)	Yes	No (yes)	No (no)	Yes	
Dallas	No	No (no)	Yes		No (no)	No	
Idlewild	Yes	Yes	Yes		Yes	Yes	
St. Louis	Yes	Yes	Yes		Yes	Yes	
Ontario	No	No (no)	Yes		No (yes)	Yes	No (yes)
Birmingham	No	No (no)	Yes		No (no)	Yes	
Los Angeles	No	Yes	Yes	Yes	Yes	No	
Minneapolis	Yes	Yes	Yes		Yes	Yes	
Houston	Yes	Yes	Yes		Yes	Yes	
Washington, D.C.	No	Yes	Yes	Yes	No (yes)	No	
Cleveland	No	No (no)	Yes		Yes	Yes	Yes
Louisville	No	Yes	Yes	Yes	No (no)	Yes	
New Orleans	No	No (no)	Yes		Yes	Yes	Yes
Burbank	No	No (no)	No		No (no)	No	
Atlanta	No	No (no)	Yes		No (no)	Yes	

NOTE:

1. "Yes" denotes that the noise and its effects are within the specified limits

2. "No" denotes that the noise and its effects are not within the specified limits

3. A conflict denotes the case wherein there was an inconsistency between the noise amplitude and performance specifications.

TABLE XXVI
COMPARISON OF EFFECTS OF APPLYING ACCEPTANCE CRITERIA
TO KC-135, DC-7, AND TF-102 AIRCRAFT

Facility	95% Prob Noise Ampl ≤ 5 μa MM-Rwy	Heading Damped System $\epsilon_y \leq 15$ (20) Feet KC-135	DC-7	TF-102	Conflict
Atlantic City	Yes	Yes	Yes	Yes	
St. Louis	Yes	Yes	Yes	Yes	
Burbank	No	No (no)	No (no)	No (no)	
Dallas	No	No (no)	No (no)	No (no)	
San Francisco	No	No (yes)	Yes	Yes	No (yes)
		Rate Damped System $\epsilon_y \leq 15$ (20) Feet			
Atlantic City	Yes	Yes	Yes	Yes	
St. Louis	Yes	Yes	No (no)	Yes	Yes
Burbank	No	No (no)	No (no)	No (no)	
Dallas	No	No (no)	Yes	Yes	
San Francisco	No	Yes	Yes	-	Yes

NOTE: See Note for Table XXV

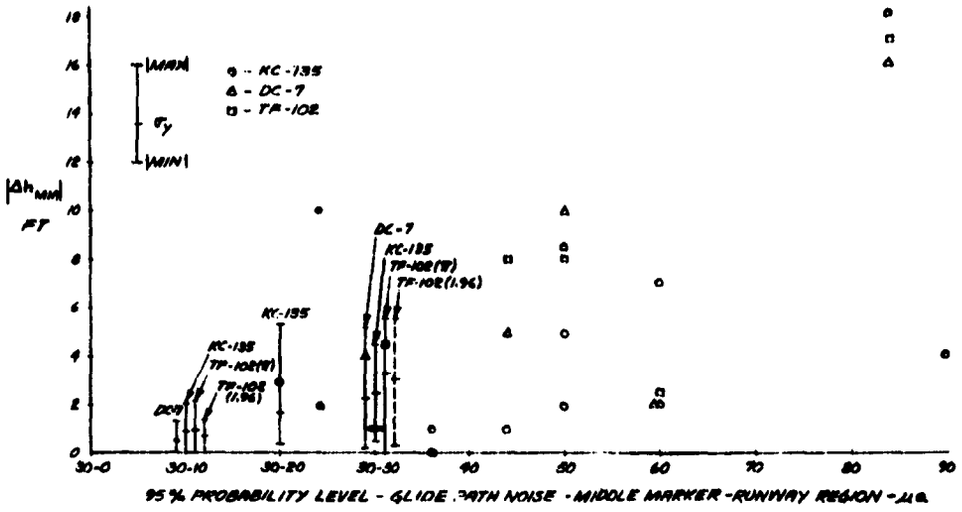

Figure 42 Glide Path - Altitude Deviation Results - Middle Marker

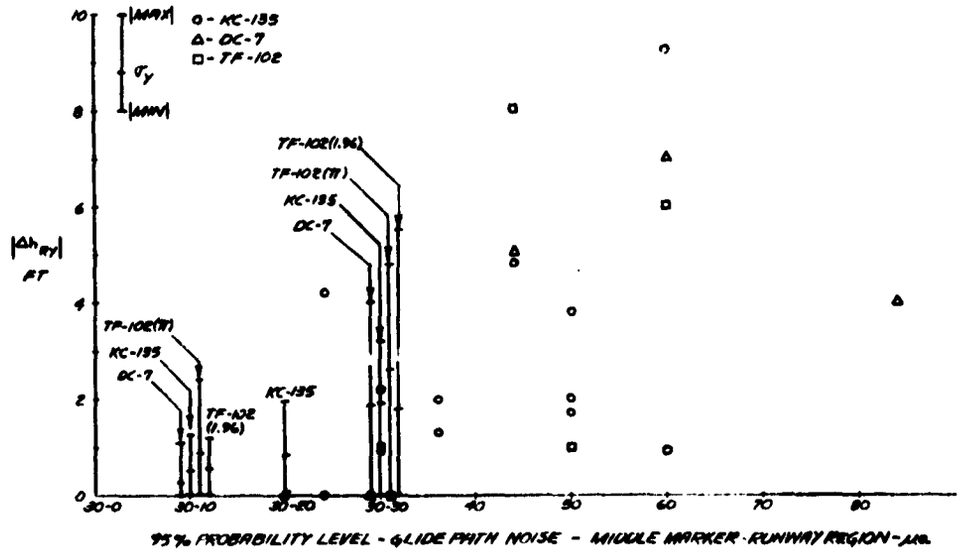

Figure 43 Glide Path - Altitude Deviation Results - Runway

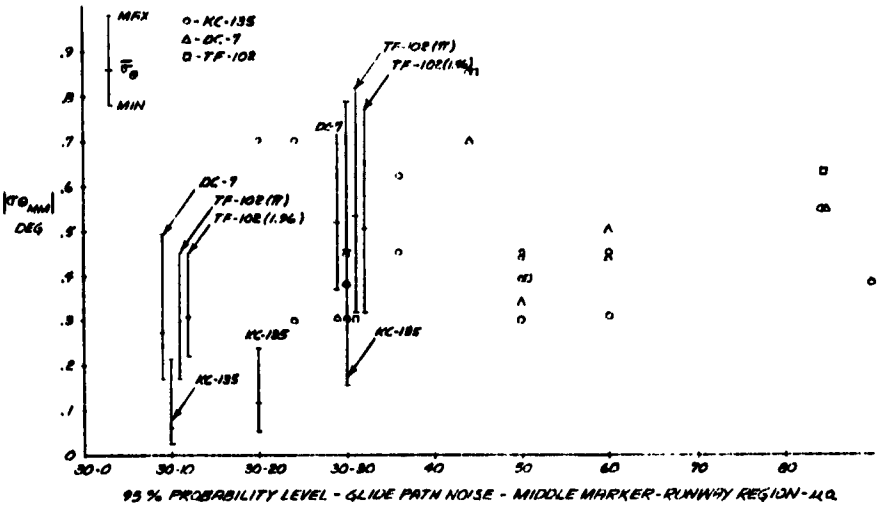

Figure 44 Glide Path - Pitch Attitude Results - Middle Marker

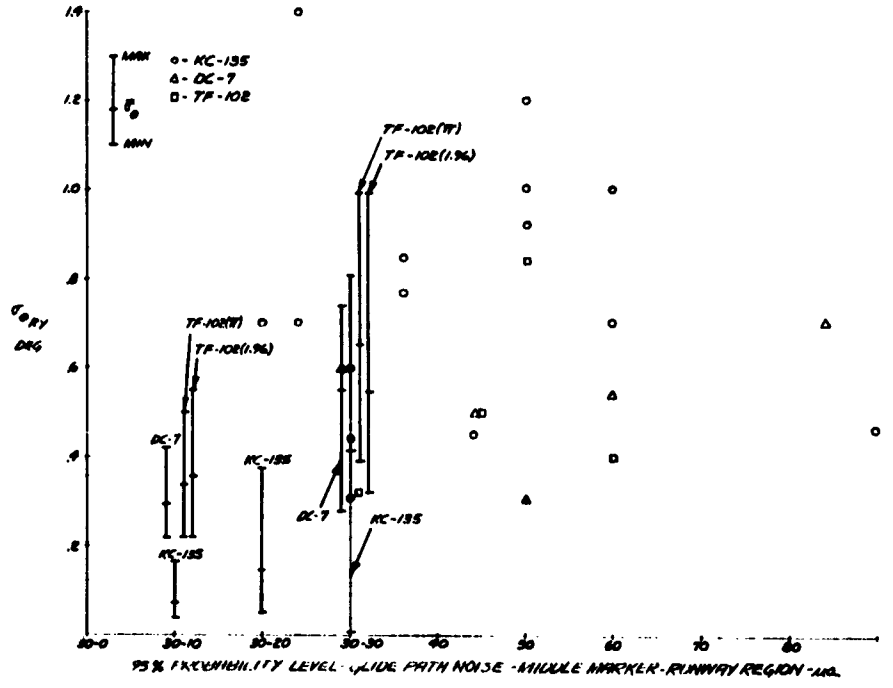

Figure 45 Glide Path - Pitch Attitude Results - Runway

It is clear that this approach of specifying a maximum allowable noise amplitude is not the best technical solution to the problem although it does provide an acceptable solution in terms of immediate and relatively simple implementation. These considerations are further expounded upon in the Appendix where the problem is treated using statistical decision theory to prove that a complete analog simulation offers the best technical approach to specifying ILS beam acceptance.

3.2.2 Glide Path Noise Variance Study

The same general comments that were just made for the localizer can be made of the glide path results. In this case, as shown in Figures 42 through 45, the 20 μa, 95% probability path noise amplitude in the middle marker-runway region is acceptable by providing pitch attitude standard deviations of less than one degree and altitude deviations of less than four feet at the runway threshold. An allowable noise amplitude between 20 and 30 μa could be chosen for those coupler systems which use attitude damping. However, the increased disperions of those coupler systems which use beam rate damping as well as the additional responses to gusts and other disturbances force the 20 μa figure to be recommended.

Table XXVII is a compilation of the glide path test facilities along with information as to which passed or failed the various performance and path noise amplitude specifications. Four conflicts between the two specifications are noted in the fourth column of Table XXVII. Of these only the Louisville facility has the undesirable characteristic of passing the noise amplitude specification and failing the performance criteria. Eight of the test facilities, including Louisville, pass the 20 μa maximum path noise amplitude specification. Table XXVIII compares the results of applying the specifications to the three test aircraft at some of the glide path facilities. The only conflict occurs at the St. Louis facility which would be rejected unnecessarily since the performance is adequate although the noise amplitude specifications is exceeded.

The results of the variance programs with the TF-102 system were repeated using a noise bandwidth of 1.96 rad/sec in addition to the 3.14 rad/sec bandwidth that was used throughout the tests. No significant differences were found to exist, as shown in Figures 42 through 45.

It is interesting to note that these glide slope responses were derived using conventional approach coupler systems with increased desensitization rates to account for the lower altitude approaches. No glide slope extension schemes were included. It would seem therefore that the need for such extension systems would decrease if the present ILS facilities could be guaranteed to have the lower noise content.

TABLE XXVII
APPLICATION OF PERFORMANCE AND PATH NOISE AMPLITUDE SPECIFICATIONS TO TEST GLIDE PATH FACILITIES KC-135

Facility	95% Prob Noise Ampl ≤ 20 μa MM-Rwy	$\Delta h_{Rwy} \leq 4$ Feet	$\sigma\theta_{Rwy} \leq 2$ Deg	Conflict
Detroit	No	-	-	
San Francisco	Yes	Yes	Yes	
Atlantic City	No	Yes	Yes	Yes
Miami	Yes	Yes	Yes	
Chicago	Yes	Yes	Yes	
Idlewild	No	Yes	Yes	Yes
St. Louis	No	-	-	
Ontario	No	No	Yes	
Minneapolis	Yes	Yes	Yes	
Houston	No	Yes	Yes	Yes
Washington, D.C.	Yes	Yes	Yes	
Cleveland	No	No	Yes	
Louisville	Yes	No	Yes	Yes
New Orleans	Yes	Yes	Yes	
Burbank	No	No	Yes	
Atlanta	Yes	Yes	Yes	
Kansas City	No	No	Yes	

NOTE: See Note for Table XXV

TABLE XXVIII
COMPARISON OF PERFORMANCE AND
PATH NOISE SPECIFICATIONS WITH GLIDE PATH
FACILITIES FOR KC-135, DC-7, TF-102

Facility	95% Prob Noise Ampl ≤ 20 μa MM-Rwy	KC-135	DC-7	TF-102	Conflict
Atlantic City	No	-	-	-	
St. Louis	No	Yes	Yes	Yes	Yes
Burbank	No	No	No	No	
San Fran.	Yes	Yes	Yes	Yes	
Ontario	No	No	No	No	

NOTE: See Note for Table XXV

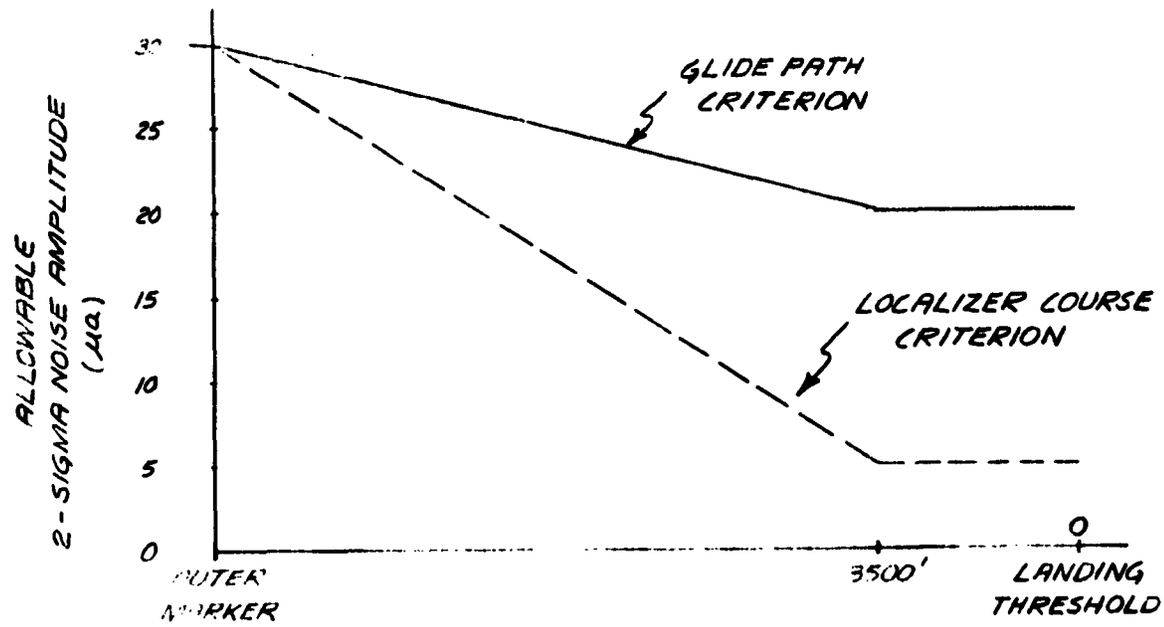

Figure 46 Recommended Course/Path Noise Amplitude Criteria

3.2.3 Use of the Recommended Course/Path Noise Amplitude Criteria

As a result of the preceding studies, Figure 46 shows the relationship between the maximum (95% probability) course/path noise amplitude and the distance from the runway threshold that is being recommended in this report. If the noise is to be evaluated in any region of the approach the theodolite-corrected flight recording should be analyzed for a time interval not less than $\pm$ 10 seconds and not more than $\pm$ 20 seconds about the midpoint of the region to be evaluated.

The 95% maximum amplitude specification is the allowable percentage of the total time interval in which the course/path noise amplitude must be less than the amount specified in Figure 46 for the region being evaluated. Figure 47 presents a typical example of the method that can be employed to evaluate the course/path noise at a particular facility. If the sum of the time intervals t_1, t_2, t_3 that the given specification is exceeded, is equal to or less than 5% of the total time, T, then the region that is being evaluated is acceptable.

Therefore, $$100\,\frac{[T - (t_1 + t_2 + \ldots)]}{T} \geq 95\%$$

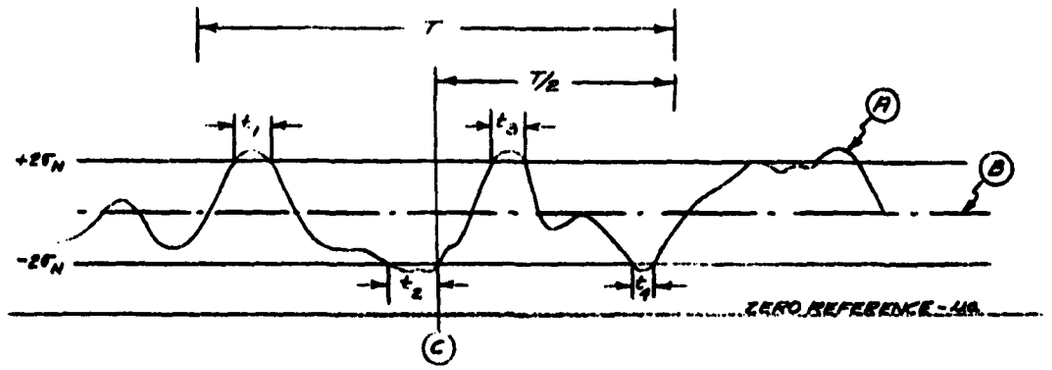

(A) - THEODOLITE CORRECTED SAMPLE OF COURSE/PATH NOISE - μa

(B) - MEAN VALUE OF COURSE/PATH NOISE - μa

T - REGION TO BE EVALUATED ($\pm$10 TO $\pm$20 SECONDS WIDE)

$\pm 2\sigma_N$ - MAX NOISE AMPLITUDE SPECIFICATION AT POINT (C) - μa

$t_1, t_2, t_3, \cdots$ - TIME INTERVALS THAT NOISE EXCEEDS ALLOWABLE $2\sigma_N$ VALUE

FOR THE FACILITY TO BE ACCEPTABLE IN THIS REGION, $100\,\frac{[T-(t_1+t_2+t_3+\cdots)]}{T} \geq 95\%$

Figure 47 Recommended Course/Path Noise Amplitude Criteria

APPENDIX
USE OF STATISTICAL THEORY IN CLASSIFYING ILS FACILITIES

1. SUMMARY

This appendix discusses the classification of ILS facilities by statistical decision theory, the type of problems the theory solves, and the validity of applying an optimization criterion of the theory to the classification of the ILS facilities (acceptable or not down to some specified altitude).

The motivation for considering the applicability of decision theoretic criteria to facility classification stems from the initial choice of the beam error power spectrum as the measurements on which the classification of each facility is to be based. In effect, the choice of the beam error spectrum, assigns to it the role of an observable, in the context of decision theory, which is to be used to predict the conditions of all the landing parameters by which the descent operation is defined as acceptable or not. The statistical character of the beam error spectra, resulting from measurements for each of 25 ILS facilities presently available, was found to be unsatisfactory, that is, the spectra turned out to be uncorrelated with the values of the landing parameters as found by exact simulation of the aircraft control system fed by the error histories of each of the facilities. Although it can easily be demonstrated theoretically, that a zero beam error spectrum results in zero landing errors, it can also be shown that the beam error spectral measurements are uncorrelated, nontrivially, with the landing errors.

Following the demonstrated failure of the beam error spectrum to correlate with the simulated landing errors, a general examination was undertaken of the applicability of statistical decision methods to the problem of facility classification. The conclusion is that the only chance of obtaining satisfactory correlation between an observable and the true landing parameter is provided by a simulation channel approximation of each of the landing parameters for its corresponding observable, thus giving up the notion that frequency distributed measurements on the input parameter, i.e., the beam error, can correlate with each of the landing parameters. This one-to-one correspondence between observable and landing parameter, admittedly requires more complex measurement equipment, and one can safely assume a trade-off between the order of approximation (and thus the complexity) of the measurement channels, and the degree of correlation.

2. ELEMENTS OF STATISTICAL DECISION THEORY

This topic is discussed following consideration of the type of conditions under which an ILS facility is to be classified as acceptable or rejectable by the FAA. A sound method for this binary classification of future facilities is, for the purposes of this report, the objective of the study. A summary of the conditions and their relation to statistical decision theory follows.

First, the FAA imposes a specification on several descriptive landing parameters, such as errors in longitudinal and lateral displacements, altitude rate, pitch and roll, these errors being specified at touchdown, or at any altitude at which a transition from automatic to manual landing is of interest. In addition to the aforesaid instantaneous parameters, a mean square time average specification imposed on control surface activity (mean square aileron elevator and rudder deflections over the duration of the ILS descent operation) would be consonant with what pilots are tactually made aware of. The specifications on the bounds of these errors are dictated by experience, and are given conditions of the problem from the point of view of statistical decision theory.

The mathematical theory enters into the problem of classifying an ILS facility, when the information available to the decision maker is no more than statistical, and the decision maker wants to find decision rules such as to minimize, or bound in the long run, his misclassification errors.

An example, taken from Reference 11 best illustrates the problem:

Suppose a weatherman is to decide each day between two hypotheses: H_0 - it will rain tomorrow, and H_1 - it will be fair tomorrow. The decision is to be made on the basis of a single observed quantity, the average rate of change, x, of the barometric pressure during the past 24 hours. From records compiled over years, the probability distribution density (p. d. d.), $p(x \mid H_0)$, describing the distribution of x on days preceding rain, and the

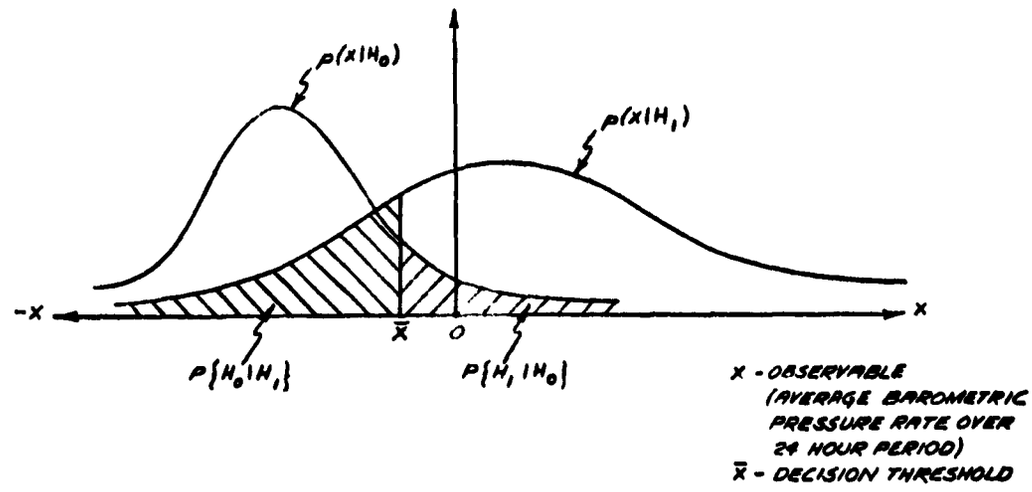

Figure 48 Conditional Distribution Densities
Single Decision Threshold

p.d.d., $p(x|H_1)$, describing the distribution of x on days preceding fair ones, are precomputed

A plausible realization of these two distributions is illustrated in Figure 43, with the 24 hour average barometric rate on days preceding rain being distributed more negatively than on days preceding fair weather days.

The weatherman can now utilize this statistical information by adopting a decision rule of the following type:

(a) Predict a rainy day, if the observed average rate x is less than some threshold, $\bar{x}$, decided upon in advance.

(b) Predict a fair day, if the observed rate x is greater than $\bar{x}$.

Now, owing to the overlap of the distributions $p(x|H_0)$ and $p(x|H_1)$, no matter what choice for the decision threshold, $\bar{x}$, that the weatherman adopts, he risks making each of two kinds of misclassifications:

(c) Predicting fair weather when in fact it will rain,

(d) Predicting rainy weather, when in fact it turns out to be fair.

(In general, if a statistical predictor is called upon to predict n categories, rather than just two as in this example, he risks making n(n-1) kinds of misclassification.)

For a choice of some particular $\bar{x}$, as a point which divides the observation parameter into the two regions, the probability of making the mistake stated in (c) is then

$$(1)\quad P\left\{H_1 \middle| H_0\right\} = \int_{\bar{x}}^{\infty} p(x \mid H_0)\,dx = Q_0(\bar{x})$$

and for the mistake stated in (d)

$$(2)\quad P\left\{H_0 \middle| H_1\right\} = \int_{-\infty}^{\bar{x}} p(x|H_1)\,dx = Q_1(\bar{x})$$

2.1 BAYES CRITERION

Now, if the weatherman has, in addition to the statistical information described by the conditional p.d.d.'s, $p(x \mid H_o)$ and $p(x \mid H_1)$, (1) the prior probabilities of the occurrence of rainy and fair days; that is independent of the observations of barometric pressure rates, he notes the relative frequency of occurrence of rainy and fair days, and, where this relative frequency of occurrence is fairly constant, assigns prior probabilities

$$(3)\quad P\{H_o\} = W, \quad P\{H_1\} = 1 - P\{H_o\} = 1 - W$$

and (2), a realistic assessment of costs or risks on some scale for erring in each of the two ways described, C_{10} and C_{01}, he can adjust $\bar{x}$, the parameter which specifies the decision strategy in this case, such as to minimize his average risk,

$$(4)\quad P\{H_1 \mid H_o\}\, P\{H_o\}\, C_{10} + P\{H_o \mid H_1\} \left[1 - P\{H_o\}\right] C_{01} = \bar{C}$$

The optimum adjustment of $\bar{x}$, following from the required information, is put in evidence by noting that $P\{H_1 \mid H_o\}$ and $P\{H_o \mid H_1\}$ are functions of $\bar{x}$, as given by (1) and (2), and that $P\ H_o$ and $P\ H_1$ have, by hypothesis, known values, W, and 1-W. Hence the average risk $\bar{C}$ is a function of $\bar{x}$, and the cost elements, C_{10} and C_{01}. Equation (4) is then rewritten

$$(4a)\quad \bar{C}(\bar{x}, R_o) = Q_o(\bar{x})\ W\ C_{10} + Q_1(\bar{x})\ (1-W)\, C_{01}$$

An optimum decision threshold, $\bar{x}_B$, can then be found from the constraint,

$$(5)\quad \frac{\partial \bar{C}}{\partial \bar{x}} \text{ set} = 0 = Q_o'(\bar{x}_B)\, W\, C_{10} + Q_1'(\bar{x}_B)\,(1-W)\, C_{01}$$

which yields

$$(6)\quad \bar{x}_B = f(W, C_{01}, C_{10}).$$

For the decision threshold, $\bar{x}$, found under such constraints, the weatherman is said to adopt a Bayes strategy.

2.2 MINIMAX CRITERION

If the weatherman does not know the prior probabilities of occurrence of rainy and fair days, W and 1-W, but can scale the costs, C_{10} and C_{01}, and can prescribe the two conditional d.d.'s, $p(x|H_o)$ and $p(x|H_1)$, he can find a decision threshold, $\bar{x}_M$, which minimizes his maximum risk. This he does by considering the prior probability, W, as a variable, and applying the constraint,

$$(7)\quad \frac{\partial \bar{C}}{\partial W} \text{ set } = 0 = Q_o(\bar{x}_M)C_{10} - Q_1(\bar{x}_M)C_{01}$$

which yields

$$(8)\quad \bar{x}_M = g(C_{10}, C_{01}).$$

It may be noted that $\bar{x}_M$ depends only on the costs, assumed by hypothesis, to be available.

Now if the prior probability, W, is considered an unknown in (4-a), the Bayes constraint (5) is applied, and $\bar{x}_M$, as obtained from (7), is substituted for $\bar{x}_B$, in (5), the result will be a constraint on the unknown prior probability, W, yielding some value, W_M, i.e.,

$$(9)\quad \frac{\partial \bar{C}}{\partial \bar{x}} (\bar{x}_M, W_M) \text{ set } = 0 = Q_o'(\bar{x}_M)W_M C_{10} + Q_1'(\bar{x}_M)(1-W_M)C_{01}$$

It can then easily be shown that the pair, $\bar{x}_M$, W_M is a saddle point of $\bar{C}(\bar{x}, W)$, and from the constraints applied to obtain $\bar{x}_M$ and W_M, it can be inferred that $\bar{C}(\bar{x}_M, W_M)$ is a minimum with respect to $\bar{x}$, and a maximum with respect to W. The value $\bar{x}_M$ as obtained from (7), thus corresponds to a Bayes strategy under the most unfavorable prior probability, W_M, and is thus optimal under a minimax criterion.

2.3 NEYMAN - PEARSON CRITERION

If the weatherman does not know either the prior probability of the occurrence of rainy and fair days, nor the costs, C_{10} and C_{01} for the two kinds of error, but has realistic models of the conditional disturbances,

$p(x|H_o)$ and $p(x|H_1)$, he obviously cannot minimize his average risk, $\bar{C}$, in any sense. He can however, arrive at a useful optimization of $\bar{x}$, the decision threshold, by imposing a constraint which practically always has significance when the prior probabilities and the costs are not available. This constraint consists in assigning a value to the probability of one of the two kinds of error, i.e.,

$$\text{either} \quad P\{H_1|H_o\} = \alpha$$

$$\text{or} \quad P\{H_o|H_1\} = \beta, \tag{10}$$

and minimizing the other error probability.

For the example chosen, it turns out that no minimization is possible, since the assignment of a value, α to $P\{H_1|H_o\}$, or β to $P\{H_o|H_1\}$ determines the decision threshold $\bar{x}$. Another example, however, of wide representation will be shown, where both an imposed constraint and a minimization constraint on the respective errors are required to adjust $\bar{x}$. Before taking up this example, a few remarks on the assigned constraint to one of the errors is in order.

Consider first, a detection radar, which is required to make automatically the binary decision, in the presence of interference: target (H_1), or no target (H_o). In terms of the output of the detector, this amounts to deciding: signal plus noise, or noise alone. Such a radar would require as stored information, $p(x|H_1)$ and $p(x|H_o)$, or the equivalent, where x is now the output voltage of the detector, and $p(x|H_1)$ and $p(x|H_o)$ are the distributions of this voltage due to signal plus noise, and noise alone. The error probabilities, $P\{H_o|H_1\}$ and $P\{H_1|H_o\}$, correspond now to the probabilities of false dismissal, and of false alarm, respectively. For a given environmental signal to noise ratio, a decrease in the decision or alarm threshold, $\bar{x}$, reduces the probability of false dismissal, but must concommitantly, increase the probability of false alarm, as may be seen from Figure 48, resulting in some costly action being taken in rain. Under such conditions, the policy taken is to impose the largest false alarm probability, α, that can be tolerated, arrived at from considerations external to the statistical criterion discussed here, and then to minimize the false dismissal probability, if minimizable.

3. THE STATISTICAL CLASSIFICATION OF ILS FACILITIES

(The classification method discussed in this paragraph is based on the Neyman-Pearson Criterion.)

Assume that the condition of a single landing parameter, y (for example, the lateral displacement at touchdown) specifies the acceptability, H_o, or the rejectability, H_1, of the ILS facility. More specifically, in terms of y,

$$H_o, \text{ if } -\bar{y} \leqslant y \leqslant \bar{y} \Rightarrow |y| \leqslant \bar{y}$$

$$H_1, \text{ if } y < -\bar{y}, \text{ or } y > \bar{y} \quad |y| > \bar{y}$$

If y were available to the decision maker, there would be no statistical problem. Owing, however to the fact that the determination of y, for a given facility and aircraft control system would require a complex simulation channel, a requirement that the decision maker prefers to avoid, an estimator of y, $\tilde{y}$, is determined for each facility and aircraft, this estimator presumably being determined from a substantially simplified simulation channel.

The decision maker now is confronted with prescribing the distribution densities:

$$(11) \quad p(\tilde{y} \,|\, |y| \leqslant \bar{y}) \triangleq p(\tilde{y} \,|\, Ho)$$

and

$$p(\tilde{y} \,|\, |y| > \bar{y}) \triangleq p(\tilde{y} \,|\, H_1)$$

As to how these two functions can be found, is admittedly a basic problem. First, the distributions concern a future population of facilities for which only $\tilde{y}$, not the exact parameter, y, will be available. Let this population consist of N members.

Second, a pilot population consisting of M members, none of which is in the N member population, is subject to the dual determinations, y_k and $\tilde{y}_k$, k = 1 , M, this pilot population being presently in existence, and for which both complete channel simulation determinations, y_k, are feasible.

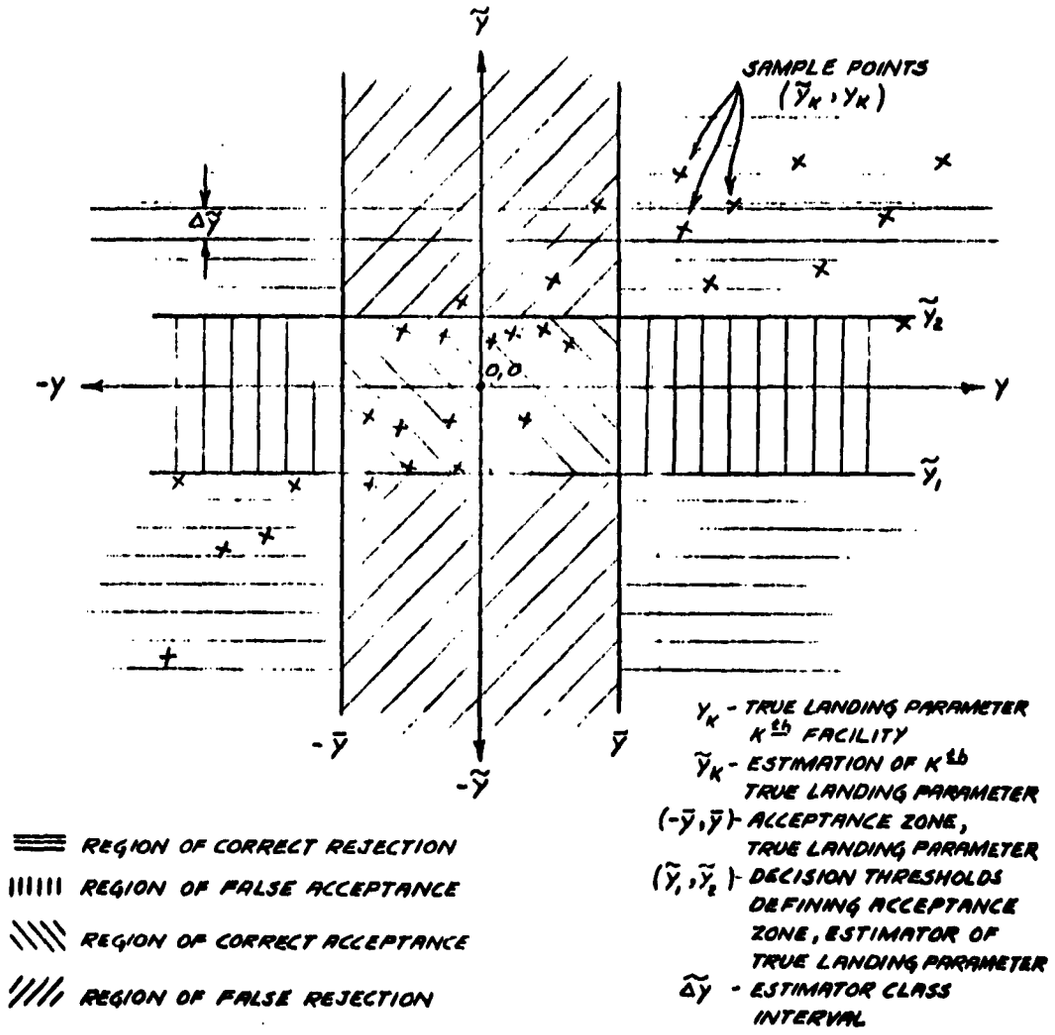

Figure 49 Empirical Correlation Graph

The two-dimensional points $(y_k, \tilde{y}_k)$ can be plotted on a graph representing the y-y plane. (A fictitious example is shown in Figure 49). The estimator axis, $\tilde{y}$, can then be partitioned by a convenient uniform class interval, $\Delta\tilde{y}$. The collection of points are now divided into two classes: those with y coordinates inside the interval $(-\bar{y}, \bar{y})$ corresponding to the H_o-class, and those outside this interval, corresponding to the H_1-class. Abstracted then from the M member population are two histograms:

$$(12)\quad h(\tilde{y}\,\big|\,|y| \leq \bar{y}) = \frac{m_o(\tilde{y}_i)}{M_o \Delta\tilde{y}} = \frac{m_{oi}}{M_o \Delta\tilde{y}}$$

and

$$h(\tilde{y}\,\big|\,|y| > \bar{y}) = \frac{m_1(\tilde{y}_i)}{M_1 \Delta\tilde{y}} = \frac{m_{1i}}{M_1 \Delta\tilde{y}}$$

where $m_o(\tilde{y}_i)$ are the number of points in the i^{th} class interval, conditional upon their y-coordinates being inside the acceptance zone, i.e., for $|y_k| \leq \bar{y}$, $m_1(y_i)$ are the number in the i^{th} class interval conditional upon $|y_k| > \bar{y}$, and M_o and M_1 are the number of points inside and outside the acceptance zone, respectively, and necessarily,

$$(13)\quad M = M_o + M_1.$$

Deferring temporarily considerations as to how well the empirically determined histograms, (12), are representative of the future population distribution as required by (11), it will now be shown how the Neyman-Pearson Criterion would be applied, if the pilot histograms were representative.

We first recognize that our problem now is that of determining two decision thresholds, $\tilde{y}_1$ and $\tilde{y}_2$ on the observable, y, which in effect will map a true finite acceptability region, $-\bar{y} \leq y \leq \bar{y}$, onto a finite acceptability region in the observation space, $\tilde{y}_1 \leq \tilde{y} \leq \tilde{y}_2$. As shown in Figure 50 , the true classification bounds $(-\bar{y}, \bar{y})$, and the decision bounds $(\tilde{y}_1, \tilde{y}_2)$, divide the y-$\tilde{y}$ plane into four regions corresponding to the four possible outcomes in a binary hypothesis test.

We must also decide whether to fix the false rejection probability and minimize the false acceptance probability, or the other way around. For the application of this criterion to radar, the analog of the former constraint (fixed false alarm probability-minimized false dismissal probability) is always applied, following from the prevailing operating condition being that a detection radar is overwhelmingly not presented with any targets.

For the landing system situation, we must expect a high dominance of safe or acceptable landings to unacceptable landings (corresponding to no target, and target, respectively for the detection radar), otherwise we have a landing system not worth taking seriously. Accordingly, we fix the false rejection probability and minimize the false acceptance probability. For the observation acceptance zone $(\tilde{y}_1 \leq \tilde{y} \leq \tilde{y}_2)$, and utilizing the empirically determined histograms, there results the false rejection probability,

$$(15)\quad P\left\{H_1 \middle| H_o\right\} = \int_{-\infty}^{\tilde{y}_1} h\left(\tilde{y} \middle| |y| \leq \bar{y}\right) dy + \int_{\tilde{y}_2}^{\infty} h\left(\tilde{y} \middle| |y| \leq \bar{y}\right) dy$$

$$= \frac{1}{M_o \, \Delta\tilde{y}} \left\{ \sum_{i=-\infty}^{i_1} m_{oi} + \sum_{i=i_2}^{\infty} m_{oi} \right\}$$

$$\triangleq Q_o(\tilde{y}_1, \tilde{y}_2) = q_o(i_1, i_2) \text{ set} = \alpha$$

(where α is an upper bound tolerable to the decision maker), and the false acceptance probability,

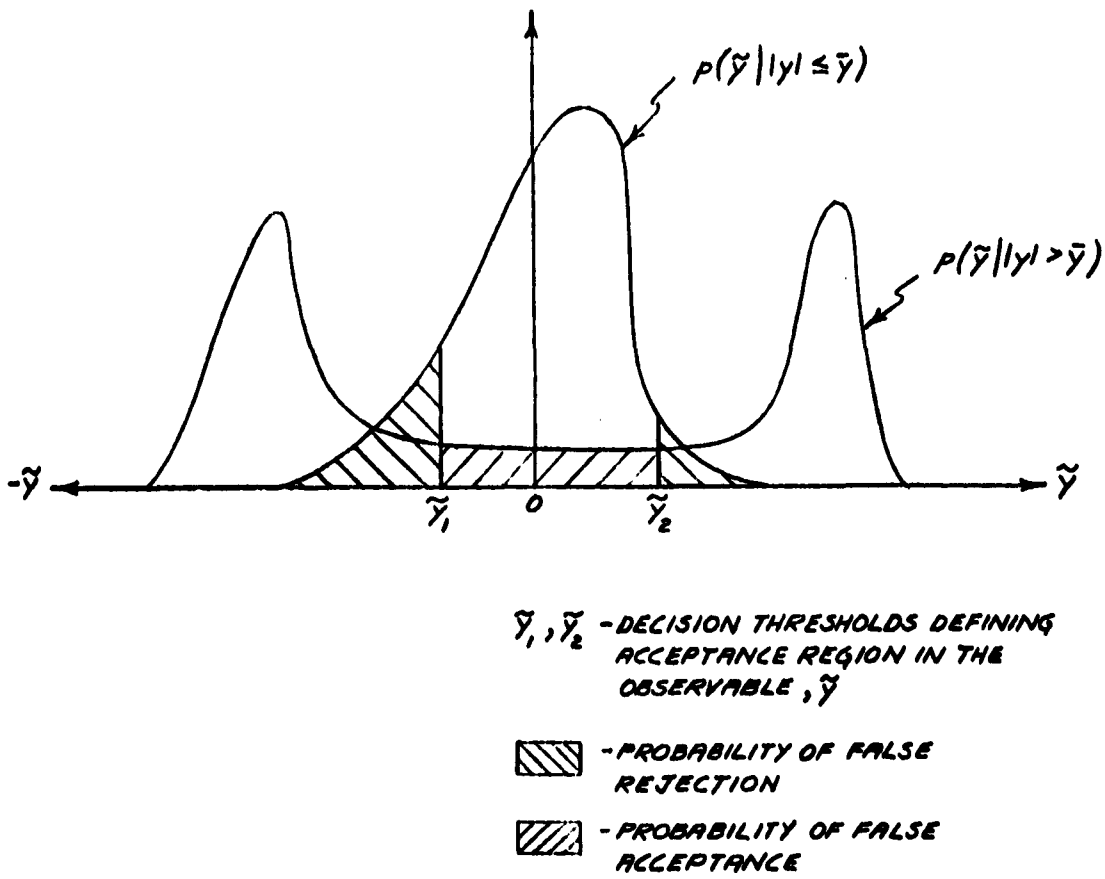

Figure 50 Conditional Distribution Densities Double Decision Threshold

$$(16)\quad P\left\{H_o \middle| H_1\right\} = \int_{\tilde{y}_1}^{\tilde{y}_2} h(\tilde{y} \middle| |y| > \bar{y})\,dy = \frac{1}{m_1\,\Delta\tilde{y}} \sum_{i=i_1}^{i=i_2} m_{1i}$$

$$\triangleq Q_1(\tilde{y}_1, \tilde{y}_2) = q_1(i_1, i_2)$$

Using the method of Lagrange multipliers for finding the pair of optimal decision thresholds $(\hat{y}_1, \hat{y}_2)$ which will satisfy the value, α, in (15), and also minimize (16), the function U is formed,

(17) $U(\tilde{y}_1, \tilde{y}_2) \triangleq Q_1(\tilde{y}_1, \tilde{y}_2) + \lambda Q_o(\tilde{y}_1, \tilde{y}_2)$, and the following conditions are imposed,

$$\frac{\partial U(\tilde{y}_1, \tilde{y}_2)}{\partial \tilde{y}_1} \text{ set } = 0 = \frac{\partial Q_1}{\partial \tilde{y}_1}(\tilde{y}_1, \tilde{y}_2) + \lambda \frac{\partial Q_o}{\partial y_1}(\tilde{y}_1, \tilde{y}_2)$$

$$(18)\quad \frac{\partial U(\tilde{y}_1, \tilde{y}_2)}{\partial \tilde{y}_2} \text{ set } = 0 = \frac{\partial Q_1}{\partial \tilde{y}_2}(\tilde{y}_1, \tilde{y}_2) + \lambda \frac{\partial Q_1}{\partial y_2}(\tilde{y}_1, \tilde{y}_2),$$

and, in addition

$\alpha = Q_o(\tilde{y}_1, \tilde{y}_2)$, as given by (15).

The first two equations of (18) can be found in terms of the given histograms as

$$(18a)\quad 0 = -h(\tilde{y}_1 \,||y| > \bar{y}) + \lambda H(\tilde{y}_1 \,||y| \leq \bar{y})$$

$$0 = h(\tilde{y}_2 \,||y| > \bar{y}) - \lambda h(\tilde{y}_2 \,||y| \leq \bar{y}),$$

and from (12) leads to

$$(18b) \quad 0 = -\frac{m_{l_{i_1}}}{M_l \Delta \tilde{y}} + \lambda \frac{m_{o_{i_1}}}{M_o \Delta \tilde{y}}$$

$$0 = \frac{m_{l_{i_2}}}{M_l \Delta \tilde{y}} - \lambda \frac{m_{o_{i_2}}}{M_o \Delta \tilde{y}}$$

where $m_{o_{i_1}}$, $m_{o_{i_2}}$, are the number of samples in the acceptable distribution in class intervals containing the decision thresholds, $\tilde{y}_1$ and $\tilde{y}_2$, and $m_{l_{i_1}}$ and $m_{l_{i_2}}$ are the corresponding numbers for the unacceptable distributions. From (15) and (18b), the unknowns λ, i_1, and i_2, can be solved, which, in combination with the histogram tables, (12), leads to the optimal decision thresholds, $\hat{\tilde{y}}_1$ and $\hat{\tilde{y}}_2$.

The generalization to a multiple measurement prescription for acceptability and nonacceptability is straightforward.

Let $y_1, y_2, \ldots . y_n$, be n measurement parameters for which acceptability is prescribed by the compound event $|y_1| \leq \bar{y}_1$ and, ... and $|y_n| \leq \bar{y}_n$, and rejectability by the compound event $|y_1| > \bar{y}_1$, or....., or $|y_n| > \bar{y}_n$.

With $\tilde{y}_1, \ldots, \tilde{y}_n$ as the estimators of $y_1, \ldots, y_n$, two empirically obtained distributions in a pilot population can be obtained:

$$h(\tilde{y}_1, \ldots, \tilde{y}_n \mid |y_1| \leq \bar{y}_1, \ldots, |y_n| \leq \bar{y}_n)$$

$$h(\tilde{y}_1, \ldots, \tilde{y}_n \mid |y_1| > \bar{y}_1, \text{ or} \ldots . \text{ or } |y_n| > \bar{y}_n),$$

a constraint is applied to the false rejection probability,

$$\alpha = \int_{-\infty}^{\tilde{y}_{11}} d\tilde{y}_1 \cdots \int_{-\infty}^{\tilde{y}_{1n}} d\tilde{y}_n \; h(\tilde{y}_1, \ldots, \tilde{y}_n \mid |y_1| \leq \bar{y}_1, \cdots |y_n| \leq \bar{y}_n)$$

$$+ \int_{\tilde{y}_{21}}^{\infty} d\tilde{y}_1 \cdots \int_{\tilde{y}_{2n}}^{\infty} d\tilde{y}_n \; h(\tilde{y}_1, \ldots, \tilde{y}_n \mid |y_1| \leq \bar{y}_1, \cdots |y_n| \leq \bar{y}_n)$$

and the false acceptance probability

$$Q_1(\tilde{y}_{11}, \tilde{y}_{21}, \ldots, \tilde{y}_{1n}, \tilde{y}_{2n}) = \int_{\tilde{y}_{11}}^{\tilde{y}_{21}} d\tilde{y}_1 \cdots \int_{\tilde{y}_{1n}}^{\tilde{y}_{2n}} d\tilde{y}_n \; h(\tilde{y}_1, \ldots, \tilde{y}_n \mid |y_1| > \bar{y}_1 \text{ or } |y_n| > \bar{y}_n)$$

is minimized via 2n-1 Lagrance multipliers in 2n minimization constraints, leading to 2n optimal decision thresholds, $\hat{\tilde{y}}_{11}, \hat{\tilde{y}}_{12}, \ldots \hat{\tilde{y}}_{n1}, \hat{\tilde{y}}_{n2}$, for the n measurements.

4. THE UNRELIABILITY OF CLASSIFYING THE ILS FACILITIES BY STATISTICAL DECISION METHODS

As stated previously in this report, a careful investigation into the possible correlation between power spectral density measurements in the geometric beam error and any of the landing parameters over a 25 facility ensemble (this ensemble being subjected to complete simulation) failed to reveal any significant correlation. Specifically, in order to reduce or eliminate the very serious error of false acceptance, one is led to apply decision thresholds to the spectral measurements (here given the role of estimator) so narrow as to result in an intolerably high false rejection probability. Note that this is a result possible from an estimator which indeed leads to zero landing error when the estimator is zero, but which otherwise is not correlated with the parameter for which it has been adopted as an estimator. It is not difficult to see why the course noise power spectrum is so trivially correlated with the landing errors.

The power spectrum (or spectral density), for any spectral frequency, is a mean square over a time interval. But a bounding of a time average mean square really leaves the course/path noise function unspecified except in the trivial case of imposing a zero mean square, in which case the noise function must be zero everywhere in the interval. Any landing parameter, on the other hand, must depend on the entire history of the course/path noise preceding the time instant at which the landing parameter is of interest, the late history being more heavily weighted than the early history. It would be very surprising if such different operations acting on a given ensemble of functions were statistically correlated.

From these considerations, it is natural to seek estimators of the landing parameter which take cognizance of the simulation channel as a point of departure, and which then approximate the weighting characteristic or dynamics of the landing parameter channel by means of a significantly simplified version of the exact simulation channel. This approach was tried on the lateral deviation channel, the exact channel being 17^{th} order and slightly nonlinear, the approximate channel being a linear 3^{rd} order filter. The results showed more correlation than for the power spectrum, but nevertheless too weak to be used for statistical prediction.

This result leads naturally to considering higher order approximations of the simulation channels. In any case, this point of view requires that each landing parameter be estimated by means of its channel approximation, thus giving up the notion that any single processing operation on the input course/path noise can result in adequate correlation between its output and all the landing parameters.

Accepting the notion of a channel-wise estimation, we arrive at a fundamental problem concerning the statistical correlation of an estimator with the parameter it is to estimate, and the confidence that can be put in empirical distributions derived from a small sample population.

If, in the absurd limit, the estimation channel were an exact replicate of the simulation channel which by definition determines the true landing parameter, no trials would be necessary for obtaining the two conditional distributions, these distributions being required for attaining Neyman-Pearson adjustments of the estimator decision thresholds. The estimator decision thresholds, in this limiting case, would be exactly the FAA specified bounds on the acceptance zone of the parameters in question.

If now, at the expense of high order approximation for each estimation channel, a high degree of correlation is attained in the pilot experiment, it can be concluded that the future population will also be highly correlated, and that the two distributions empirically obtained from the pilot population can serve with confidence as the corresponding distributions for the future populations. Stated in other terms, a strongly correlated estimator, results in only slight overlap of the two distributions, a characteristic which is more likely to be extrapolable from a small to large population than for a large overlap. Hence, there arises the question: Given the two distributions, empirically derived from a small population, and not necessarily with small overlap, are the probabilities of misclassification (false rejection and false acceptance) resulting from a Neyman-Pearson adjustment of the decision thresholds of the estimator for the pilot population necessarily close to or not close to the corresponding misclassification probabilities for the large future population? This question has not been resolved at present. However it seems very doubtful that small population estimation distributions which (1) result from poorly correlated estimators, and which (2) are, for the ILS facility classification problem, multivariate distributions, will be necessarily close to the large and decisive problem distributions.

Moreover, since it may be the intention that only these 25 facilities or small sampling of the total number of facilities will be used for lower

altitude approaches, there is no point in using statistical decision methods for classifying these facilities. The implications of this statement are either (1) investigate higher and higher order estimation channels until very strong correlation is found between the outputs of the estimation and exact channels or (2) classify the activity on the basis of exact simulation only. In view of the complications of Item (1) with its nonelimination of misclassification error, Item (2) is recommended as the technically best method to be followed.

REFERENCES

1. ILS Beam Characteristics for Low Approach and All-Weather Capability - K. Moses and J. Doniger
IATA Radio System Group Meeting - November 13, 1961
Paper No. 6RSG-4FTSC/WP-6

2. Aeronautical Systems Division - Technical Report 61-114 Automatic Landing System Study Part I - Air Force Contract No: AF33(616)-6925 - Flight Control Laboratory

3. Interim Report on Standard Performance Criteria for Autopilot/Approach Coupler Equipment - Special Committee 79 of RTCA - September, 1961

4. The Application of Statistics to the Flight Vehicle Vibration Problem - Aeronautical Systems Division - Technical Report 61-123 - J. S. Bendat et al - June 1961 - Flight Dynamics Laboratory Contract AF33(616)-7434

5. S. S. L. Chang - Synthesis of Optimum Control Systems - McGraw Hill - 1961

6. The Measurement of Power Spectra from the Point of View of Communications Engineering, Parts I and II - Blackburn and Tukey - Bell System Technical Journal - March 1958

7. Monthly Progress Report - FAA Contract FAA/ARDS-451 for November 30 and December 31, 1961

8. Monthly Progress Report - FAA/ARDS-451 for January 31 and February 28, 1962

9. Monthly Progress Report - FAA/ARDS-451 for March 31, 1962

10. Phase I Final Report - FAA/ARDS-451 - May 1962

11. Statistical Theory of Signal Detection - C. W. Helstrom - G. Pergamon Press - 1960